รายงานวิจัยฉบับสมบูรณ์

โครงการ หน้าที่ของ miRNAs ในระบบภูมิคุ้มกันของกุ้งต่อเชื้อก่อโรค

Role of miRNAs in shrimp immunity against pathogens

โดย

รองศาสตราจารย์ ดร. กุลยา สมบูรณ์วิวัฒน์

มิถุนายน 2562

สัญญาเลขที่ RSA5980055

รายงานวิจัยฉบับสมบูรณ์

หน้าที่ของ miRNAs ในระบบภูมิคุ้มกันของกุ้งต่อเชื้อก่อโรค

Role of miRNAs in shrimp immunity against pathogens

ผู้วิจัย

รองศาสตราจารย์ ดร.กุลยา สมบูรณ์วิวัฒน์

สังกัด

จุฬาลงกรณ์มหาวิทยาลัย

สนับสนุนโดยสำนักงานกองทุนสนับสนุนการวิจัย

และจุฬาลงกรณ์มหาวิทยาลัย

(ความเห็นในรายงานนี้เป็นของผู้วิจัย สกว. และจุฬาลงกรณ์มหาวิทยาลัย

ไม่จำเป็นต้องเห็นด้วยเสมอไป)

บทคัดย่อ

รหัสโครงการ : RSA5980055

ชื่อโครงการ : หน้าที่ของ miRNAs ในระบบภูมิคุ้มกันของกุ้งต่อเชื้อก่อโรค

ชื่อนักวิจัย : รองศาสตราจารย์ ดร.กุลยา สมบูรณ์วิวัฒน์ จุฬาลงกรณ์มหาวิทยาลัย

E-mail Address : kunlaya.s@chula.ac.th

ระยะเวลาโครงการ : 16 มิถุนายน 2559 – 15 มิถุนายน 2562

ไมโครอาร์เอ็นเอ (miRNAs) เป็น noncoding RNA ขนาดเล็ก ที่ทำหน้าที่สำคัญในกระบวนการควบคุมการแสดงออกหลังการเกิดการถอดรหัส ของยีนในกระบวนการต่างๆ ของเซลล์ อย่างไรก็ตามหน้าที่ของ miRNA ในระบบภูมิคุ้มกันของกุ้งยังไม่เป็นทราบแน่ชัด ในปัจจุบันโรคระบาดที่มีความรุนแรงในกุ้ง ได้แก่ โรคตายด่วน หรือ acute hepatopancreatic necrosis disease (AHPND) ซึ่งเกิดจากเชื้อแบคทีเรีย *Vibrio parahaemolyticus* (VP_{AHPND}) ที่สามารถผลิตโปรตีนสารพิษ Pir และโรคตัวแดงดวงขาว (White spot syndrome virus; WSSV) ที่เกิดจากการติดเชื้อไวรัสตัวแดงดวงขาว ดังนั้นในงานวิจัยนี้จึงมีวัตถุประสงค์เพื่อค้นหาและศึกษาหน้าที่ของ miRNA ในระบบภูมิคุ้มกันของกุ้ง จากการศึกษาก่อนหน้านี้พบว่าการทำให้กุ้งขาว *Penaeus vannamei* เครียดด้วยความร้อน (non-lethal heat shock; NLHS) ส่งผลให้กุ้งต้านทานการติดเชื้อ VP_{AHPND} มากขึ้นและเหนี่ยวนำการแสดงออกของยีนในระบบภูมิคุ้มกัน ในงานวิจัยนี้ได้วิเคราะห์ทรานสคริปโตมของเซลล์เม็ดเลือดของกุ้งขาวที่ติดเชื้อ VP_{AHPND} หลังจากถูกกระตุ้นด้วย NLHS สามารถแยกยีนที่มีการแสดงออกเปลี่ยนแปลง (DEGs) และ miRNA ที่มีการแสดงออกเปลี่ยนแปลงในสภาวะ NLHS และทำการวิเคราะห์ปฏิสัมพันธ์ของ miRNA และ mRNA พบว่าสภาวะ NLHS สามารถเหนี่ยวนำยีนในกระบวนการโพรฟีนอลออกซิเดส (proPO) วิถีธำรงค์ดุลของเซลล์เม็ดเลือด และกระบวนการผลิตเปปไทด์ต้านจุลชีพให้มีการแสดงออกเปลี่ยนแปลงไป จากผลการศึกษา miRNA ที่ตอบสนองต่อการติดเชื้อ VP_{AHPND} ที่น่าสนใจพบว่า lva-miR-4850 สามารถจับบริเวณ 3′-UTR ของยีน *PO2* ส่งผลให้เกิดการยับยั้งการแสดงออกของยีน *PO2* และแอกติวิตีของฟีนอลออกซิเดส แต่มีการเพิ่มขึ้นของจำนวนแบคทีเรียในกุ้งภายหลังจากการฉีด lva-miR-4850 นอกจากนี้ ได้ศึกษา miRNA ที่มีการแสดงออกตอบสนองต่อการติดเชื้อไวรัส WSSV ที่พบในเซลล์เม็ดเลือดของกุ้งกุลาดำ *Penaeus monodon* คือ pmo-miR-315 ซึ่งจากการทำนายโดยใช้โปรแกรมทางคอมพิวเตอร์พบว่ายีนเป้าหมายของ pmo-miR-315 คือ ยีน *PmPPAE* ชนิดใหม่ ในที่นี้เรียกว่า *PmPPAE3* โดยจากงานวิจัยนี้พบว่า *PmPPAE3* ทำหน้าที่เกี่ยวข้องกับการกระตุ้นระบบโพรฟีนอลออกซิเดสในกุ้ง จากนั้นศึกษาการแสดงออกและปฏิสัมพันธ์ระหว่าง pmo-miR-315 และ *PmPPAE3* พบว่า การแสดงออกของ pmo-miR-315 มีรูปแบบที่แปรผกผันกับการแสดงออกของ *PmPPAE3* โดย pmo-miR-315 สามารถจับกับบริเวณจับบนยีน *PmPPAE3* ได้ ทั้งนี้ยังพบว่าการให้ pmo-miR-315 เข้าสู่กุ้งกุลาดำที่ติดเชื้อไวรัส WSSV ส่งผลให้การแสดงออกของยีน *PmPPAE3* และแอกติวิตีของฟีนอลออกซิเดสลดลง แต่มีผลให้จำนวนไวรัส WSSV ในเซลล์เม็ดเลือดเพิ่มขึ้น จากผลการทดลองนี้แสดงให้เห็นว่า pmo-miR-315 ทำหน้าที่ลดการกระตุ้นระบบโพรฟีนอลออกซิเดสผ่านการยั้บยั้งการแสดงออกของยีน *PmPPAE3* ซึ่งมีผลช่วยให้ไวรัส WSSV เพิ่มจำนวนมากขึ้นในกุ้ง จากผลการวิจัยข้างต้นจึงสรุปได้ว่า ข้อมูลทรานสคริปโตมของกุ้งที่ติดเชื้อก่อโรคและ NLHS รวมกับการศึกษาหน้าที่ของโปรตีนในระบบภูมิคุ้มกัน แสดงให้เห็นถึงความซับซ้อนของการตอบสนองภูมิคุ้มกันของกุ้งเพื่อส่งเสริมกลไกการป้องกันตัวเองอย่างมีประสิทธิภาพในกุ้ง องค์ความรู้ด้านหน้าที่ของ miRNA และปฏิสัมพันธ์ของ miRNA กับยีนเป้าหมาย จากงานวิจัยนี้จะนำมาประมวลเพื่อหาแนวทางการป้องกันและควบคุมโรคระบาดในกุ้ง ซึ่งมีความสำคัญยิ่งต่อความยั่งยืนของอุตสาหกรรมการเลี้ยงกุ้ง

คำหลัก : ไมโครอาร์เอ็นเอ ภาวะเครียดจากความร้อน ยีนในระบบภูมิคุ้มกัน ภูมิคุ้มกันของกุ้ง เชื้อก่อโรคในกุ้ง

Abstract

Project Code : RSA5980055

Project Title : Role of miRNAs in shrimp immunity against pathogens

Investigator : Associate Professor Dr. Kunlaya Somboonwiwat Chulalongkorn University

E-mail Address : kunlaya.s@chula.ac.th

Project Period : 16 June 2016 – 15 June 2019

MicroRNAs (miRNAs), the small noncoding RNAs, play a pivotal role in posttranscriptional gene regulation in various cellular processes. However, the miRNA function in shrimp immunity against pathogens is still elusive. Currently, acute hepatopancreatic necrosis disease (AHPND) caused by *Vibrio parahaemolyticus* producing Pir toxin (VP_{AHPND}) and white spot disease (WSD) caused by white spot syndrome virus (WSSV) are the severe bacterial and viral diseases in shrimp. Hence, this research aims to identify and uncover the function of miRNAs in shrimp immunity. As reported previously, non-lethal heat shock (NLHS) could enhance the resistance of *Penaeus vannamei* to VP_{AHPND} infection and induce the expression of immune-related genes. Herein, transcriptomic analysis of *P. vannamei* hemocyte infected with VP_{AHPND} upon NLHS treatment identified NLHS-induced differentially expressed genes (DEGs) and differentially expressed miRNAs (DEMs) and the miRNA/mRNA regulatory network. Pathway analysis of the NLHS-induced DEMs and their target DEGs which have immune-related functions demonstrated that NLHS induces changes in expression of genes involved in prophenoloxidase (proPO) system, hemocyte homeostasis and antimicrobial peptide production in *P. vannamei*. Among the VP_{AHPND}-responsive miRNAs identified, lva-miR-4850, targeting 3′-UTR of prophenoloxidase 2 (*PO2*) gene was of interest. Introducing the lva-miR-4850 mimic into the VP_{AHPND}-infected shrimp caused the reduction of the *PO2* transcript and the PO activity but significantly increased the number of bacteria in the VP_{AHPND} targeted shrimp tissues. Moreover, the WSSV-responsive miRNA, pmo-miR-315, identified from *Penaeus monodon* hemocytes was characterized. The predicted pmo-miR-315 target mRNA is a novel *PmPPAE* gene called *PmPPAE3*. Therefore, *PmPPAE3* was characterized and its function in PO activity activation was shown. The negative correlation of expression and the interaction of pmo-miR-315 and *PmPPAE3* were revealed. Introducing the pmo-miR-315 into the WSSV-infected shrimp caused the reduction of the *PmPPAE3* transcript level and, hence, the PO activity activated by the *Pm*PPAE3 whereas the WSSV copy number in the shrimp hemocytes was increased. Our findings state a significant role of pmo-miR-315 in attenuating proPO activation via *PPAE3* gene suppression and facilitating the WSSV propagation in shrimp upon WSSV infection. In conclusions, the profiling of transcriptome-wide interactions during pathogen infections and NLHS and protein function analysis, revealed the complexity of the shrimp innate immune responses to promote effective host defense. The knowledge of miRNA function and interaction with target genes will be used in establishing a new strategy for disease control which will lead to sustainable shrimp aquaculture.

Keywords: miRNA, Non-lethal heat stress, Immune-related genes, Shrimp immunity, Shrimp pathogens

Executive summary

อุตสาหกรรมการเลี้ยงกุ้งนำรายได้เข้าประเทศปีละหลายหมื่นล้านบาท ซึ่งเป็นอุตสาหกรรมที่มีความสำคัญต่อเศรษฐกิจของประเทศไทย อย่างไรก็ตามการระบาดของโรคติดเชื้อซึ่งมีสาเหตุมาจากไวรัสและแบคทีเรีย เช่น โรคตัวแดงดวงขาว ที่เกิดจากไวรัสตัวแดงดวงขาว (WSSV) และโรคตายด่วน หรือ early mortality syndrome (EMS) หรือเรียกอีกชื่อหนึ่งว่า Acute hepatopancreatic necrosis syndrome (AHPND) ที่เกิดจากการติดเชื้อแบคทีเรีย *Vibrio parahaemolyticus* สายพันธุ์ที่มีการสร้างโปรตีนสารพิษ (VP_{AHPND}) เป็นสาเหตุหลักที่ทำให้เกิดความไม่มั่นคงทางการผลิต และเนื่องจากยังไม่วิธีการควบคุมโรคที่มีประสิทธิภาพ ดังนั้น งานวิจัยด้านระบบภูมิคุ้มกันโดยเฉพาะอย่างยิ่งการตอบสนองและการควบคุมการทำงานของระบบภูมิคุ้มกันของกุ้งจึงมีความสำคัญต่อความยั่งยืนของอุตสาหกรรมการเลี้ยงกุ้ง เนื่องจากเป็นแกนความรู้สำคัญที่จะนำมาประยุกต์ใช้เพื่อเป็นแนวทางในการป้องกันและควบคุมโรคระบาดในกุ้ง

จากงานวิจัยที่มีมาก่อนหน้าชี้ให้เห็นว่าไมโครอาร์เอ็นเอ (miRNA) เป็น อาร์เอ็นเอขนาดเล็กที่ทำหน้าที่ควบคุมการแสดงออกของยีน จึงมีความสำคัญในการควบคุมกระบวนการต่างๆ ภายในเซลล์ รวมถึง ระบบภูมิคุ้มกัน ซึ่งในปัจจุบัน มีการนำไปทดลองรักษาโรคในคนที่เกิดจากความผิดปกติของการทำงานระดับยีนหลายชนิด ถึงแม้ว่าในปัจจุบันจะมีงานวิจัยที่ศึกษาหน้าที่ของ miRNA ในระบบภูมิคุ้มกันของกุ้งเพิ่มขึ้น แต่ยังขาดความเข้าใจหน้าที่ของ miRNA อีกมาก ดังนั้นในงานวิจัยนี้ จึงมุ่งเน้นการศึกษาหน้าที่ของ miRNA ที่พบในเซลล์เม็ดเลือดที่เป็นเซลล์ของระบบภูมิคุ้มกันที่สำคัญ และมีการแสดงออกตอบสนองต่อสภาวะที่กุ้งติดเชื้อก่อโรคทั้งไวรัสและแบคทีเรีย VP_{AHPND} แต่เนื่องจากยังไม่มีข้อมูล miRNA ในกุ้งขาวที่ติดเชื้อแบคทีเรีย ในเบื้องต้นผู้วิจัยจึงได้ทำการศึกษาทรานสคริปโตมของยีนและอาร์เอ็นเอขนาดเล็ก เพื่อระบุชนิดและศึกษาความสัมพันธ์ระหว่าง miRNA และยีนเป้าหมายในกลุ่มที่ทำหน้าที่ในระบบภูมิคุ้มกันที่ถูกควบคุมการแสดงออกโดย miRNA โดยศึกษาในสภาวะที่กุ้งถูกทำให้เครียดด้วยความร้อนและติดเชื้อ VP_{AHPND} เนื่องจากมีรายงานก่อนหน้าที่ระบุว่ากุ้งขาวที่ถูกทำให้เครียดด้วยความร้อน มีความสามารถในการต้านทานการติดเชื้อ VP_{AHPND} ได้เพิ่มขึ้น ดังนั้นในการวิจัยนี้จึงแบ่งการศึกษาออกเป็น 3 ส่วน โดยสรุปผลงานในส่วนต่างๆ ดังต่อไปนี้

1) การค้นหาและระบุชนิดของ miRNA ที่ตอบสนองต่อเชื้อ VP_{AHPND} ภายใต้สภาวะความเครียด จากความร้อน

จากผลการวิเคราะห์การแสดงออกของยีนและ miRNA ในเซลล์เม็ดเลือดของกุ้งที่ถูกทำให้เครียดด้วยความร้อน (Non-lethal heat stress; NLHS) และติดเชื้อ VP_{AHPND} ด้วยเทคนิค Next Generation Sequencing (NGS) พบ ยีน และ miRNA จำนวน 2,662 และ 41 ชนิด ตามลำดับ ที่ตอบสนองต่อ NLHS และตอบสนองต่อการติดเชื้อ VP_{AHPND} และได้ยืนยันการแสดงออกยีนและ miRNA ที่สนใจในสภาวะที่ถูกทำให้เครียดด้วยความร้อนด้วยเทคนิค quantitiative realtime RT-PCR และ qRT-PCR ตามลำดับ เมื่อนำ miRNA ที่ตอบสนองต่อ NLHS ที่มีการแสดงออกแปรผกผันกับยีนเป้าหมายในกลุ่มที่ทำหน้าที่ในระบบภูมิคุ้มกันที่ตอบสนองต่อ NLHS ที่พบในเซลล์เม็ดเลือดของกุ้งมาวิเคราะห์ร่วมกันเพื่อศึกษาความเชื่อมโยงระหว่าง miRNA และ mRNA พบว่า NLHS สามารถเหนี่ยวนำยีนในกระบวนการโพรฟีนอลออกซิเดส (proPO) วิถีธำรงค์ดุลของเซลล์เม็ดเลือด และกระบวนการผลิตเปปไทด์ต้านจุลชีพให้มีการแสดงออกเปลี่ยนแปลงไป และสามารถระบุชนิดของ miRNA ที่คาดว่าทำหน้าที่ควบคุมการแสดงออกของยีนในกระบวนการดังกล่าวในสภาวะ NLHS ได้ ทั้งนี้แสดงให้เห็นว่า miRNA ทำหน้าที่ในการควบคุมการแสดงออกของยีน

ในกลุ่มของระบบภูมิคุ้มกันในสภาวะ NLHS ซึ่งส่งผลต่อการเพิ่มความสามารถในการต้านทานการติดเชื้อ VP_{AHPND} ของกุ้ง

2) การศึกษาหน้าที่ของ miRNA ที่มีการแสดงออกตอบสนองต่อการติดเชื้อ VP_{AHPND}

จากข้อมูล NGS ข้างต้นสามารถระบุชนิดของ miRNA ที่มีการแสดงออกตอบสนองต่อการติดเชื้อ VP_{AHPND} จากเซลล์เม็ดเลือดของกุ้งขาว และได้ยืนยันการแสดงออกของ miRNA ที่สนใจจำนวน 10 ชนิด ด้วยเทคนิค stem-loop quantitiative realtime RT-PCR ทั้งในสภาวะที่กุ้งติดเชื้อ VP_{AHPND} จากผล NGS นำ miRNA ที่มีการแสดงออกเปลี่ยนแปลงเมื่อมีการติดเชื้อ VP_{AHPND} ไปทำนายหายีนเป้าหมายในระบบภูมิคุ้มกันที่มีรูปแบบการแสดงออกแบบแปรผกผันกัน โดยพบว่า miRNA ที่มีการตอบสนองต่อการติดเชื้อ VP_{AHPND} ทำหน้าที่ควบคุมยีนในกลุ่ม Heat shock protein โปรติเนสและตัวยับยั้งโปรติเนส RNA interference pattern recognition protein เปปไทด์ต้านจุลชีพ Toll pathway IMD pathway endocytosis ระบบโพรฟีนอลออกซิเดส วิถีธำรงค์ดุลของเซลล์เม็ดเลือด และกระบวนการแข็งตัวของเลือด ทั้งนี้สนใจศึกษาหน้าที่ของ lva-miR4850 ซึ่งมียีนเป้าหมายคือ ยีนโพรฟีนอลออกซิเดส 2 (PO2) จากการวิจัยสามารถยืนยันการจับกันของ lva-miR4850 กับยีน *PO2* และ lva-miR4850 ยับยั้งการแสดงออกของยีน *PO2* และส่งผลให้แอกติวิตีของโพรฟีนอลออกซิเดสลดลงด้วย

3) การศึกษาหน้าที่ของ miRNA ที่มีการแสดงออกตอบสนองต่อการติดเชื้อไวรัสตัวแดงดวงขาว

จากข้อมูล NGS ในงานวิจัยของกลุ่มวิจัยที่ผ่านมา พบ miRNA จากกุ้งกุลาดำที่มีการแสดงออกตอบสนองต่อการติดเชื้อไวรัสตัวแดงดวงขาวที่สนใจ คือ pmo-miR-315 ที่มีการแสดงออกเพิ่มขึ้นสูงที่เวลา 48 ชั่วโมงหลังการติดเชื้อไวรัสตัวแดงดวงขาว ซึ่งจากการทำนายโดยใช้โปรแกรมทางคอมพิวเตอร์พบว่ายีนเป้าหมายของ pmo-miR-315 คือ ยีน *PmPPAE3* โดยจากงานวิจัยนี้พบว่า *PmPPAE3* ทำหน้าที่เกี่ยวข้องกับการกระตุ้นระบบโพรฟีนอลออกซิเดสในกุ้ง และ pmo-miR-315 สามารถจับกับ *PmPPAE3* และทำให้การแสดงออกของยีน *PmPPAE3* ถูกยับยั้ง ในกุ้งกุลาดำที่ติดเชื้อไวรัส WSSV ส่งผลให้แอกติวิตีของฟีนอลออกซิเดสลดลง และจำนวนไวรัส WSSV ในเซลล์เม็ดเลือดเพิ่มขึ้น จากผลการทดลองนี้แสดงให้เห็นว่า pmo-miR-315 ทำหน้าที่ลดการกระตุ้นระบบโพรฟีนอลออกซิเดสผ่านการยับยั้งการแสดงออกของยีน *PmPPAE3* ซึ่งมีผลช่วยให้ไวรัส WSSV เพิ่มจำนวนมากขึ้นในกุ้ง

ผลงานวิจัย

1. Jaree P, Wongdontri C, Somboonwiwat K. White spot syndrome virus-induced shrimp miR-315 attenuates prophenoloxidase activation via PPAE3 gene suppression. Frontiers in Immunology. Front Immunol. 2018, 25;9:2184
2. Boonchuen P, Maralit BA, Jaree P, Tassanakajon A, Somboonwiwat K. MicroRNA and mRNA interactions contribute to coordinating the immune response in chronic non-lethal heat stressed *Litopenaeus vannamei* against acute hepatopancreatic necrosis disease-causing strain of *Vibrio parahaemolyticus*. PLOS Pathogens. (submitted)
3. Boonchuen P, Somboonviwat K, Tassanakajon A, Somboonwiwat K. Identification of miRNA from *Penaeus vannamei* in response to *Vibrio parahaemolyticus* AHPND infection (manuscript in preparation)

1. Introduction

Thailand shrimp farming has been continuing affected by serious infectious disease outbreaks caused mainly by viruses and bacteria especially the white spot syndrome virus (WSSV) and Vibrio species. In 2013, Thai shrimp production has declined nearly 50 percent because of the spread of a deadly disease outbreak named "early mortality syndrome" (EMS) or acute hepatopancreatic necrosis disease (AHPND). It has later been shown to be caused by toxin-harboring *Vibrio parahaemolyticus* (VP_{AHPND}) (Tran et al, 2013). As shrimp farmers adopt several strategies to cope with the diseases, the devastating effect of these diseases still exist. Understanding the fundamental basis of disease pathogenesis and how the shrimp immune system works during the diseased conditions will lead to the development of effective and efficient management strategies to prevent the VP_{AHPND} infection. Likewise, the information on the molecular mechanisms of AHPND tolerance can lead to platforms for the development of AHPND- resistant shrimp either through marker- assisted selective breeding or transcriptome analyses at different rearing conditions. Therefore, the research to support disease control and prevention in shrimp farming remains very important for the sustainability of the industry.

MicroRNAs (miRNAs) are small non-coding RNA molecules that play important functions in RNA silencing and post-transcriptional regulation (Bartel et al, 2004). The biogenesis of miRNA is a process in which the primary transcripts (pri-miRNA) containing the hairpin loop domains are cut by the RNase III-like enzyme, Drosha, into a 60–70 nucleotide-long precursor miRNA (pre-miRNA). The pre-miRNA is exported to the cytoplasm by Exportin-5 and further cleaved by the RNase-III enzyme, Dicer, producing the miRNAs of 18-24 double-stranded oligonucleotides. A strand of miRNA is incorporated into the RNA-induced silencing complex (RISC) rendering specific interaction to the target mRNA. The complementary target mRNA is degraded and, hence, translational repressed (Azzam et al, 2012).

Generally, a single miRNA regulated multiple target genes, furthermore, a single gene might be regulated by multiple mature miRNAs. So far, miRNAs have been identified in a wide range of organisms and they are involved in developmental and physiological processes as well as the immune system (Lagos-Quintana et al., 2002; Lu and Liston, 2009). The miRNAs do respond to bacterial components, such as LPS as reported by Taganov et al., 2006. miRNAs that are expressed in response to various mycobacteria infection in dendritic cells have been identified. The specific miRNA responses that reflect mechanisms by which certain pathogens interfere with

the host response to infection have been revealed (Siddle et al., 2015). In mammals, *in vitro* study suggested that several cellular miRNAs play a role in antiviral response. For example, in mice, cellular miR-24 and miR-93 down-regulate vesicular stomatitis virus (VSV) protein expression and other miRNAs, including miR-28, miR-125b, miR-150, miR-223 and miR-382, inhibit human immunodeficiency virus-1 (HIV-1) replication via binding sites located within the viral genome (for review: Umbach and Cullen, 2009). The expression level of several cellular miRNAs increases after HIV-1 infection, including miR-297, miR-370 and miR-122. However, miR-17-92 expression level is suppressed upon HIV-1 infection resulted in increased HIV-1 replication (Triboulet et al., 2007).

In crustaceans, there are many reports showing that the host miRNAs can regulate the expression of the host and viral genes and vice versa. In 2012, the first large-scale miRNA characterization in WSSV-infected *Marsupenaeus japonicas* lymphoid organ has been reported (Huang et al, 2012). Several cellular WSSV-responsive miRNAs play important roles in shrimp immunity including apoptosis pathway (Yang et al, 2014, Gong et al, 2015), phagocytosis (Shu et al, 2016), NF-kB pathway (Xu et al, 2016) and JAK/STAT pathway (Huang et al, 2016). Furthermore, the WSSV miRNAs were also identified and probably could target either the host or viral genes. In the WSSV-infected *M. japonicas,* the viral miRNAs could target virus transcripts and further promote virus infection (He et al, 2014). In the meantime, a viral miRNA, WSSV-miR-N24, could target the shrimp apoptotic gene, caspase 8, and further represses the apoptosis of shrimp hemocytes (Huang wt al, 2014). Receently, the role of miRNA in regulating the DCP1-DCP2 complex that functions in regulating the stability of viral mRNA has been revealed. The miRNA miR-87 of *M. japonicus* inhibited WSSV infection by targeting the host DCP2 gene and viral miRNA WSSV-miR-N46 took a negative effect on WSSV replication by targeting the host DCP1 gene (Sun and Zhang 2019).

In *Penaeus monodon*, the 60 known miRNA homologs that are expressed in the hemocytes of WSSV-challenged shrimp at the early and late phases of infection have been identified (Kaewkascholkul et al, 2016). Their immune-related gene targets in apoptosis pathway, antimicrobial peptide, prophenoloxidase system, signal transduction, proteinase and proteinase inhibitor, blood clotting system and heat shock protein have also been predicted. Among them, the pmo-miR-315 was found to be a highly up-regulated miRNAs in response to WSSV challenge and their target genes were confirmed to be a novel prophenoloxidase-activating enzyme, called *PmPPAE3*. In this research, the roles of pmo-miR-315 in WSSV-infected shrimp were investigated.

The study of the host miRNA responses to bacteria has progressed at a slower pace than that of viral infection. The emerging roles of miRNAs in mammalian host signaling and defense against bacterial pathogens have been revealed. In the aquatic animals, zebrafish (*Danio rerio*) and mud crab (*Scylla paramamosain*), miRNAs that are expressed in response to bacterial infection were identified (Li et al., 2013; Wu et al, 2012). Recently, the next generation sequencing was used to identify differentially miRNA expression from *Penaeus vannamei* hemocytes upon VP_{AHPND} infection. Among them, they have been shown to target 222 genes that are involved in various biological functions and shrimp immune response related such as proteinase inhibitors, apoptosis and heat shock proteins (Zheng et al, 2018). The miRNA expression profiles in response to bacterial infections have revealed the miRNAs as players in the host innate immune responses and, thus, providing key evidences on the general role of miRNAs in immunity (Eulalio et al, 2012).

It has been proven that the immune-related genes and heat shock proteins (Hsps) become up-regulated after non-lethal heat shock (NLHS) facilitate some form of tolerance or resistance to the pathogens (Yik Sung et al, 2007, Loc et al, 2013). For instance, the Hsp70 transcript is increased in the hepatopancreas of Chinese shrimp *Fenneropenaeus chinensis* after WSSV infection (Wang et al, 2006). The Hsp70 and Hsp90 mRNAs become up-regulated in the gills *P. monodon* upon *Vibrio harveyi* infection (Rungrassamee et al, 2010). In *P. vannamei,* the *Lv*Hsp60 protein is significantly up-regulated in the gills, hepatopancreas and hemocytes after bacterial challenge (Zhou et al, 2010). These observations in different shrimp species indicates the conserved functional role of Hsps in shrimp, which also highlights the presence of an organized system of resistance to pathogenic infection related to heat stress in shrimp and perhaps in invertebrates in general.

In the present study, the next-generation sequencing of small RNA and the RNA-seq data of the hemocytes of *P. vannamei* under the NLHS condition was performed and analyzed. The inferred relationships among the target genes and miRNAs revealed important aspects of miRNA and their targets pertaining to AHPND resistance or tolerance were shown. The interesting pathogen-responsive miRNAs were selected for further functional characterization. Their involvement in regulating prophenoloxidase activating system was clearly elucidated.

2. Methods

2.1 Integrated analysis of microRNA and mRNA expression in hemocytes of *P. vannamei* challenged with *Vibrio parahaemolyticus* AHPND under heat stress conditions

2.1.1 Shrimp samples

Shrimp, weighing 2-4 grams, were obtained from a local shrimp farm and acclimatized in rearing tanks with ambient temperature of 30 °C, water salinity of 20 parts per thousand (ppt), and constant aeration before used in the experiments. The shrimp were fed with commercial pellets 4 times a day during the course of experiments. Due to the Ethical Principles and Guidelines for the use of animals for scientific purposes by the National Research Council of Thailand, this project was conducted according to the animal use protocol number 1823006 approved by the Chulalongkorn University Animal Care And Use Committee (CU-ACUC).

This project was reviewed and approved by the CU-IBC (Approval number: SCI-01-001) to be in accordance with the levels of risk in pathogens and animal toxins listed in the Risk Group of Pathogen and Animal Toxin (2017) published by the Department of Medical Sciences, Ministry of Public Health, the Pathogen and Animal Toxin Act (2015) and Biosafety Guidelines for Modern Biotechnology, BIOTEC (2016).

2.1.2 Non-lethal heat stress (NLHS) and bacterial challenge experiments

The bacterial inoculum was prepared by culturing the bacteria overnight in 3 mL of tryptic soy broth (TSB) containing 1.5% NaCl at 30 °C and 250 rpm. Then, the starter culture was transferred to 200 mL TSB with 1.5% NaCl and further incubated at 30 °C and 200 rpm until the OD_{600} reached 2.0 (approximately 10^8 CFU/mL).

After rearing at 30 °C, the chronic non-lethal heat stress (NLHS) was applied to the shrimp. The shrimp were divided into 4 groups of 10 shrimp each. Two groups were NLHS-treated byplacing in tanks containing 10 L sea water at 38 °C for 5 min daily for 7 days and allowed a 3-day recovery period in their respective rearing tanks. They were, then, challenged with $VP_{AHPND}$by immersion.adding the bacterial inoculum to a final concentration of 10^6 CFU/mL. The shrimp survival was observed for 53 h. The experiment was done in triplicate. Statistical analyses of the results were conducted using GraphPad Prism version 6.

2.1.3 RNA extraction

Approximately 500 µL of hemolymph was drawn out from the ventral sinus of a shrimp using a sterile syringe with an equal volume of anticoagulant (27 mM sodium citrate, 336 mM NaCl, 115 mM glucose and 9 mM EDTA, pH 5.6) (Somboonwiwat et al, 2010) Hemocytes were immediately collected by centrifugation at 800×*g* for 10 min at 4 °C and kept in liquid nitrogen. The hemocytes from 30 individuals of VP_{AHPND}-challenged NLHS-treated and VP_{AHPND}-challenged NH control shrimp at time points 0, 6 and 24 h post infection (hpi) were pooled and extracted for large and small RNAs using *mir*Vana™ miRNA Isolation Kit (Ambion, Life Technologies) following the manufacturer's protocol. The experiment was done in triplicate. The integrity of RNA was evaluated in Agilent 2100 Bioanalyzer chip using RNA 6000 Pico Kit and Small RNA Kit (Agilent) for large and small RNA preparations, respectively. The RNA concentrations were determined by Qubit® RNA HS Assay Kit (ThermoFisher Scientific) on the Qubit® 2.0 flourometer.

2.1.4 RNA sequencing and data analysis

Six cDNA libraries including 0 NLHS-VP, 6 NLHS-VP, 24 NLHS-VP, 0 NH-VP, 6 NH-VP and 24 NH-VP were prepared from 4 µg total RNA following the manufacturer's protocol for TruSeq® Stranded mRNA LT Sample Prep Kit (Illumina). In a run, ten indexed libraries were normalized, pooled and then sequenced with a 1% PhiX spike-in control using NextSeq 500 Mid Output v2 Sequencing Kit (Illumina) in a NextSeq 500 desktop sequencer (Illumina). Additional adapter trimming and quality control of raw reads was performed using FastQ Toolkit available through the BaseSpace (Illumina) public app repository. High quality reads were assembled together to form a reference assembly in Trinity v2.06 software (Grabherr et al, 2011). Transcript abundance was estimated using RSEM wrapped by scripts included in Trinity. Differentially expressed transcripts and genes (DEGs) were detected using edgeR software (Robinson et al, 2010) in each treatment group and checked for sequence quality and correlation.

Gene ontology enrichment analysis for differentially expressed features was done by the Trinotate protocol (http://trinotate.github.io/), leveraging different software for functional annotation, such as BLAST (Altschul et al, 1990), PFAM (Punta et al, 2011), HMMER (Finn et al, 2011), SignalP (Petersen et al, 2011), tmHMM (Krogh et al, 2001), KEGG (Kanehisa et al, 2012), GO (Ashburner et al, 2002), and eggnog (Powell et al, 2012), and, then, running the GO-Seq (Powell et al, 2012). Using the UniProt Retrieve/ID mapping tool (http://www.uniprot.org/uploadlists/),

the UniProt accession numbers from the Trinotate protocol were mapped into the Entrez GeneIDs, which were then used in the KOBAS 2.0 (http://kobas.cbi.pku.edu.cn/home.do) to map the KEGG Orthology or conduct the enrichment analysis. The subsequent KEGG orthology was then used as input in the KEGG Mapper – Search Pathway tool (http://www.kegg.jp/kegg/tool/map_pathway1.html) for mapping to the reference KEGG Pathways and determining the distribution. The BLAST2GO (Conesa et al, 2005) was also used for some supplementary annotation. The Fasta tools, Trinity software, BLAST+ and other supplementary tools from galaxy services of the National Center for Genome Analysis Support (https://galaxy.ncgas-trinity.indiana.edu/) (Afgan et al, 2016) and Galaxy Queensland (http://galaxy-qld.genome.edu.au/galaxy) were also used.

2.1.5 The small RNA next generation sequencing and data analysis

The cDNA libraries from small RNA from VP_{AHPND}-infected NLHS-treated shrimp hemocytes at 0, 6 and 24 hpi were constructed following the manufacturer's instruction for TruSeq® Small RNA Library Preparation Kit (Illumina). The three indexed libraries were normalized, pooled and, then, sequenced with a PhiX control spiked in at 7.5% using MiSeq Reagent Kits v2 (Illumina) in a MiSeq sequencer (Illumina). The 5′-, 3′-adapter trimming and quality control of raw reads were performed using tools in a Galaxy instance (https://usegalaxy.org/). High quality small RNA sequences with length shorter than 18 nucleotides and longer than 24 nucleotides were removed. Homology search for contaminating RNA such as mRNA, rRNA and tRNA was conducted using BLASTn against the NCBI nucleotide and Rfam database. After discarding the contaminating RNA, the remaining sequences were searched against miRBase 22.1 (http://www.mirbase.org/) in order to identify known miRNA homologs.

2.1.6 Quantitative Real-time PCR analysis

Several transcripts from the reference assembly were selected for quantitative real-time PCR analysis (RT-qPCR) to evaluate and confirm the differential expression profiles reported by RNA-seq analysis. The gene specific primers were designed by Primer3 as packaged in Geneious R6 (Biomatters) (Untergasser et al, 2012). Using 1 µg total RNA, the first strand cDNA synthesis was carried out in a reaction containing 1 mM dNTP, 10 units of RNase inhibitor, 0.5 µM oligo-dT (Promega), 1× RevertUP buffer (BiotechRabbit), and 100 units of RevertUP Reverse Transcriptase (BiotechRabbit). The RT-qPCR reactions were composed of 5- or 10-fold diluted cDNA template,

1× QPCR Green Master Mix (LRox) (BiotechRabbit) and 0.5 or 0.25 μM forward and reverse primers, and were run in MiniOpticon Real-time PCR system (Bio-Rad). Relative expression of each gene was determined and analyzed using the *EF-1α* gene as a control gene and the zero time point of non-heat shrimp as a control group.

The miRNAs of interest consisting of lva-miR-7170-5p, lva-miR-2169-3p, lva-miR-184, lva-miR-92b-5p, lva-miR-317, lva-miR-92a-3p, lva-miR-4901, lva-miR-61, lva-miR-2898 and lva-miR-6090 were selected for expression analysis using stem-loop RT-qPCR. The pooled total small RNA samples from the VP_{AHPND}-infected NLHS-treated and control shrimp hemocytes at 0, 6 and 24 hpi were prepared using the mirVana miRNA Isolation Kit (Ambion, Life technologies). The extracted total small RNA was, then, used as a template for the first strand stem-loop cDNA synthesis using the stem-loop primers by RevertAid First Strand cDNA Synthesis Kit (Thermo Fisher Scientific). The *U6* gene expression was used as an internal control.(Kaewkascholkul et al. 2016) Stem-loop RT-qPCR was performed using an appropriate amount of cDNA for each gene, specific oligonucleotide primers and QPCR Green Master Mix (Biotechrabbit) in MiniOpticon™ RealTime PCR System (Bio-Rad) with the following conditions: 95 °C for 3 min, 40 cycles of 95 °C for 30 s, 60 °C for 30 s and 72 °C for 30 s. Relative expression was calculated and data were analyzed using paired-samples t-test and then presented as means ± standard deviations (Pfaffl 2001). The statistical significance was considered at *P*-value < 0.05. The experiment was performed in triplicates.

2.1.7 miRNA target prediction

The miRNA targets were identified by comparing the miRNA sequences with transcriptome data using CU-mir software developed by our research group (Kaewkascholkul et al, 2016). The software searched for the sequences on mRNA targets that match perfectly or mismatch by one nucleotide to the seed sequences (2-8 nucleotides from the 5′ end) of miRNA. The percent complementary was calculated from the number of nucleotides that perfectly match the target mRNAs per total length of miRNA sequences. The percent complementary cutoff was set at 55%. The RNAhybrid (http://bibiserv.techfak.uni-bielefeld.de/rnahybrid/) was also used to predict genes targeted by the miRNAs with the parameters of free energy < −15.0 kcal/mol (Krüger et al, 2006).

2.1.8 miRNA/mRNA interaction network analysis

In order to define all possible miRNA-mRNA interactions involved in a specific dataset of immune-related genes, the miRNA-mRNA interaction network was constructed. The immune responsive genes from the transcriptome were specifically chosen and included in the integrated analysis of the miRNA/mRNA network. The differentially expressed miRNAs (DEMs) from shrimp challenged with VP_{AHPND} under NLHS were used as queries to search for mRNA targets and to construct the miRNA/mRNA network. Again, the binding of target mRNAs of differentially expressed miRNAs were predicted using RNAhybrid with the parameters of free energy < −15 kcal/mol. These target mRNAs were mapped against our RNA-Seq data to determine their immune-related functions.

2.2 Functional characterization of miRNAs from *P. vannamei* hemocyte in response to VP_{AHPND} infection

2.2.1 Small RNA library preparation

After the small RNA libraries of were sequenced using the MiSeq instrument, data was obtained in FASTQ format, which contained both nucleotide sequences and their corresponding quality scores. The 5′- and 3′-adapter trimming and quality control of raw reads were performed using tools in a Galaxy instance (https://usegalaxy.org/). High quality small RNA sequences with lengths shorter than 18 nucleotides and longer than 24 nucleotides were removed. A homology search of contaminating RNA (e.g. mRNA, rRNA, and tRNA) was conducted using BLASTn against the NCBI nucleotide and Rfam database. After discarding econtaminating RNA, remaining sequences were searched against miRBase 22.1 (http://www.mirbase.org/) in order to identify known miRNA homologs (Figure 2.1).

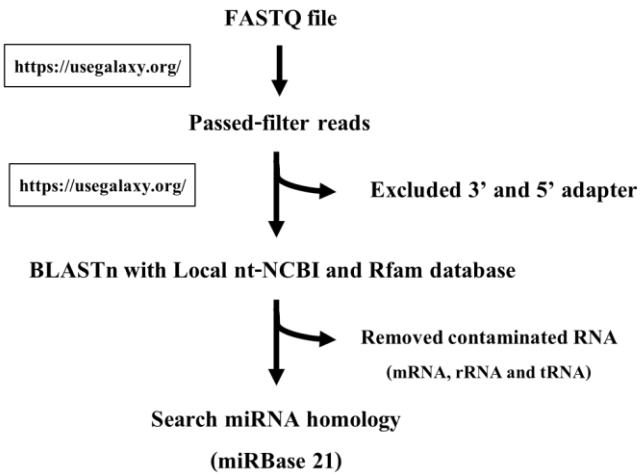

Figure 2.1. Small RNA data analysis workflow.

2.2.2 Stem-loop quantitative Real-time PCR analysis

The miRNAs of interest consisted of lva-miR-7170-5p, lva-miR-2169-3p, lva-miR-184, lva-miR-92b-5p, lva-miR-317, lva-miR-92a-3p, lva-miR-4901, lva-miR-61, lva-miR-2898, and lva-miR-6090, which were selected for expression analysis using stem-loop qRT-PCR. Pooled total small RNA from both VP_{AHPND}-infected, NLHS-treated, and control shrimp hemocyte at 0, 6, and 24 hpi was prepared using the mirVana miRNA Isolation Kit (Ambion, Life technologies). Extracted total small RNA was then used as a template for first-strand stem-loop cDNA synthesis. The stem-loop primer (Table 2.1) (CDS-3M primer: 5′-AAGCAGTGGTATCAACGCAGAGTGGCCGAGGCGGCCTTTTTTTTTTTTTTTTTTVN-3′) was used to synthesize first-strand cDNA using the RevertAid First-strand cDNA Synthesis Kit (Thermo Fisher Scientific). U6 gene expression was used as internal control. Stem-loop qRT-PCR was performed using an appropriate amount of cDNA for each gene, specific oligonucleotide primers (Table 2.1), and QPCR Green Master Mix (Biotechrabbit) in the MiniOpticon™ Real-time PCR System (Bio-Rad) under the following conditions: 95 °C for 3 min, 40 cycles of 95 °C for 30 s, 60 °C for 30 s, and 72 °C for 30 s. Relative expression was calculated and data were analyzed using a paired-samples t-test, with data being presented as mean ± standard deviation. Statistical significance was considered at $P < 0.05$. The experiment was performed in triplicate.

Table 2.1 Primers used for qRT-PCR in stem-loop qRT-PCR

miRNA name	Primer name	Sequence
lva-miR-61	miR-61-F	GGGGTGACTAGACTCTTAC
	miR-61_RT	GTTGGCTCTGGTGCAGGGTCCGAGGTATTCGCACCAGAGCCAACAGATGA
lva-miR-184	miR-184-F	GTTGTGGACGGAGAACTGA
	miR-184_RT	GTTGGCTCTGGTGCAGGGTCCGAGGTATTCGCACCAGAGCCAACCCCTTA
lva-miR-4901	miR-4901-F	GTTGGGGGTAACTTATTTTTGG
	miR-4901_RT	GTTGGCTCTGGTGCAGGGTCCGAGGTATTCGCACCAGAGCCAACGTTTGT
lva-miR-92a-3p	miR-92a-3p-F	GTTTTCGTCTCGTGTCTCG
	miR-92a-3p_RT	GTTGGCTCTGGTGCAGGGTCCGAGGTATTCGCACCAGAGCCAACCTAAGG
lva-miR-7170-5p	miR-7170-5p-F	GTTGAACTGGAGGACCGAA
	miR-7170-5p_RT	GTTGGCTCTGGTGCAGGGTCCGAGGTATTCGCACCAGAGCCAACAGTCGG
lva-miR-317	miR-317-F	GTTGAACACAGCTGGTGGT
	miR-317_RT	GTTGGCTCTGGTGCAGGGTCCGAGGTATTCGCACCAGAGCCAACTGAGAT
lva-miR-92b-5p	miR-92b-5p-F	TTGTGGGGACGAGAAGCG
	miR-92b-5p_RT	GTTGGCTCTGGTGCAGGGTCCGAGGTATTCGCACCAGAGCCAACAAGCAC
lva-miR-2169-3p	miR-2169-3p-F	GTTTGATTTAAAGTGGTACGCG
	miR-2169-3p_RT	GTTGGCTCTGGTGCAGGGTCCGAGGTATTCGCACCAGAGCCAACCCAGCT
lva-miR-2898	miR-2898-F	TTGGGGTGGTGGAGATGC
	miR-2898_RT	GTTGGCTCTGGTGCAGGGTCCGAGGTATTCGCACCAGAGCCAACTACCCC
lva-miR-6090	miR-6090-F	TTGTTGGACTGGGCGAGG
	miR-6090_RT	GTTGGCTCTGGTGCAGGGTCCGAGGTATTCGCACCAGAGCCAACTGGCCG
Universal primer		GTGCAGGGTCCGAGGT
U6	U6-qRTF	GTACTTGCTTCGGCAGTACATATAC
	U6-qRTR	TGGAACGCTTCACGATTTTGC

2.2.3 miRNA target prediction

The miRNA targets were identified by comparing with transcriptome data using CU-mir software that was previously developed by our research group (Kaewkascholkul et al., 2016) This software searched for locations on mRNA targets that seed sequences (2-8 nucleotides from 5′ end) of miRNA and can bind with perfect complementary or 1 mismatch at identified seed sequences. Percent complementary is calculated from the number of nucleotides that perfectly match the target mRNAs per total length of miRNA sequences. The percent complementarily cutoff was set at 55%. RNAhybrid (http://bibiserv.techfak.uni-bielefeld.de/rnahybrid/) was also used to predict genes targeted by miRNAs with the parameters of free energy < −15.0 kcal/mol (Kaewkascholkul et al., 2016).

2.2.4 miRNA/mRNA interaction network analysis

In order to define all possible miRNA-mRNA interactions involved in a specific dataset of immune-related genes, a miRNA-mRNA interaction network was constructed. Immune responsive genes from the transcriptome were specifically chosen for inclusion in the integrated analysis of the miRNA/mRNA network. The differentially expressed miRNAs from shrimp challenged with VP_{AHPND} under NLHS were used to identify mRNA targets and to construct the miRNA/mRNA network. Again, the binding of target mRNAs of differentially expressed miRNAs were predicted using RNAhybrid with the parameters of free energy < −15 k cal/mol. These target mRNAs were mapped against our RNA-Seq data to determine their immune-related functions.

2.2.5 Dual-luciferase reporter assay

The luciferase reporter system was used in order to confirm the interaction between miRNAs of interest and their target genes. The lva-miR-4850 was predicted to target PO2 that was also of interest. Gene-specific primers for target mRNA amplification were designed. The PO2 sequence at 3′UTR containing the predicted lva-miR-4850 target site were amplified from the cDNA of the VP_{AHPND} *P. vannamei* hemocyte. The PCR products of each target sequence were cloned into pmiRGLO plasmid (Promega) producing pmirGLO-PO2 plasmid.

To construct the experimental control, the binding element at position 2-8 nucleotide was mutated by using QuikChange II XL Site-Directed Mutagenesis Kit (Agilent Technology). Briefly, the primers were designed by switching the bases of a seed sequence from purine to

pyrimidine or pyrimidine to purine with a melting temperature (Tm) of ≥78 °C. Then, the recombinant pmiRGLO-PO2 was amplified by *PfuUltra* HF DNA polymerase and then, the PCR product was treated with *Dpn*I restriction enzyme. The treated PCR product was transformed into *E. coli* Top10. The mutant plasmids were then randomly chosen and sequenced.

After validating the sequences, 200 ng of plasmids were co-transfected into HEK293-T cells along with 20 pmol of lva-miR-4850 mimic (5′-AUAACAUGACUGAAAACAUUU-3′) (GenePhama) or miR-4850 scramble (5′-GUUAAUACCUAAGAUAUACAA-3′) (GenePhama) using the Effectene transfection reagent (Qiagen). After 48 h post transfection, the luciferase activity of Firefly and Renilla luciferases were measured by the Dual-Luciferase® Reporter assay system (Promega) following the manufacturer's instructions. Three independent experiments were performed. GraphPad Prism 6.0 software was used for statistical analyses including a paired-samples t-test, with data presented as means ± standard deviations.

2.2.6 Functional analysis of lva-miR-4850 in *P. vannamei* upon VP_{AHPND} infection

2.2.6.1 Mimic, scramble mimic, anti-miRNA oligonucleotide (AMO), and AMO scramble

To investigate whether lva-miR-4850 is involved in the prophenoloxidase system of shrimp, *in vivo* RNAi experiments were performed. The mimic, scramble mimic, anti-miRNA oligonucleotide (AMO), and AMO scramble RNA of lva-miR-4850 were synthesized by Shanghai GenePharma Co., Ltd., P.R. China (Table 2.2).

Table 2.2 Mimic, scramble mimic, anti-miRNA oligonucleotide (AMO), and AMO scramble RNA sequences

Gene	Name	Sequence	
		Sense (5'-3')	Antisense (5'-3')
Lva-miR-4850	Mimic	AUAACAUGACUGAAAACAUUU	AUGUUUUCAGUCAUGUUAUUU
	Scramble mimic	GUUAAUACCUAAGAUAUACAA	GUAUAUCUUAGGUAUUAACUU
	AMO	AAAUGUUUUCAGUCAUGUUAU	
	AMO scramble	GAUUUAUCCAUAUUGAUUAGU	

2.2.6.2 *In vivo* lva-miR-4850 Introducing and silencing in shrimp

Shrimp (2-3 g) were divided into five groups of three individuals each. Experimental shrimp were intramuscularly injected with 50 µl of 0.85% NaCl solution containing 2 nmole of mimics-lva-miR-4850 or AMO-lva-miR-4850, while the control group was injected with 2 nmole of scrambler mimics-lva-miR-4850 or AMO-lva-miR-4850 scramble or 50 µl of 0.85% NaCl. After 24 h post injection, VP_{AHPND} was challenge as described in Section 2.3. At 24 h post challenge, shrimp hemolymph was collected. Total RNA was extracted and used for first-strand cDNA production. The expression levels of lva-miR-4850 and *PO2* were determined by qRT-PCR.

On the other hand, stomach and hepatopancreas were individually collected from 3 shrimp per group, crushed, and serially 10-fold diluted in sterile 0.85% NaCl. The diluted hemolymph samples (at 10^{-1} to 10^{-6} fold) were dropped onto TCBS agar and incubated at 30 °C for 12-14 h. The bacterial colonies were then counted and calculated as CFU/ml. All experiments were performed in triplicate, and statistical analyses were performed using one-way ANOVA followed by Duncan's new multiple ranges test and presented as means ± standard deviations. Statistical significance was set at $P < 0.05$.

2.2.6.3 Phenoloxidase activity assay

Phenoloxidase (PO) activity was determined in the hemolymph of VP_{AHPND}- infected shrimp. The shrimp hemolymph from each siRNA-injected group (as described in Section 2.24.3) were collected at 24 h post VP_{AHPND} infection. PO activity was measured using a method modified from Sutthangkul et al. (2017). Briefly, 50 µl of hemolymph was mixed with 25 µl of 3 mg/mL freshly prepared L-3, 4-dihydroxyphenylalanine (L-DOPA; Fluka), and 25 µL of 20 mM Tris-HCl (pH 8.0). The absorbance at 490 nm was monitored. The amount of hemolymph proteins was measured using the Bradford method. PO activity was recorded as A_{490}/mg total protein/min.

2.3. Functional characterization of miRNAs in WSSV-infected *P. monodon*

2.3.1. Shrimp and WSSV

Healthy black tiger shrimp, *P. monodon*, of about 3-5 g and 15-20 g in size were purchased from a farm in Surat Thani Province, Thailand. Due to the Ethical Principles and Guidelines for the use of animals for scientific purposes by the National Research Council of Thailand, this project was conducted according to the animal use protocol number 1823006

approved by the Chulalongkorn University Animal Care And Use Committee (CU-ACUC). The animals were reared in laboratory tanks at ambient temperature, and maintained in aerated water with a salinity of 15 ppt for at least 7 days before use. The WSSV stock used for the experimental infection was prepared according to the method described by Xie and Yang (2005) and stored at -80 °C until used. One microliter of WSSV stock was 10-fold serially diluted with 0.85% NaCl to 10^{-7} dilution. The diluted WSSV of 50 µL was injected into the second abdominal segment of the shrimp. The mortality was recorded daily. This dosage caused 100% mortality within 3-4 days after injection and was used for all subsequent viral infection experiment. This project has been reviewed and approved by the CU-IBC (Approval number: SCI-01-001) to be in accordance with the levels of risk in pathogens and animal toxins listed in the Risk Group of Pathogen and Animal Toxin (2017) published by the Department of Medical Sciences, Ministry of Public Health, the Pathogen and Animal Toxin Act (2015) and Biosafety Guidelines for Modern Biotechnology, BIOTEC (2016).

2.3.2. Pmo-miR-315 mimic and its scramble miRNA

The mimic microRNAs used in this research were synthesized by a commercial service GenePharma (Shanghai). The sequences of mimic pmo-miR-315 and pmo-miR-315 scramble were 5′-UUUUGAUUGUUGCUCAGAAG-3′ and 5′-GUGGUUAGCGUUAAUUCUAU-3′, respectively. The sequences of miR-315 inhibitor (AMO-miR-315) and miR-315 inhibitor scramble were 5′-CUUCUGAGCAACAAUCAAAA-3′ and 5′-ACGAACCUACGAUAAUAAUC-3′.

2.3.3. Pmo-miR-315 expression in WSSV-infected shrimp tissues

The expression of pmo-miR-315 in various shrimp tissues including hemocytes, gill, lymphoid organ and stomach of WSSV-infected *P. monodon* was determined by stem-loop quantitative real time RT-PCR (qRT-PCR). The pooled total RNA of each tissue from 3 WSSV-infected individuals at 0, 6, 24 and 48 hpi was prepared using mirVana miRNA Isolation Kit (Life Technologies) and 1 µg was used as templates for the first strand stem-loop cDNA synthesis using Superscript III Reverse Transcriptase (Invitrogen). The qPCR was performed using SsoFast™ EvaGreen® Supermix (Bio-Rad) on CFX96 touch real-time PCR detection system (Bio-Rad), where each sample was analyzed in triplicate. The amplification condition was 98 °C for 2 min, followed by 40 cycles of 95 °C for 5 sec and 60 °C for 30 sec. A non-coding small nuclear RNA, U6, was used as a reference. The primer sequences for stem-loop cDNA synthesis, pmo-miR-315: RT-

pmo-miR315_F and RT-pmo-miR315_R, and for U6: RT-U6-F and RT-U6-R, are shown in Table 2.3. The miRNA relative expression level was calculated using the equation by Pfaffl, 2001. In addition, the expression of the target mRNA of pmo-miR-315, a putative prophenoloxidase-activating enzyme (*Pm*PPAE3), was determined in hemocytes of shrimp infected with WSSV at 0, 6, 24, and 48 hpi. The total RNA from hemocytes of 3 individuals was reverse-transcribed into the first strand cDNA using oligo (dT) as a primer following the manufacturer's instruction for RevertAid First Strand cDNA Synthesis Kit (Thermo scientific). Quantitative real-time PCR was performed as described previously using *EF-1*α gene as an internal control.

2.3.4 Specificity and inhibitory activity of pmo-miR-315 on target *Pm*PPAE3 mRNA

First, the pmirGLO vector (Promega) harboring the 200 bp *Pm*PPAE3 gene fragment that contained the pmo-miR-315 binding region (Figure 2A) was constructed. The *PmPPAE3* gene fragment was PCR amplified from *P. monodon* hemocyte cDNAs using the gene specific primers, pmirG_*Pm*PPAE_F and pmirG_*Pm*PPAE_R (**Table 2.3**), digested with *Sac*I and *Xba*I (New England Biolabs), cloned into the likewise double digested pmirGLO, and transformed into an *Escherichia coli* stain XL1-blue. The recombinant plasmid, pmir-T315, was extracted and sequenced to confirm the correctness of the sequences (Macrogen, Korea).

To investigate the inhibitory activity of pmo-miR-315 on the *PmPPAE3* gene target sequence, dual-luciferase activity assay was performed. The HEK293T cell culture of 8×10^4 cells/well was seeded into a 24-well plate. At 24 h after seeding, 200 ng of pmir-T315 and 20 pmole of mimic miRNA (pmo-miR-315 or scramble) were co-transfected into the HEK293T cells using the Effectene® transfection reagent (Qiagen). The luciferase activity was measured using Dual-luciferase® Reporter Assay System (Promega) at 48 h post transfection. The control cells were transfected with pmir-T315 alone and co-transfected pmir-T315 with mimic miRNA scramble.

Table 2.3 Primer used in this study

Primer name	Sequence (5′ - 3′)
Stem-loop pmo-miR-315	GTCGTATCCAGTGCAGGGTCCGAGGTATTCGCACTGGATACGACGGGATA
RT-pmo-miR315_F	CGGGCGTTTTGATTGTTGCTCAG
RT-pmo-miR315_R	CCAGTGCAGGGTCCGAGGTA
RT-U6-F	CTCGCTTCGGCAGCACA
RT-U6-R	AACGCTTCACGAATTTGCGT
RT-PmPPAE3-F	GGACGAGTGCCAGTTCAACA
RT-PmPPAE3-R	GGTCGTTGTGGTGGTGGTCACT
RT-EF1α-F	GGTGCTGGACAAGCTGAAGGC
RT-EF1α-R	CGTTCCGGTGATCATGTTCTTGATG
knPPAE3-F	CAACATTGCCGGACTGCCTA
knPPAE3-R	GGCAGAAGCACGACACGAAC
knPPAE3-T7-F	TAATACGACTCACTATAGGCAACATTGCCGGACTGCCTA
knPPAE3-T7-R	TAATACGACTCACTATAGGGGCAGAAGCACGACACGAAC
knGFP-F	ATGGTGAGCAAGGGGGAGGA
knGFP-R	TTACTTGTACAGCTCGTCCA
knGFP-T7-F	GGATCCTAATACGACTCACTATAGGATGGTGAGCAAGGGGGAGGA
knGFP-T7-R	GGATCCTAATACGACTCACTATAGGTTACTTGTACAGCTCGTCCA
pmirG_PmPPAE3_F	CTAGCGAGCTCCCAACGACCAGTAGGCCTGTGA
pmirG_PmPPAE3_R	CTAGCTCTAGAGGCAGAAGCACGACACGAA
VP28-140Fw	AGGTGTGGAACAACACATCAAG
VP28-140Rv	TGCCAACTTCATCCTCATCA
pri-PmPPAE3	GGTCGTTGTGGTGGTGGTCACT
nested PmPPAE3	TCCTGACATCCTCCGTTGTTGCTCAC

2.3.5 Introducing and silencing of pmo-miR-315 in WSSV-infected *P. monodon*

To confirm the inhibitory effect of pmo-miR-315 on the *PmPPAE3* target gene expression in shrimp after WSSV infection, the exogenous pmo-miR-315 mimic and anti-pmo-miR-315 (AMO-miR-315) were introduced into the WSSV-infected shrimp and the expression levels of pmo-miR-315 and target gene were quantified.

To study the effect of pmo-miR-315 *in vivo*, the exogenous pmo-miR-315 was introduced into the shrimp by injection. For pmo-miR-315 silencing, the AMO-miR-315 was injected into the shrimp. In these experiments, shrimp were divided into five groups of three individuals each. The first group was injected with 0.85% NaCl used as an injection control. The miRNA and AMO control groups were shrimp injected with scramble miRNA or scramble AMO-miR-315, respectively. The two test groups were shrimp injected with pmo-miR-315 mimic or AMO-miR-315. At 2 h after the first injection, all groups were muscularly injected with WSSV. After 48 h post-WSSV infection, shrimp hemolymph was collected. The total RNA was extracted and used for the first-strand cDNA production. The expression level of pmo-miR-315 and putative *PmPPAE3* was determined by qRT-PCR.

2.3.6 Analysis of WSSV copy number in shrimp overexpressing pmo-miR-315 using qRT-PCR

To study the effect of pmo-miR-315 and on WSSV replication, the WSSV copy number was also investigated according to a method described by Mendoza-Cano and Sánchez-Paz (2013). The genomic DNA of WSSV-infected shrimp hemocytes was extracted using a FavorPrep™ Tissue Genomic DNA Extraction Mini Kit (Favorgen). The quantity and quality of genomic DNA was determined by NanoDrop 2000c spectrophotometer (Thermo Sciencetific) and 1.2 % agarose gel electrophoresis.

The qRT-PCR was performed in triplicates of 10 μL reaction containing 5 μL Luna® Universal qPCR Master mix (New England Biolabs) and 1.5 μL genomic DNA template (10 ng/μL) and 250 nM VP28-140Fw and VP28-140Rv (**Table 2.3**). The amplification condition was 98 °C for 2 min, followed by 40 cycles of 95 °C for 5 sec and 61 °C for 30 sec. The plasmid containing a highly conserved region of the WSSV *VP28* gene, was used to generate a standard curve for the determination of WSSV copy number.

2.3.7 Phenoloxidase activity assay in shrimp silencing/overexpressing pmo-miR-315 using qRT-PCR

The phenoloxidase (PO) activity was determined in the hemolymph of WSSV- infected shrimp. The shrimp hemolymph was collected at 48 h post WSSV infection and the PO activity was measured using a method modified from Sutthangkul et al. (2017). Briefly, 50 μL of hemolymph was mixed with 25 μL of 3 mg/mL freshly prepared L-3, 4-dihydroxyphenylalanine (L-DOPA; Fluka) and 25 μL of 20 mM Tris -HCl pH 8.0. The absorbance at 490 nm was monitored. The amount of hemolymph proteins was measured by the Bradford method (Bradford et al, 1976) (Bradford 1976). The PO activity was recorded as A_{490}/mg total protein/min.

2.3.8 Identification of *Pm*PPAE3

According to our previous report on pmo-miR-315 target prediction (Kaewkascholkul et al, 2016), the partial nucleotide sequence of *PmPPAE3* was obtained from *P. monodon* EST database. To identify the full-length cDNA, the 5′-RACE was performed using a SMARTer™ RACE cDNA Amplification Kit (Clontech, USA) according to the manufacturer's instructions. The specific primers of partial putative *PmPPAE3* gene were designed, which are pri-*Pm*PPAE3 and nested *Pm*PPAE3 (**Table 2.3**). The primary and nested-PCR were used to amplify the 5′-RACE cDNA library using Advantage® 2 polymerase mix (Clontech). The PCR product was analyzed by 1.2% agarose gel electrophoresis. The nested PCR product was purified and cloned into the pGEM-T easy vector (Promega) and transformed into *E. coli* XL1-blue. The positive clone was selected and sequenced by a commercial service (Macrogen, Korea). The 5'-RACE *PmPPAE3* nucleotide sequence was analyzed and combined with the starting *PmPPAE3* sequence from the EST library. The full-length cDNA of putative *PmPPAE3* was analyzed using a Blast program (http://www.ncbi.nlm.nih.gov/BLAST/). The open reading frame and the encoded amino acid sequence were predicted using ExPASy software (http://web.expasy.org/translate/). The putative signal peptide cleavage site was predicted by SignalP 4.1 server (http://www.cbs.dtu.dk/services/SignalP/). Moreover, the structural protein domains were analyzed by a simple modular architecture research tool program (SMART) (http://smart.embl-heidelberg.de/).

Multiple amino acid sequence alignment was performed using the Clustal Omega program (http://www.ebi.ac.uk//Tools/msa/clustalo/). The deduced amino acid sequence of *Pm*PPAE3 was aligned with other insect and crustacean PPAEs including *Bombyx mori* PO-

activating enzyme (*Bm*PAE: NP_001036832.1); *Manduca sexta* proPO-activating proteinase 1 (*Ms*PAP1: AF059728), *Holotrichia diomphalia* proPO-activating factor I (*Hd*PPAFI: AB013088), *Glossina morsitans* (*Gm*PPAE: ABC84592) and *Drosophila melanogaster* melanization protease1 (*Dm*MP1: NM141193); *P. monodon* proPO-activating enzyme 1, 2 and 3 (*Pm*PPAE1: FJ595215, *Pm*PPAE2: FJ620685, *Pm*PPAE3: MH325330), *P. vannamei* proPO-activating enzyme (*Lv*PPAE: AFW98991.1), *F. chinensis* proPO-activating enzyme (*Fc*PPAE: AFW98985.1) and *Pacifastacus leniusculus* proPO-activating enzyme (*Pl*PPAE: AJ007668). An unrooted phylogenetic tree was constructed by the neighbor-joining method based on the amino acid sequences using MEGA 7 software (Kumar et al, 2016). The bootstrap sampling was reiterated 1000 times.

2.3.9 Tissue distribution analysis of *Pm*PPAE3 gene

The *PmPPAE3* gene expression in various tissues including hemocytes, gill, lymphoid organ, and stomach of healthy unchallenged *P. monodon* was analyzed by semi-quantitative RT-PCR. The total RNA of each tissue was extracted by Tri reagent (Geneaid) and used for the first-strand cDNA synthesis using RevertAid First Strand cDNA Synthesis Kit (Thermo Scientific). The PCR reaction was performed using the *PmPPAE3* specific primer pair (**Table 2.3**) and the *EF-1α* was used as an internal control. The expression profile was analyzed by 1.5% agarose gel electrophoresis.

2.3.10 Effect of *Pm*PPAE3 gene silencing on PO activity in shrimp

The function of *Pm*PPAE3 in shrimp was characterized using a RNA interference technique. The *PmPPAE3* DNA template was amplified from normal shrimp cDNA with gene specific primers (knPPAE3-F, knPPAE3-R, knPPAE3-T7-F and knPPAE3-T7-R) as shown in **Table 2.3**. In addition, the dsRNA of the green fluorescent protein (*GFP*) as the negative control, was prepared from the pEGFP-1 vector (Clontech) using the knGFP-F, knGFP-R, knGFP-T7-F, and knGFP-T7-R (**Table 2.3**). The *PmPPAE3*-dsRNA- and GFP-dsRNA were prepared using T7 RiboMAX™ Express Large Scale RNA Production System (Promega) according to the manufacturer's instruction. The *P. monodon* of approximately 3 g body weight were divided into two groups of three individuals each. The first (control) group was injected with 5 μg/g shrimp of *GFP*-dsRNA, whilst the second group, the *PmPPAE3* knockdown, was injected with 5 μg/g shrimp *PmPPAE3*-

dsRNA. The hemolymph of individual shrimp was collected at 48 h post injection. Then, the expression level of *PmPPAE3* gene and also the PO activity were measured as described above.

2.3.11 Statistical analysis

All experiments were performed in triplicate. One-way ANOVA with Duncan's multiple range test was used to identify statistically significant differences with SPSS software (version 17.0). Data are presented as means ± 1 standard deviations of three biological replications. The statistical significance of differences among means was calculated by the paired-samples t-test where the significance was accepted at the *P*-value < 0.05.

3. Results

3.1 Integrated analysis of miRNA and mRNA expression in hemocytes of *P. vannamei* challenged with VP_{AHPND} under heat stress conditions

3.1.1 Effect of NLHS on shrimp survival upon VP_{AHPND} challenge

Herein, we had confirmed that shrimp treating with NLHS prior to VP_{AHPND} infection showed significantly higher survival rate than the non-heat control, as previously demonstrated by Jungprung et al. (2017). This survival experiment was set-up by dividing shrimp into 4 groups of no heat treatment control (NH), NLHS control (NLHS), VP_{AHPND} challenge (NH-VP), and NLHS plus VP_{AHPND} challenge (NLHS-VP) (Figure 3.1). For the NLHS treatment, shrimp were placed in tanks with a temperature of 38 °C for 5 min daily for 7 days and allowed to recover in control tanks at ambient temperature without any disturbance for 3 days. No mortality was observed until the end of the experiment in heat treatments without any VP_{AHPND} challenge. With VP_{AHPND} challenge, the survival rates were reduced and there was significantly different between the NH-VP (24.53%) and NLHS-VP (58.33%) groups based on Log-rank test indicating a possible modulation of the shrimp immune system to tolerate or fight against bacterial infection.

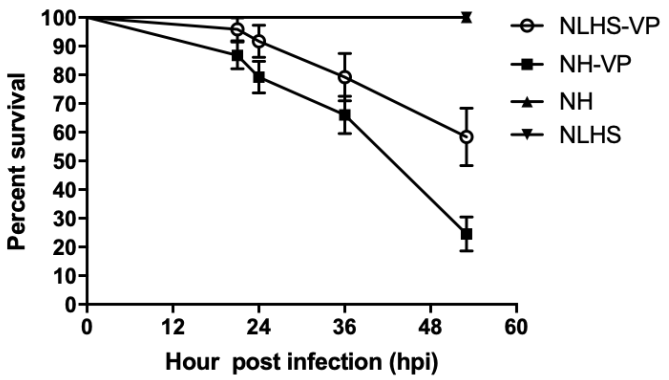

Figure. 3.1. Effect of chronic non-lethal heat stress on the survival of VP_{AHPND}-challenged shrimp. Shrimp were stressed under NLHS condition or reared normally under NH condition. After 3 days recovery time, the NLHS (○) and NH (■) treated shrimp were challenged with VP_{AHPND}. The NLHS (▼) and NH (▲) treated shrimp immersed with 1.5% NaCl were used as controls. Shrimp survival was observed every 6 h post-infection for 53 h. The experiment were performed in triplicate and the survival percentage was calculated as mean ± 1 standard error (S.E.) at each time point.

3.1.2. Gene expression profiling in *P. vannamei* hemocytes under NLHS condition

The hemocytes from 30 individuals each of NH-VP and NLHS-VP groups were collected at 0, 6, and 24 h after the bacterial challenge, pooled and subjected to cDNA library construction. The experiment was done in triplicate for a total of 18 cDNA libraries that were subjected to Illumina Sequencing in the Next-Seq 500 (Table 3.1). Two sequencing runs, each with 10 normalized libraries pooled into 1, had an average %Q30 of 81.975% and a sequence range of 30-151 bp. Total raw single-pass reads for all the libraries amounted to 400,232,814 reads, which were reduced to 399,998,390 reads after additional adapter trimming, quality filtering and size selection (50-151 bp). Each library had an average number of filtered reads of 22,222,133. Sequencing reads were deposited in the Short Read Archive (SRA) of the National Centre for Biotechnology Information (NCBI), and can be accessed using accession numbers: SRR3993813, SRR3997616, SRR3997617, SRR3997618, SRR3997619, SRR3997620, SRR3997621, SRR3997622, SRR3997623, SRR3997631, SRR3998867, SRR3998869, SRR3998870, SRR3998871, SRR3998872, SRR3998873, SRR3998874, and SRR3998992.

All clean reads were concatenated and subjected to *de novo* assembly using Trinity, which generated 174,835 putative genes or 205,137 isotigs. This reference assembly has an N50

isotig length of 1,074 and an isotig length ranging from 201 bp to 22,966 bp (Table 3.2). The isotigs/transcripts were annotated by searching their sequences using BLASTX against Swiss-Prot, GO, Cluster of Orthologous Groups (COG) and KEGG Pathway databases. The 47,401 (or 23.11%) sequences had significant hits (E-value ≤ 10^{-5}) to the Swiss-Prot database and the majority of these sequences were homologous to *Homo sapiens* (26.54%), *Mus musculus* (16.77%) and *Drosophila melanogaster* (13.55%) genes (Figure 3.2A). The 184,422 level 2 gene ontologies (Figure 3.2B) had been mapped using BLAST2GO, while the 11,350 sequences were categorized in COGs (Figure 3.2C). The 33,475 sequences were successfully mapped to KEGG orthology but only 20,183 were grouped into the reference pathways. The metabolic pathways, biosynthesis of secondary metabolites and biosynthesis of antibiotics were among the top 20 KEGG pathways (Figure 3.2D) represented in the transcriptome assembly.

3.1.3 Differentially expressed genes (DEGs) in NLHS-treated *P. vannamei* upon VP_{AHPND} challenge

The differentially expressed genes (DEGs) in NLHS-treated *P. vannamei* upon VP_{AHPND} challenge were identified by pairwise comparisons among the relevant groups of 3 biological replicates and expressed as fold changes against a specific group. (Table 3.3). Between the 0 NH-VP and 6 NH-VP, 14 transcripts were differentially expressed and 8 of these are significantly upregulated ($P < 0.05$) in 6 NH-VP. The gene, identified as *P. vannamei* Relish small isoform gene (FJ416145), had the highest upregulation (8.5-fold) in this particular comparison. Between the 0 NH-VP and 24 NH-VP, 78 transcripts were differentially expressed, and 68 transcripts were upregulated in 24 NH-VP group. The Relish small isoform gene was also upregulated in this group (7.7-fold) together with *P. monodon* triosephosphate isomerase gene homolog (7.4-fold). Between the 0 NLHS-VP vs 6 NLHS-VP, 52 transcripts were differentially expressed, and 43 transcripts were significantly upregulated in the 6 NLHS-VP group. The gene homolog of lipoprotein aminopeptidase is 5.3-fold upregulated in the 6 NLHS-VP group as well as 6 NH-VP and 24 NH-VP groups (3.9- and 3.7-fold, respectively). Between the 0 NLHS-VP and 24 NLHS-VP, 7 transcripts were upregulated in the 24 NLHS-VP group out of 11 differentially expressed genes.

Table 3.1 Number of sequences obtained from RNA-Seq in each cDNA library of *P. vannamei* hemocytes after NH or NLHS treatment and VP_{AHNPD} infection.

ID	Condition	Time Point)hpi(	Replicate No.	Number of reads
0NH-VP	non-heat	0	replicate 1	24,914,546
0NH-VP	non-heat	0	replicate 2	18,790,695
0NH-VP	non-heat	0	replicate 3	20,783,002
6NH-VP	non-heat	6	replicate 1	22,850,301
6NH-VP	non-heat	6	replicate 2	23,616,635
6NH-VP	non-heat	6	replicate 3	22,809,007
24NH-VP	non-heat	24	replicate 1	23,665,724
24NH-VP	non-heat	24	replicate 2	23,782,913
24NH-VP	non-heat	24	replicate 3	23,155,408
0 NLHS-VP	heat	0	replicate 1	23,480,445
0 NLHS-VP	heat	0	replicate 2	20,214,421
0 NLHS-VP	heat	0	replicate 3	21,731,765
6 NLHS-VP	heat	6	replicate 1	24,793,063
6 NLHS-VP	heat	6	replicate 2	21,750,763
6 NLHS-VP	heat	6	replicate 3	20,503,721
24 NLHS-VP	heat	24	replicate 1	21,347,015
24 NLHS-VP	heat	24	replicate 2	20,746,438
24 NLHS-VP	heat	24	replicate 3	21,296,952
Total				400,232,814

Table 3.2 Trinity assembly statistics of RNA-Seq of *P. vannamei* hemocytes after NH or NLHS treatment and VP_{AHPND} infection.

Statistics for isotig lengths:	**Value**
Min isotig length:	201
Max isotig length:	22,966
Mean isotig length:	672.14
Median isotig length:	357
N50 isotig length:	1,074
Statistics for numbers of isotigs:	
Total trinity 'genes':	174,835
Number of isotigs:	205,137
Number of isotigs >=1kb:	31,106
Number of isotigs in N50:	28,762
Statistics for bases in the isotigs:	
Number of bases in all isotigs:	137,880,518
Number of bases in isotigs >=1kb:	71,369,224
GC Content of isotigs:	41.32%

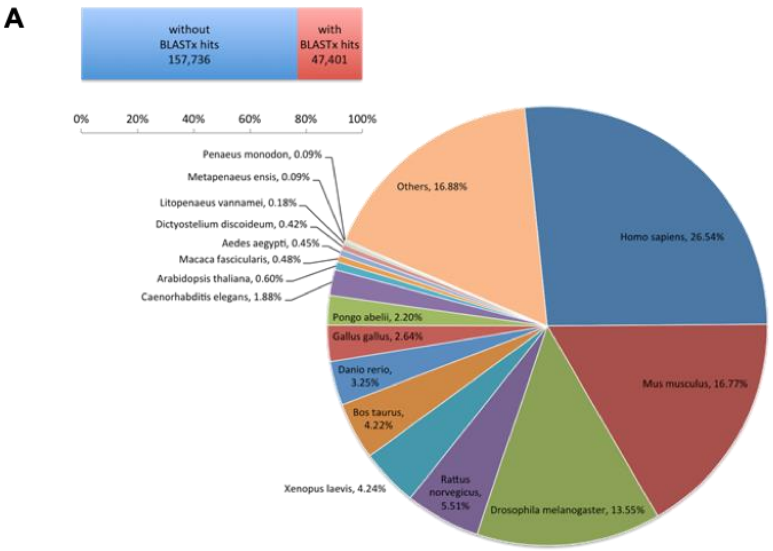

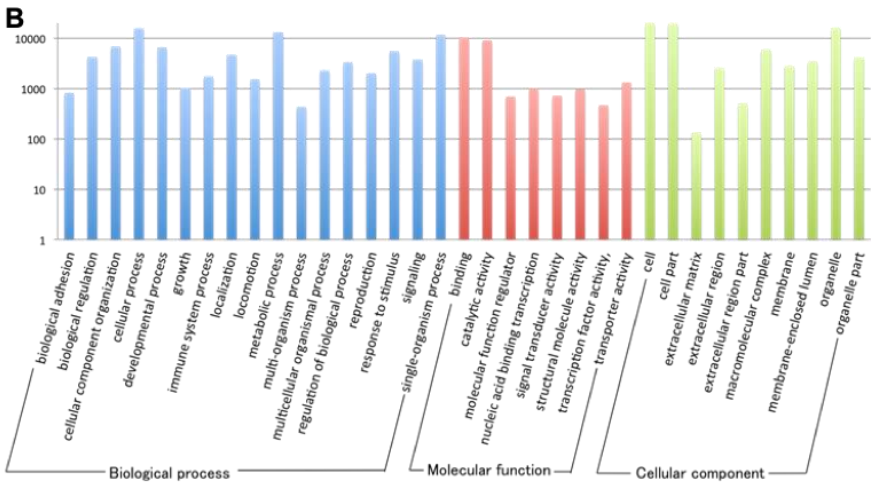

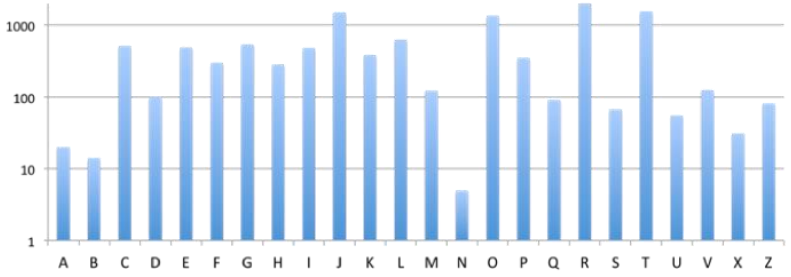

A RNA processing and modification
B Chromatin structure and dynamics
C Energy production and conversion
D Cell cycle control, cell division, chromosome partitioning
E Amino acid transport and metabolism
F Nucleotide transport and metabolism
G Carbohydrate transport and metabolism
H Coenzyme transport and metabolism
I Lipid transport and metabolism
J Translation, ribosomal structure and biogenesis
K Transcription
L Replication, recombination and repair
M Cell wall/membrane/envelope biogenesis
N Cell motility
O Post-translational modification, protein turnover, chaperones
P Inorganic ion transport and metabolism
Q Secondary metabolites biosynthesis, transport and catabolism
R General function prediction only
S Function unknown
T Signal transduction mechanisms
U Intracellular trafficking, secretion, and vesicular transport
V Defense mechanisms
W Extracellular structures
X Mobilome: prophages, transposons
Y Nuclear structure
Z Cytoskeleton

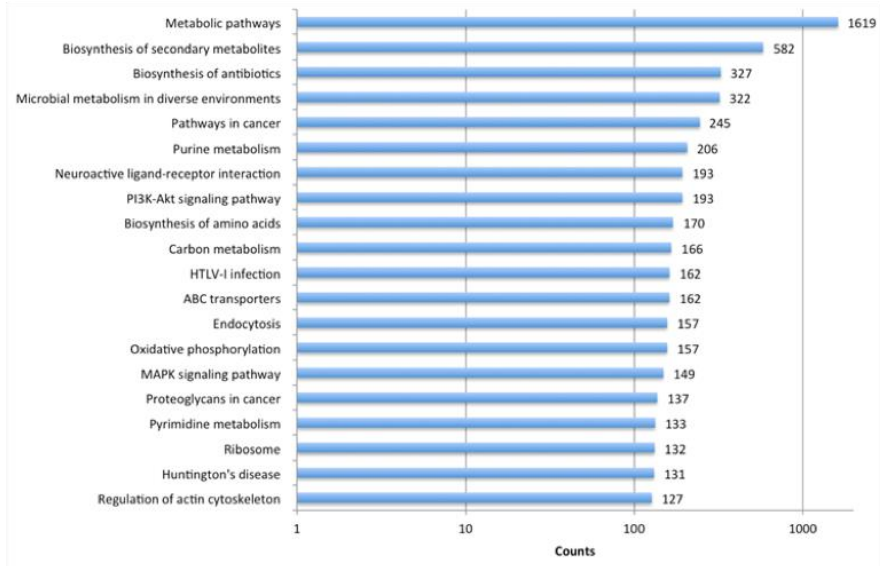

Figure 3.2. Sequence analysis and functional annotation of assembled unigenes. Number of BLAST hits in the reference transcriptome and sequence distribution in different organisms (A), gene ontologies (GO level 2) with specific hits to the reference assembly sequences (B), number of sequences in the transcriptome assembly that are mapped according to the Cluster of Orthologous Group (C), and top 20 KEGG Pathways mapped in the assembly (D) are shown.

Regardless of the time points post VP_{AHPND} challenge, a total number of NLHS-VP responsive transcripts was 3,980 genes and that of NH-VP responsive transcripts was 3,141 genes. A Venn diagram was used to highlight specific groupings of DEGs (Figure. 3.6A). A grouping of 2,664 DEGs were considered as the NLHS-VP responsive transcripts only while another grouping of 1,825 DEGs were the NH-VP responsive transcripts only. Their intersection of 1,316 DEGs were expressed in response to VP_{AHPND} infection whether or not the shrimp were treated with NLHS. In the future work, it will be interested to further analyze the DEGs that are specifically found in the NLHS-VP group to broaden the knowledge on how the NLHS enhance the shrimp immune response against VP_{AHPND} infection.

The specific NLHS-VP responsive transcripts were annotated using the NCBI Genbank database through blastx and mapped against available shrimp transcript databases to identify immune-related genes. Some of the identified immune-related genes include: *prophenoloxidase 1* (*PO1*) and *prophenoloxidase 2* (*PO2*) in the proPO system, *ALF-AAK*, *penaeidin 4a* and *AMP type2* in AMP production system, and *tranglutaminase* and *apoptosis inhibitor* in hemocyte homeostasis, all of which were up-regulated upon NLHS-VP. On the other hand, the down-regulated gene of NLHS-VP was *caspase* (Figure. 3.8). This result indicated that the NLHS triggered an immune response regulated by the proPO system, AMP production, and hemocyte homeostasis similar to the molecular responses for a bacterial infection. Therefore, the NLHS trigger could be considered as a prior conditioning and preparation for the shrimp to fight the later infections, thereby enhancing bacterial immunity against VP_{AHPND} and improving the survival rates.

Table 3.3. Fold changes in each relevant pairwise comparison presented in separate worksheets. Green highlights indicate significantly low false discovery rates (FDR)

Gene homolog	log2 (Fold change)			
	Normalized with 0 NH-VP		Normalized with 0 NLSH-VP	
	6 NH-VP	24 NH-VP	6 NLHS-VP	24 NLHS-VP
PREDICTED: Vollenhovia emeryi enhancer of split mbeta protein-like (LOC105567088), mRNA	5.49			
PREDICTED: Sinocyclocheilus rhinocerous E3 ubiquitin-protein ligase TRIP12 (LOC107710892), transcript variant X6, mRNA	8.38			
FJ416145 Penaeus vannamei relish small isoform gene, complete cds	8.49			
Takifugu rubripes HoxCa gene cluster, complete sequence	4.15			
Culex quinquefasciatus enhancer of split mgamma protein, mRNA	5.48			
PREDICTED: Anser cygnoides domesticus histidyl-tRNA synthetase (HARS), transcript variant X1, mRNA		11.04		
PREDICTED: Aplysia californica Golgi-specific brefeldin A-resistance guanine nucleotide exchange factor 1-like (LOC101846877), mRNA		8.91		
Gryllus bimaculatus GbTdc2 mRNA for tyrosine decarboxylase 2, complete cds		6.65		
Marsupenaeus japonicus alr mRNA for alanine racemase, complete cds		3.90		
PREDICTED: Cynoglossus semilaevis actinin, alpha 4 (actn4), transcript variant X1, mRNA		8.22		
PREDICTED: Sinocyclocheilus rhinocerous E3 ubiquitin-protein ligase TRIP12 (LOC107710892), transcript variant X5, mRNA		7.95		
PREDICTED: Vollenhovia emeryi enhancer of split mbeta protein-like (LOC105567088), mRNA		4.70		
Ixodes scapularis aromatic amino acid decarboxylase, putative, mRNA		3.69		
Penaeus vannamei relish small isoform gene, complete cds		7.72		
PREDICTED: Oryctolagus cuniculus acyl-CoA synthetase short-chain family member 1 (ACSS1), mRNA		4.13		
Gryllus bimaculatus GbTdc2 mRNA for tyrosine decarboxylase 2, complete cds		3.72		
Fenneropenaeus chinensis heat shock protein 70 mRNA, complete cds		6.19		
Penaeus monodon triosephosphate isomerase mRNA, complete cds		7.39		
Marsupenaeus japonicus scavenger receptor B1 mRNA, complete cds		2.96		
PREDICTED: Cephus cinctus diphthine methyltransferase (LOC107265617), transcript variant X2, mRNA		3.52		
Gryllus bimaculatus GbTdc2 mRNA for tyrosine decarboxylase 2, complete cds		3.62		
PREDICTED: Monodelphis domestica OPA1, mitochondrial dynamin like GTPase (OPA1), transcript variant X4, mRNA			9.28	
RecName: Full=Probable lipoprotein aminopeptidase LpqL; AltName: Full=Leucine aminopeptidase; AltName: Full=Lipoprotein LpqL; Flags: Precursor			5.29	
PREDICTED: Vollenhovia emeryi enhancer of split mbeta protein-like (LOC105567088), mRNA			4.86	

Table 3.3. (continue)

Gene homolog	log2 (Fold change)			
	Normalized with 0 NH-VP		Normalized with 0 NLSH-VP	
	6 NH-VP	24 NH-VP	6 NLHS-VP	24 NLHS-VP
PREDICTED: Crassostrea gigas pleckstrin homology domain-containing family H member 1-like (LOC105336836), transcript variant X9, mRNA			7.68	
Penaeus monodon AV gene, complete cds			4.31	
Penaeus vannamei serine proteinase inhibitor (SERPIN) mRNA, complete cds			4.44	
Cherax quadricarinatus clone V1-1690 DNA helicase B-like protein mRNA, partial cds			3.62	
Penaeus monodon AV gene, complete cds			4.49	
PREDICTED: Microplitis demolitor disks large homolog 5 (LOC103578467), transcript variant X8, mRNA				7.12
PREDICTED: Sarcophilus harrisii SATB homeobox 1 (SATB1), transcript variant X2, mRNA				9.12
PREDICTED: Crassostrea gigas pleckstrin homology domain-containing family H member 1-like (LOC105336836), transcript variant X9, mRNA				7.92
PREDICTED: Diaphorina citri serine/threonine-protein kinase D3 (LOC103509158), mRNA				8.58

3.1.4 Sequence analysis of *P. vannamei* miRNAs

To supplement the information derived from the transcriptome, we also explored the global miRNA expression to get a glimpse of some regulators that were associated with the observed gene expression. To do this, we analyzed the miRNAs expressed in VP_{AHPND}-infected and NLHS-treated shrimp (mir_NLHS-VP), by sequencing them at various sampling times (0, 6 and 24 hpi). The high-throughput sequencing generated total raw reads of 1,086,629 in the 0 mir_NLHS-VP, 879,272 in the 6 mir_NLHS-VP and 1,114,328 in the 24 mir_NLHS-VP. The high quality sequences that passed initial quality filters were 948,089, 771,799 and 956,249 reads, respectively.

Analyses showed that the majority of the non-redundant sequences were 20–22 nucleotides (nt) in length (Figure 3.3A). Searching against NCBI nucleotide database demonstrated that, on the average, 25% of the sequences were most likely contaminating RNAs (Figure 3.3B). After removal of these contaminating mRNA, rRNA and tRNA homologs, the final counts of sequences were 78,000 sequences, 77,415 of which were mappable to miRBase 22.1. The percentage of matched mature miRNA sequences was 93.86%, 93.93% and 94.19%, respectively,

for the 0 mir_NLHS-VP, 6 mir_NLHS-VP and 24 mir_NLHS-VP libraries. Sequences with unknown identities and homologs were also listed. Of those, forty-one miRNA homologs were identified from the NLHS-VP experimental group.

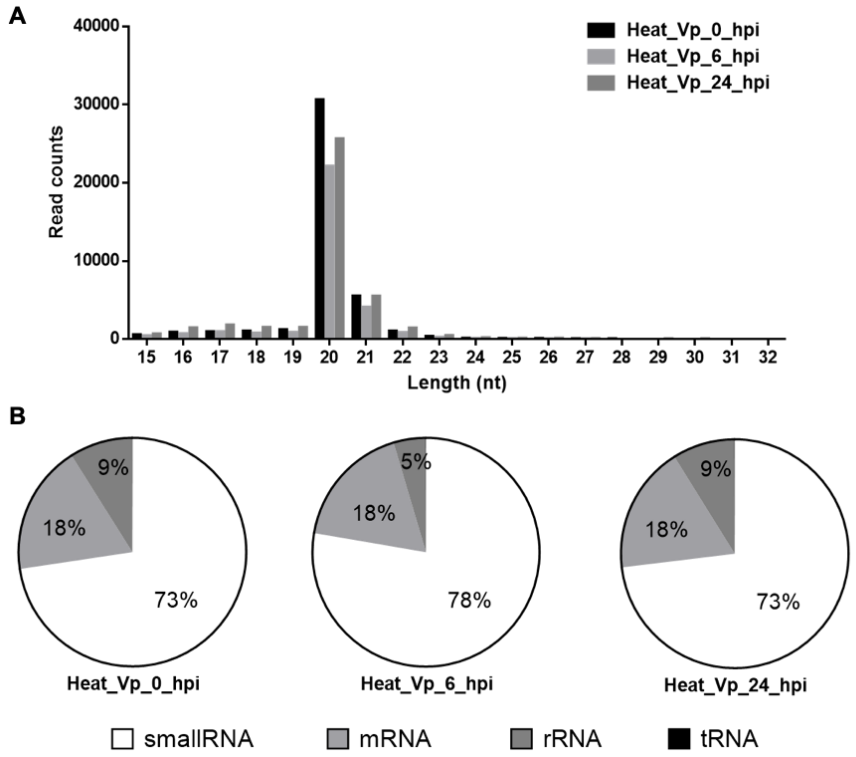

Figure. 3.3 Length distribution, abundance and composition of small RNAs in shrimp *P. vannamei*. Length distribution and abundance of small RNAs in VP_{AHPND}-infected and NLHS-treated *P. vannamei* hemocytes collected at 0, 6 and 24 hpi (A). Composition of small RNAs in the small RNA-NGS libraries (B). Heat_Vp_0_hpi represents 0 mir_NLHS-VP library, Heat_Vp_6_hpi represents 6 mir_NLHS-VP library and Heat_Vp_24_hpi represents 24 mir_NLHS-VP library.

3.1.5 RT-qPCR validation of significant differentially expressed miRNAs (DEMs) and DEGs

In order to confirm the presence of the identified miRNAs and mRNAs as well as analyze the expression of interesting *P. vannamei* miRNAs and mRNAs in response to VP_{AHPND} infection under NLHS and control conditions, the expression profiles of 10 DEMs (lva-miR-7170-5p, lva-miR-2169-3p, lva-miR-184, lva-miR-92b-5p, lva-miR-317, lva-miR-92a-3p, lva-miR-4901, lva-miR-61, lva-miR-2898 and lva-miR-6090) and 8 DEGs which were identified from the sequencing data (*Relish*, *lipoprotein receptor*, *dynamin*, *importin7, juvenile hormone epoxide hydroxylase*

1; *JHEH-1*, *DNAJ5*, *prophenoloxidase 1*; *PO1* and *prophenoloxidase 2*; *PO2*), were analyzed for their expression using RT-qPCR.

Under the NLHS-VP condition, the *Relish* gene expression was significantly higher in all experimental groups than the respective controls. The *dynamin* gene was upregulated by 2-fold at 6 hpi and down-regulated by 2-fold at 24 hpi. The *lipoprotein receptor* gene was up-regulated about 2-fold at only 6 hpi. *Importin7, JHEH-1, DNAJ5, PO1* and *PO2* were significantly down-regulated around 1.5- to 10-fold at 6 hpi and 24 hpi (Figure 3.4). It should be noted that the expression pattern from the NGS data had similar trend as compared with the RT-qPCR results of selected DEGs.

Meanwhile, the stem loop RT-qPCR analysis revealed that the expression levels of all 10 chosen DEMs were altered in shrimp hemocytes following NLHS treatment and VP_{AHPND} challenge by about 1.5- to 8-fold. For the NH-VP condition, only some of these DEMS had significant changes in their expression levels. These were lva-miR-2898, lva-miR-2169-3p, lva-miR-7170-5p and lva-miR-92b-5p, which were all up-regulated at 6 and 24 hpi by about 1.5- to 10-fold (Figure 3.5). It was also found that the expression of 7 of 10 selected miRNAs were significantly altered under the NLHS-VP condition in consistent with our small RNA-Seq data.

3.1.6 Correlation of DEMs and DEGs of NLHS-treated shrimp in response to VP_{AHPND} infection

In order to analyze the interaction between the miRNAs and their targets based on their differential expression profiles, the DEMs of NLHS-VP and NH-VP (unpublished data) were analyzed altogether. As with the expression profiles of the DEMs, a Venn diagram was also created to highlight specific groupings of DEMs between the libraries of NLHS-VP and NH-VP. The 18 DEMs were specifically grouped into NLHS-VP while only 2 DEMs were grouped into NH-VP (Figure 3.6A).

These DEMs from the NLHS-VP with their corresponding predicted target mRNAs from our sequencing dataset were analyzed using in-house and RNA-hybrid software for functionalizing their specific miRNA-mRNA interactions as a clue to the general regulatory mechanisms underlying the immune response of shrimp under the NLHS and VP_{AHPND} infection. The 1,183 DEM-DEG pairs, with both positive and negative correlations, were identified and included in the miRNA-target network. Some of the biological functions that might be regulated by the NLHS-VP

miRNAs were: “Defense & Homeostasis”, “Energy & Metabolism”, “Cell cycle & DNA Synthesis/repair”, “Gene expression & Protein synthesis/degradation”, “Receptor”, “Signaling & Communication”, “Transporter”, “Hypothetical protein” and “Unknown”. The Lva-miR-7278-5p, lva-miR-6831-5p, lva-miR-745b, lva-miR-9041-5p, lva-miR-502b-3p and lva-miR-2898 had high degrees of connectivity and might play crucial roles in this regulatory network. Meanwhile, the genes involved in “Defense & Homeostasis”, “Energy & Metabolism”, and “Cell cycle & DNA Synthesis/repair” were the most common miRNA targets (Figure 3.6B-C).

In order to further characterize the identified biological pathways, an enrichment analysis specific for immune-related pathways was done for the identified DEGs of miRNA-mRNA pairs. The 3 pathways that changed significantly (*P*-value < 0.05) were “hemocyte homeostasis”, “prophenoloxidase system” and “AMP production”. Given these immune pathways and the information on the canonical members of these pathways in related literature, we were able to find sequence homologs of these members in our NGS dataset. We ,then, used publicly available information on shrimp to further annotate these homologs as well as other sequences in our transcriptome data. We also used our sequence information to lookup gene expression patterns in the identified pathways using RT-qPCR.

The RT-qPCR was used to quantify the expression profiles of some canonical members of the identified pathways (Figure 3.7). The expression profile of *PO1* and *PO2* under the NLHS condition was modified and re-presented from Figure 3.4 As expected, the *PO1* and *PO2* in proPO pathway were highly up-regulated from 1.5- to 8-fold in NLHS-VP group. The *IMD*, *IKK*β and *Relish* in the IMD pathway had higher gene expression while the *Toll1*, *Toll2*, *Toll3*, *MyD88*, *TRAF6*, *Pelle* and *Dorsal* in the Toll pathway were not significantly changed in the NLHS-VP group. For the hemocyte homeostasis pathway, the *transglutaminase* and *inhibitor of apoptosis* were analyzed and found to be highly up-regulated whereas the *caspase* was down-regulated in NLHS-VP. These findings confirmed the results of the pathway enrichment analysis. The information obtained finally suggested that the biological immune pathways, “hemocyte homeostasis”, “Prophenoloxidase system” and “AMP production via IMD pathway”, might play important roles in the enhancement of shrimp antibacterial immunity against VP_{AHPND} upon modulation of NLHS.

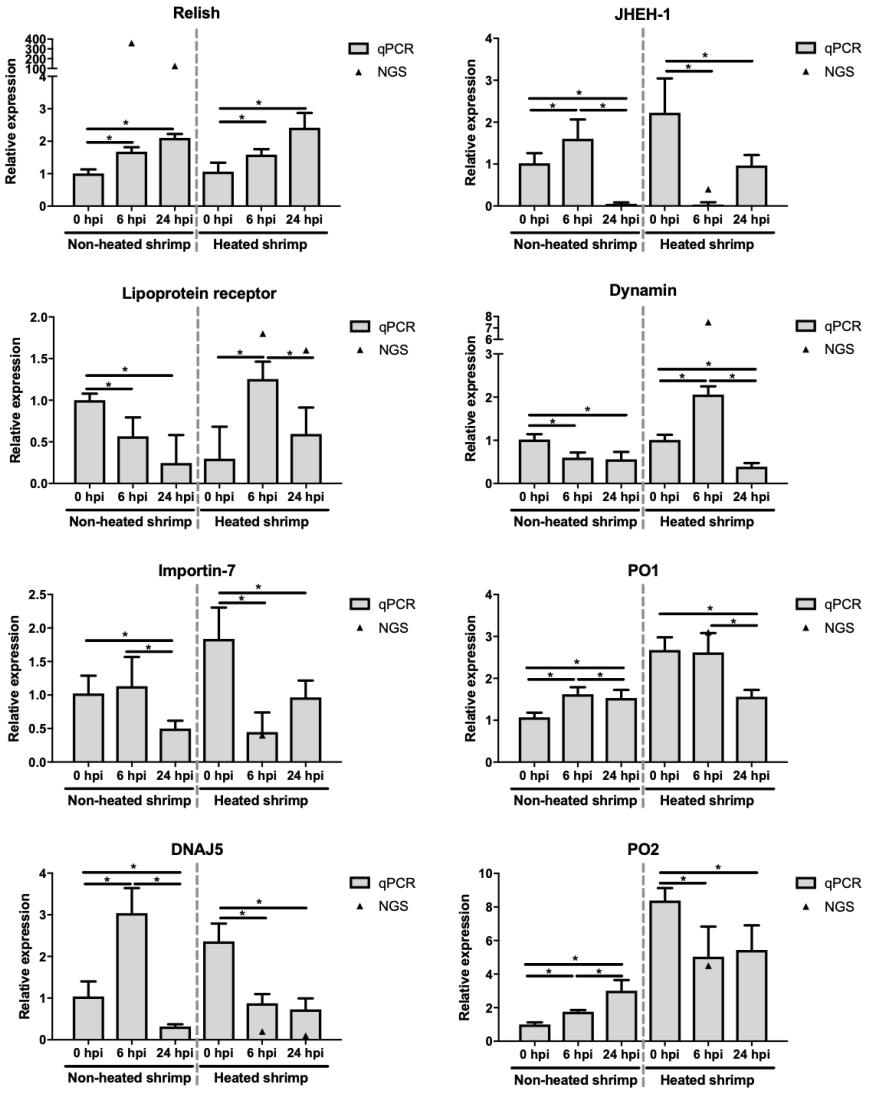

Figure. 3.4. Validation of RNA-Seq using RT-qPCR. Eight genes (*Relish*, *lipoprotein receptor*, *dynamin*, *importin7, juvenile hormone epoxide hydroxylase 1*; *JHEH-1*, *DNAJ5*, *prophenoloxidase 1*; *PO1* and *prophenoloxidase 2*; *PO2*) were evaluated for their expression in hemocytes from *P. vannamei* under the NLHS and NH conditions in response to VP_{AHPND} infection. Total RNA from hemocytes of VP_{AHPND}-infected and NH/NLHS-treated *P. vannamei* at 0, 6 and 24 hpi was used for cDNA synthesis. The relative expression levels of 8 genes were determined by RT-qPCR and standardized against *EF-1*α, the internal reference. The relative expression ratio was calculated using the $2^{-\Delta\Delta CT}$ method. The bar graphs are the data from RT-qPCR presented as means ± standard deviations and the triangles (▲) are the data from the NGS. The experiment was done in triplicate. The expression level was calculated relative to that of the normal shrimp under NH condition at 0 h after VP_{AHPND} challenge. Asterisks indicate significant difference (P<0.05) from the respective VP_{AHPND} infected NH shrimp at 0 hpi.

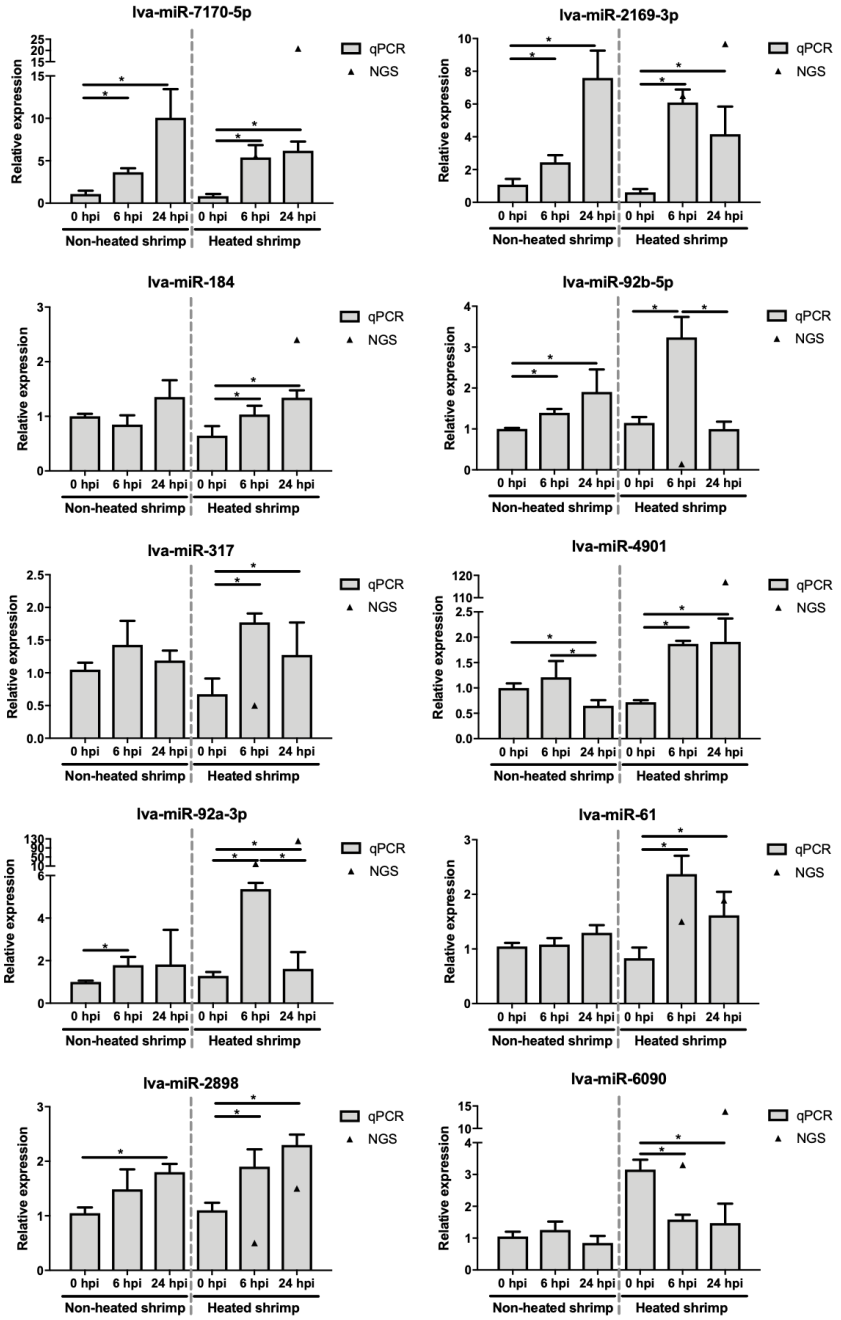

Figure. 3.5. Relative expression analysis of miRNAs in response to VP_{AHPND} infection following the NLHS and NH treatments. Total small RNAs from VP_{AHPND}-infected *P. vannamei* hemocytes of shrimp treating under NH and NLHS conditions were used as template for specific stem-loop first strand cDNA synthesis. Relative expression levels of 12 miRNAs were determined by RT-qPCR and standardized against the U6, the internal reference, at 0, 6 and 24 hpi. The bar graphs are the data from RT-qPCR presented as means ± standard deviations and the triangles (▲) are data from the NGS. The results were derived from triplicate experiments. Asterisks indicate significant differences at $P < 0.05$.

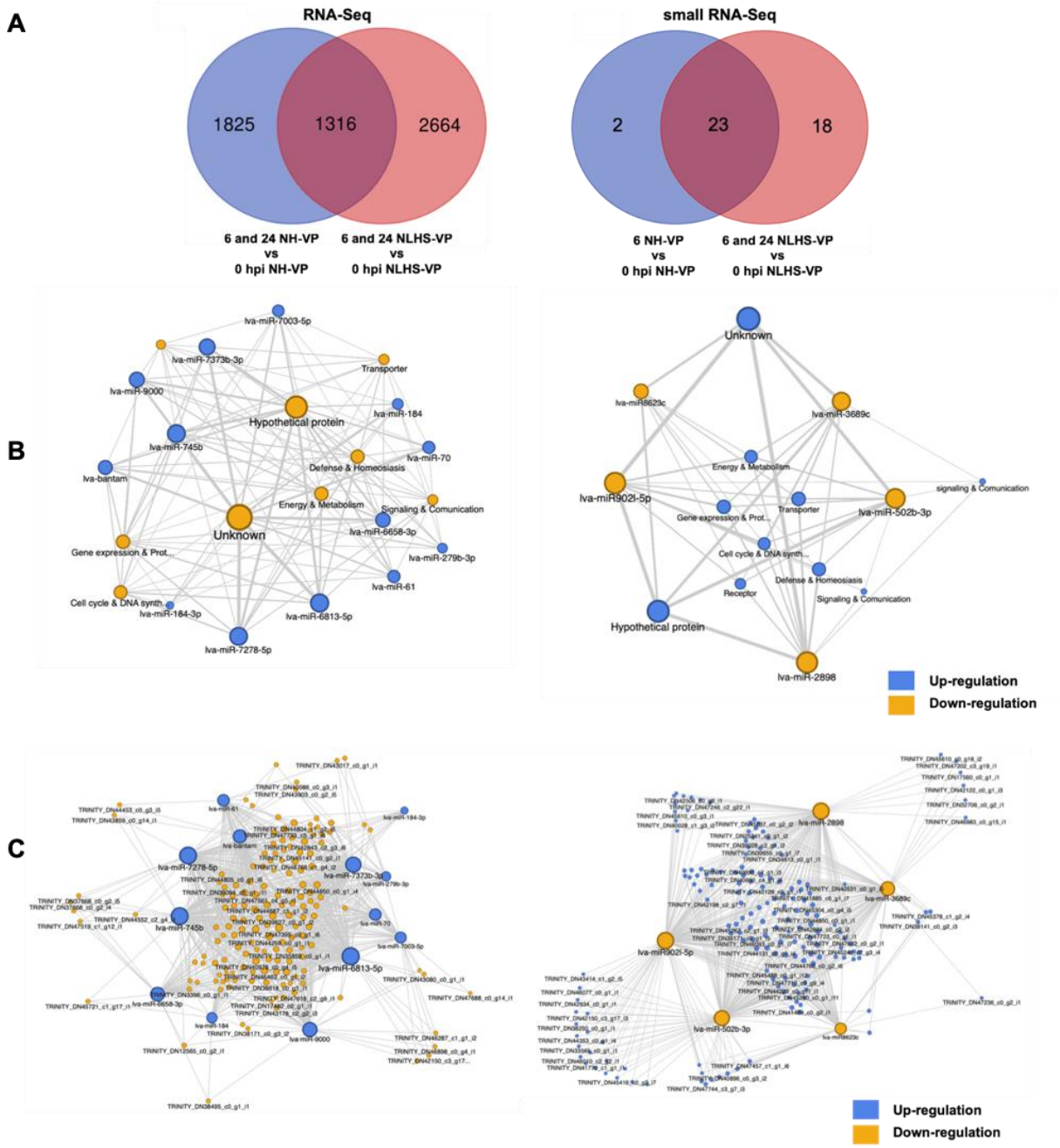

Figure. 3.6. Network analysis for miRNA/mRNA interaction. The Venn diagrams represent unique and common *P. vannamei* mRNAs and miRNAs in response to VP_{AHPND} infection following the NLHS and NH treatments (A). The miRNA-mRNA negative correlation network based on the predicted miRNA target function (B) and unique isotig (C). The circular nodes represent mRNAs and miRNAs. The degree of connectivity, which represents the number of genes regulated by a given miRNA, is indicated by the size of the node; the higher the degree of connectivity, the larger the node is.

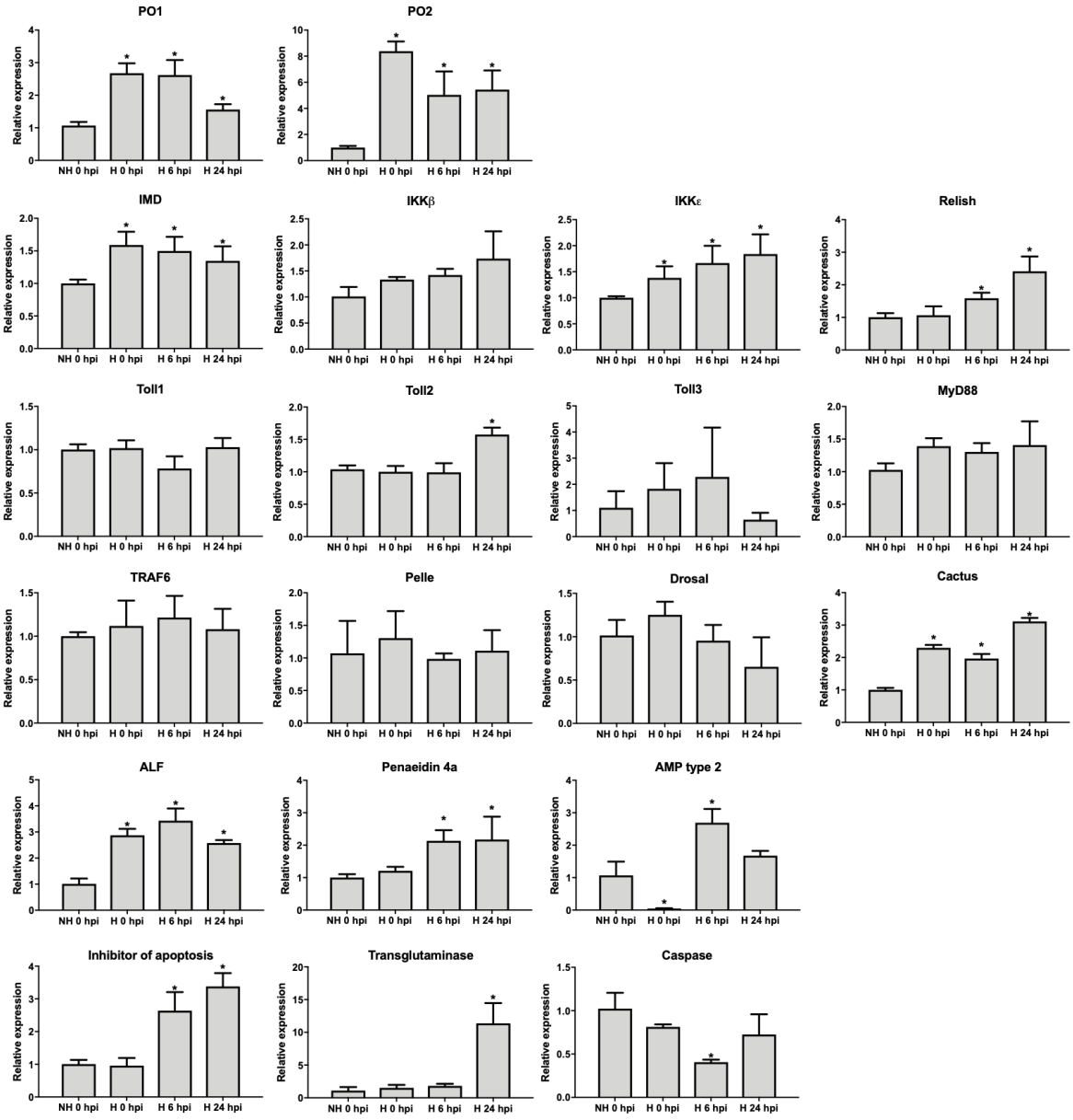

Figure. 3.7. Relative expression analysis of genes in the NLSH modulated immune pathways. Expression of genes in the prophenoloxidase system, Toll pathway, IMD pathway, and hemocyte homeostasis in VP_{AHPND}-infected *P. vannamei* hemocytes following the NLHS treatment were analyzed by RT-qPCR using the same cDNAs of the RT-qPCR validation experiment. Relative expression levels were normalized with the NH-VP at 0 hpi to observe the effect of both NLHS and VP_{AHPND} challenge and standardized against *EF-1α* as the internal control. The results were derived from triplicate experiments. Asterisks indicate significant differences at $P < 0.05$. The expression profile of *PO1* and *PO2* under the NLHS condition was modified and re-presented from Fig.3.

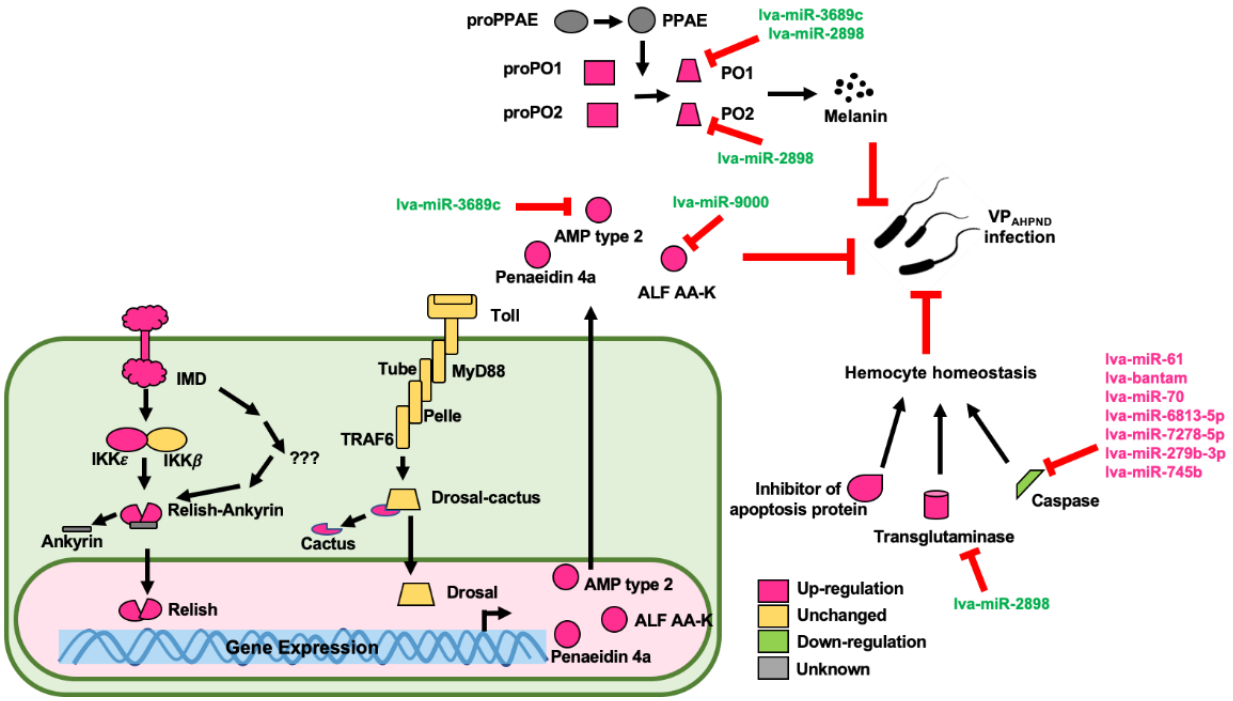

Figure. 3.8. A schematic representation of the predicted interactions between miRNAs and target immune genes of *P. vannamei* under NLHS-VP condition.

3.2 Function analysis of a VP_{AHPND}-responsive miRNA in *P. vannamei* hemocyte

3.2.1 miRNA expression analysis upon VP_{AHPND} infection using stem-loop real-time PCR

In order to confirm the presence of the identified miRNAs and to analyze the expression of *P. vannamei* miRNA in response to VP_{AHPND} infection only, the expression levels of 10 NH-VP responsive miRNAs (lva-miR-9000, lva-miR-8522c, lva-miR-2169-3p, lva-miR-4850, lva-miR-92b-5p, lva-miR-D9-3p, lva-miR-184, lva-miR-4901, lva-miR-7170-5p, and lva-miR-92a-3p) were evaluated using stem-loop RT-PCR. The relative expression levels of miRNAs were determined in VP_{AHPND}-infected *P. vannamei* hemocyte at 0, 6, and 24 hpi, using U6 as the internal reference (Figure 3.9). The results indicated that the expression levels in 8 out of 10 miRNAs were altered in shrimp hemocyte following VP_{AHPND} challenge. The expression levels of lva-miR-8522c and lva-miR-184 remained unchanged at 6 and 24 hpi. For lva-miR-9000, the expression level at 6 and 24 hpi were down-regulated by approximately 1.5- and 1.75-fold, respectively. Moreover, the expression level of lva-miR-D9-3p and lva-miR-4850 remained unchanged at 6 hpi but were then down-regulated by approximately 2-fold at 24 hpi. For lva-miR-2169-3p and lva-miR-7170-5p,

the expression level was up-regulated by approximately 2- and 3-fold at 6 hpi and 2.5- and 10-fold at 24 hpi, respectively. For lva-miR-4901, the expression level was up-regulated by 1.7-fold at 6 hpi and remained unchanged at 24 hpi. The expression level of lva-miR-92a-3p increased by approximately 2-fold at 6 hpi and remained unchanged at 24 hpi. The expression level of lva-miR-92b-5p was unchanged at 6 hpi but increased by approximately 1.75-fold at 24 hpi.

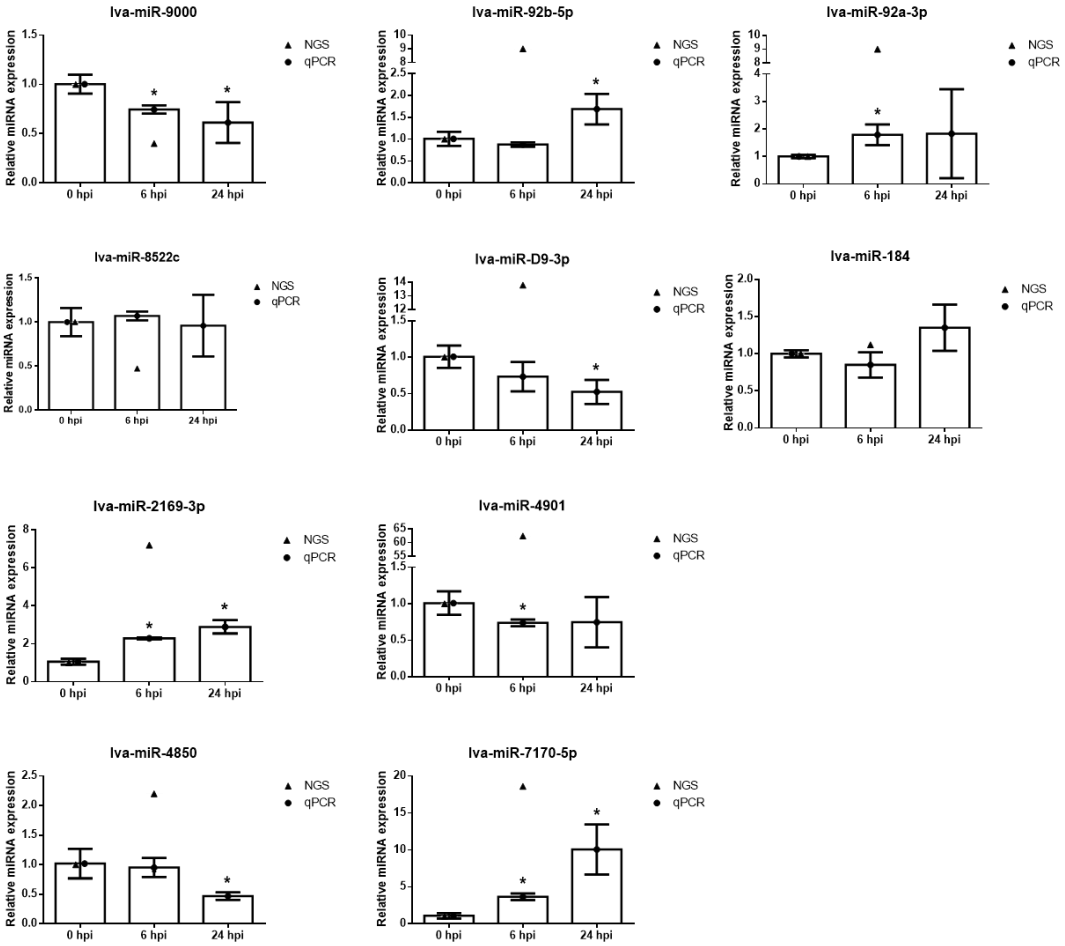

Figure 3.9 Relative expression analysis of miRNAs in response to VP_{AHPND} infection. Total RNA from VP_{AHPND}-infected *P. vannamei* hemocyte was used as a template for specific stem-loop first-strand cDNA synthesis. The relative expression levels of 10 miRNAs were determined by qRT-PCR and standardized against U6 as the internal reference at 0, 6, and 24 hpi. Results were derived from triplicate experiments. Data are presented as means ± standard deviations. Asterisks indicate significant differences at $P < 0.05$.

3.2.2 miRNA target prediction

The function of miRNA on gene expression regulation depends on its ability to directly bind the target mRNA. Therefore, identification of the target mRNA of each miRNA could provide clues regarding the role of miRNA in shrimp immune response against VP_{AHPND} infection. The transcriptome database of VP_{AHPND}-infected *P. vannamei* was used for mRNA target prediction using the developed miRNA target prediction program (Kaewkascholkul et al., 2016). The criteria for searching miRNA targets included: the presence of a seed sequence (2-8 nucleotides from the 5′-end) of miRNA with perfect complementarity or 1 mismatch position to mRNA at any different region; an open reading frame (ORF); 3′-UTR and 5′-UTR; and an overall complementarity of miRNA to target mRNA no lower than 65%. It was determined that VP_{AHPND}-responsive miRNAs might target several shrimp immune-related genes (Figure 3.10).

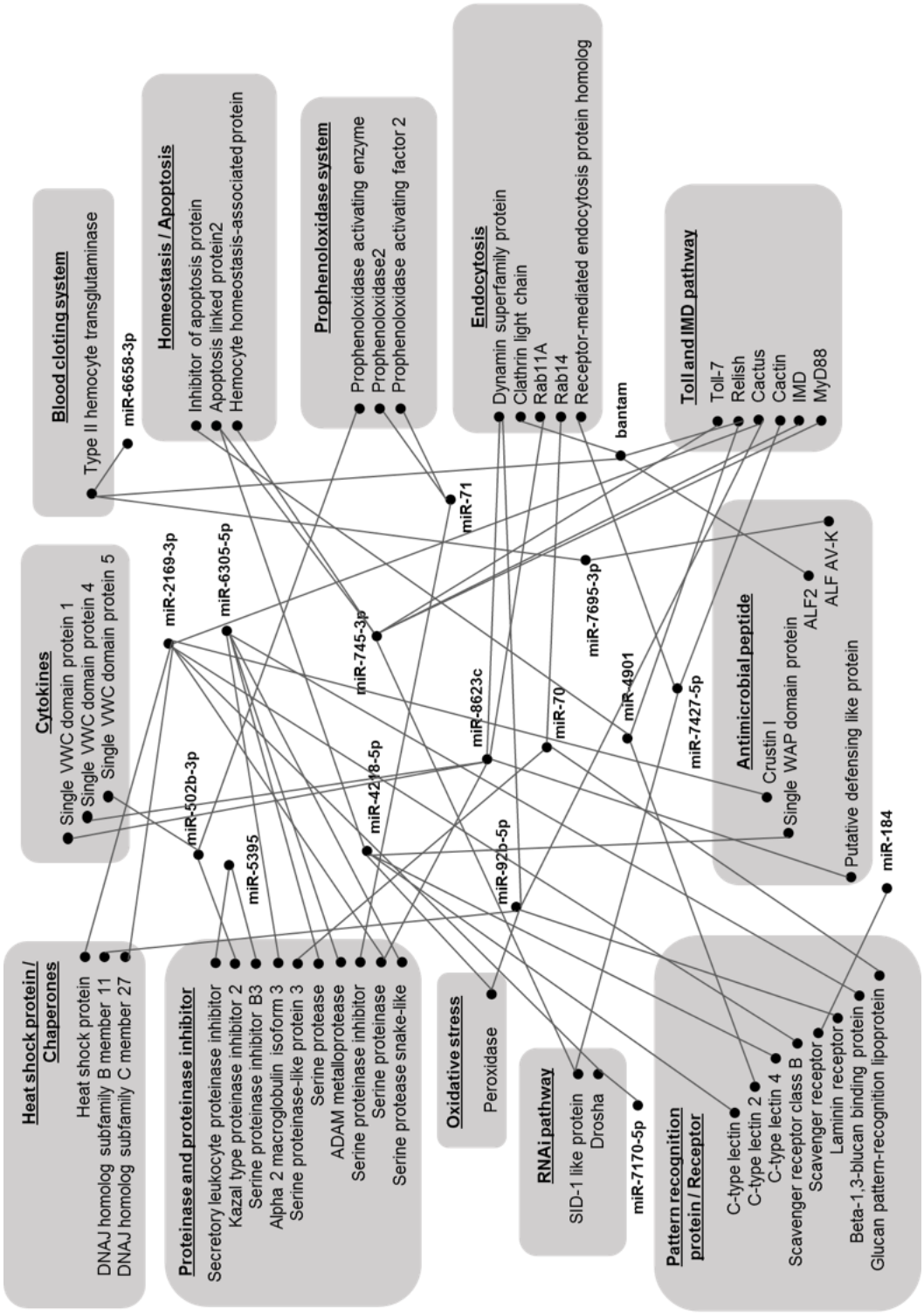

Figure 3.10 The predicted interactions between miRNAs and target *P. vannamei* immune genes. The target genes of VP_{AHPND}-responsive miRNAs were predicted against the *P. vannamei* transcriptome database using the developed miRNA target prediction program. Target genes were grouped according to immune-related function.

3.2.3 Expression analysis of the target mRNA of lva-miR4850 in *P. vannamei* shrimp by qRT-PCR

Based on the results presented in Section 3.12.2, lva-miR4850 was selected for further miRNA/target interaction analysis. Notably, lva-miR4850 was predicted to target the 3'UTR of *PO2* at position 2319 to 2338 and *Dicer1* at position 11,779 to 11,795, which were a gene in the prophenoloxidase system and RNA interference pathway, respectively (Figure 3.11A-B). The expression analysis of putative lva-miR4850 target genes revealed that PO2 and Dicer1 were up-regulated after VP_{AHPND} infection in *P. vannamei* hemocyte by approximately 1.8- to 3-fold (Figure 3.11C). The result suggested that *PO2* and *Dicer1* might be lva-miR4850 target genes.

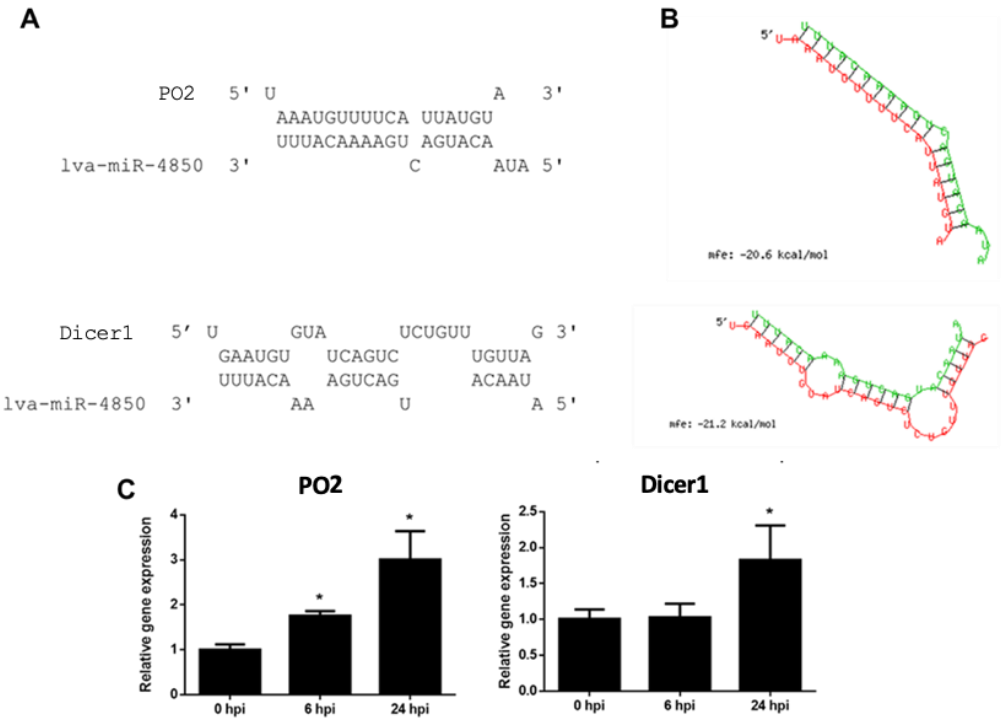

Figure 3.11 Prediction of target genes, miRNA binding site and expression analysis of lva-miR-4850. The binding of lva-miR-4850 to target mRNA were predicted using in-house software (A) and RNAhybrid software (B). Relative expression analysis of the mRNA targets of lva-miR-4850 in response to VP_{AHPND} infection in *P. vannamei* hemocyte. Relative expression levels were determined by qRT-PCR and standardized against EF-1α as the internal control. Results were derived from triplicate experiments. Asterisks indicate significant differences at $P < 0.05$.

3.2.4 Confirmation of target mRNA of lva-miR4850 by dual-luciferase reporter assay

Based on lva-miR-4850 target, PO2 is one of key enzyme in the melanization cascade that also participates in cuticle sclerotization and wound healing. Sclerotized cuticle presents a barrier to infection, and melanization around pathogens help to kill invading pathogens (Amparyup et al., 2013). In this study, *PO2* and lva-miR-4850 interaction was further characterized

To confirm the miRNA/target interaction, DNA fragments corresponding to the putative miRNA-binding region of the PO2 gene was cloned into a pmirGLO vector downstream of the firefly luciferase gene (Figure 3.12) and used as the parental construct (pmiR). Then, it was mutated at the seed region (pmiRGLO-mutant) and used for the experiment. Reporter constructs were then transfected into HEK293-T cells with either respective miRNA mimics or scramble. The results showed that the luciferase activity of pmirGLO-PO2 was reduced by approximately 35% (Figure 3.13). The reduction of firefly luciferase expression indicates the binding of miRNA to the cloned miRNA target sequence. On the other hand, the mutated seed sequence of lva-miR-4850 did not affect luciferase activity compared to that of the control group (Figure 3.13). These results indicated that the PO2 gene was a target gene of lva-miR-4850.

```
PO2-WT          GCGGTTTCTGTATTAGAGTTAGAAATGGCTATTGTGTACATTTCTTTTGTATCTGTTTAA 60
PO2-mutant      GCGGTTTCTGTATTAGAGTTAGAAATGGCTATTGTGTACATTTCTTTTGTATCTGTTTAA 60
                ************************************************************

PO2-WT          TATTTGGATTTTGGTACATTGTTGTATAATATATTTTGTATCTGCAGATACAGAAATACT 120
PO2-mutant      TATTTGGATTTTGGTACATTGTTGTATAATATATTTTGTATCTGCAGATACAGAAATACT 120
                ************************************************************

PO2-WT          AAATGTTTTCATTATGTATAAAATGTGAAAACTGTGTTCCCTGTAATACTGTATTATCTG 180
PO2-mutant      AAATGTTTTCAaatacaATAAAATGTGAAAACTGTGTTCCCTGTAATACTGTATTATCTG 180
                **********      ****************************************

PO2-WT          TAATAACTACTTACACATATCAGTATTAGATAGTTGTATATTTTATTCATTATAATCATG 240
PO2-mutant      TAATAACTACTTACACATATCAGTATTAGATAGTTGTATATTTTATTCATTATAATCATG 240
                ************************************************************

PO2-WT          ATATTTGAACAGACGAAATGCGTTTAAATAA    271
PO2-mutant      ATATTTGAACAGACGAAATGCGTTTAAATAA    271
                ******************************
```

Figure 3.12 Sequence alignment of the lva-miR-4850 binding site for the PO2 gene between the wild type and seed sequence mutant. Yellow color represents the lva-miR-4850 binding sequence.

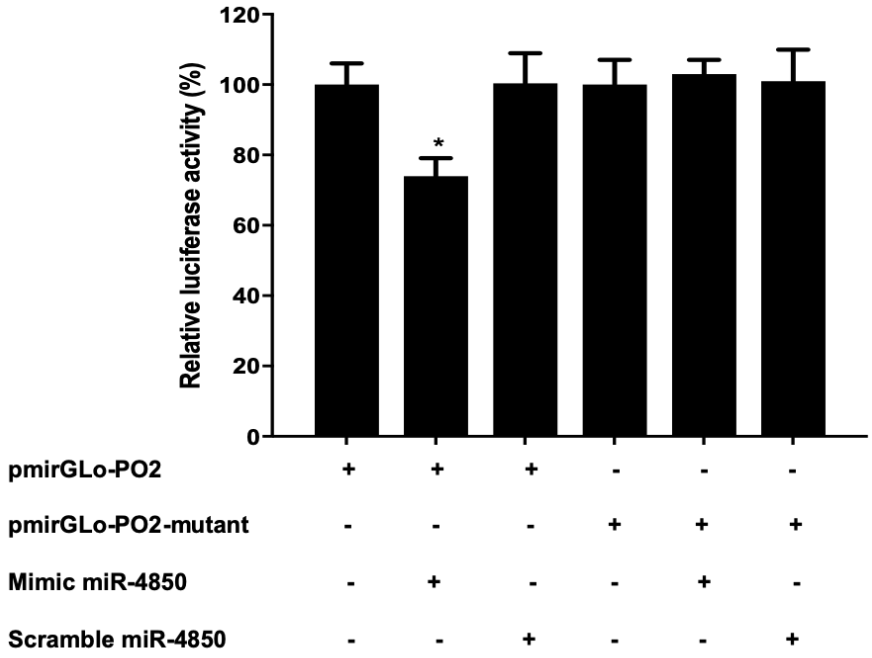

Figure 3.13 *In vitro* miRNA/target interaction analysis. Synthetic lva-miR-4850 or lva-miR-4850 scramble were co-transfected with pmirGLO-PO2 or pmirGLO-PO2 mutant into HEK293-T cells. Luciferase activity was measured at 48 h after transfection. The experiments were performed triplicate. Asterisk indicates significant differences at $P < 0.05$.

3.2.5 Regulation of *PO2* gene and proPO activating system by lva-miR-4850 in VP_{AHPND}-infected shrimp

To investigate whether lva-miR-4850 regulates PO2 gene in shrimp, *in vivo* RNAi experiments were performed. Shrimp were injected with either mimic-lva-miR-4850, scramble mimic-lva-miR-4850, AMO-lva-miR-4850, scramble AMO-lva-miR-4850, or 0.85% NaCl. After 24 hpi, each injected shrimp was challenged with VP_{AHPND}, and then, the total RNA was extracted from the hemocyte at 24 h post VP_{AHPND} challenge and subjected to qRT-PCR analysis and phenoloxidase activity assay. The qRT-PCR analysis showed that the lva-miR-4850 transcription level increased significantly by approximately 2-fold in mimic-lva-miR-4850 injected shrimp, when compared to the scramble mimic-lva-miR-4850 and 0.85% NaCl-injected shrimp. The transcription level of *PO2* exhibited a negative correlation to that of lva-miR-4850. (Figure 3.14). The *PO2* expression level was significantly decreased by approximately 4-fold in mimic-lva-miR-4850-injected shrimp as compared to the control of scramble mimic-lva-miR-4850- and 0.85% NaCl-injected shrimp. As the same trend of *PO2* expression, injection of mimic-lva-miR-4850 showed a negative correlation to lva-miR-4850 expression. The prophenoloxidase activity was

significant decreased by about 2-fold when compared to the control of scramble mimic-lva-miR-4850- and 0.85% NaCl-injected shrimp (Figure 3.15)

On the other hand, shrimp injected with AMO-lva-miR-4850 to inhibit lva-miR-4850 and challenged with VP_{AHPND} exhibited significant reduction of lva-miR-4850 expression level (approximately 1.5-fold), when compared to the scramble AMO-lva-miR-4850- and 0.85% NaCl-injected shrimp. Considering *PO2* expression level, there is inverse relationship between lva-miR-4850 and *PO2.* AMO-lva-miR-4850 injected shrimp increased significantly approximately by 1.5-fold in AMO-lva-miR-4850-injected shrimp but decreased significantly by 4-fold in mimic-lva-miR-4850 injection (Figure 3.14). In addition, shrimp injected with AMO-lva-miR-4850 challenged with VP_{AHPND} increased prophenoloxidase activity approximately 1.5 fold, when compared to the scramble AMO-lva-miR-4850- and 0.85% NaCl-injected shrimp (Figure 3.15).

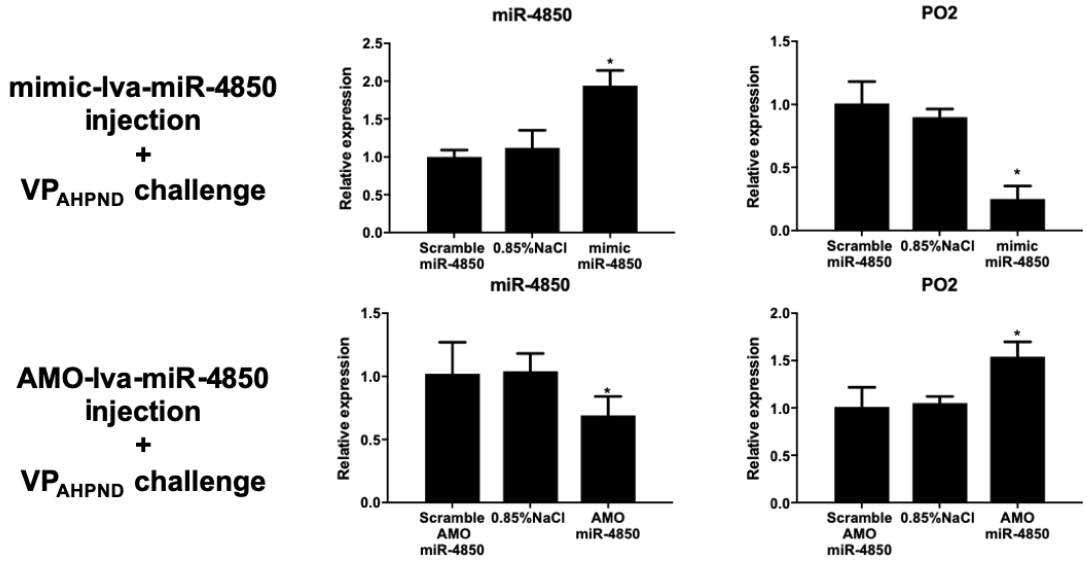

Figure 3.14 Regulation of *PO2* gene by lva-miR-4850 in VP_{AHPND} infected *P. vannamei*. Expression analysis of lva-miR-4850 and PO2 in mimic-lva-miR-4850-, scramble mimic-lva-miR-4850-, AMO-lva-miR-4850-, scramble AMO-lva-miR-4850-, or 0.85% NaCl-injected shrimp challenged with VP_{AHPND}. The experiment was performed in triplicate. Data are presented as means ± standard deviations. Asterisks indicate significant differences between data for scramble mimic- or scramble AMO-injected shrimp at $P < 0.05$.

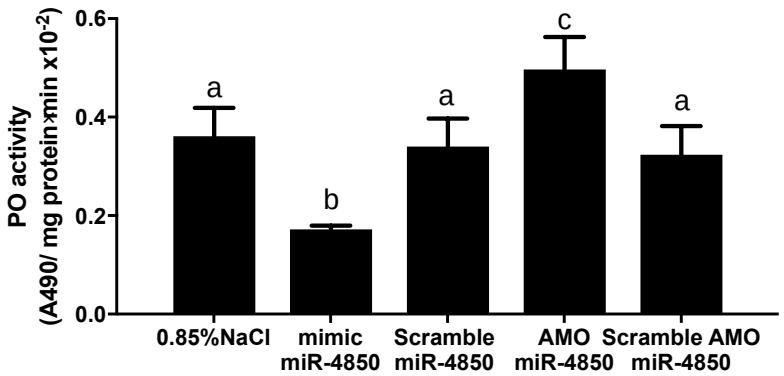

Figure 3.15 Regulation of proPO activating system by lva-miR-4850 in VP_{AHPND} infected shrimp. Phenoloxidase activity of mimic-lva-miR-4850-, scramble mimic-lva-miR-4850-, AMO-lva-miR-4850-, scramble AMO-lva-miR-4850-, or 0.85% NaCl-injected shrimp challenged with VP_{AHPND} was determined in hemolymph collected at 24 h post VP_{AHPND} challenge. The experiment was performed in triplicate. Data are presented as means ± standard deviations. Different small letters indicate significant differences between data at $P < 0.05$.

3.2.6 Effects of mimic and AMO lva-miR-4850 on the number of bacteria in stomach and hepatopancreas of VP_{AHPND}-infected shrimp

Based on the results of the challenge test for mimic-lva-miR-4850- and AMO lva-miR-4850-injected shrimp, we further investigated whether they had an effect on the number of bacterial cells present in VP_{AHPND} targeted shrimp tissues, stomach and hepatopancreas. The amount of total Vibrio in shrimp stomach and hepatopancreas was counted after either mimic-lva-miR-4850, scramble mimic-lva-miR-4850, AMO-lva-miR-4850, scramble AMO-lva-miR-4850, or 0.85% NaCl injection and challenge with VP_{AHPND}. The results revealed that the number of green colonies in both stomach and hepatopancreas increased in shrimp injected with mimic-lva-miR-4850. The number of VP_{AHPND} (CFU/ml) in AMO-lva-miR-4850 injected shrimp was reduced by approximately 10-fold compared to the scramble AMO-lva-miR-4850- and 0.85% NaCl-injected groups (Figure 3.16).

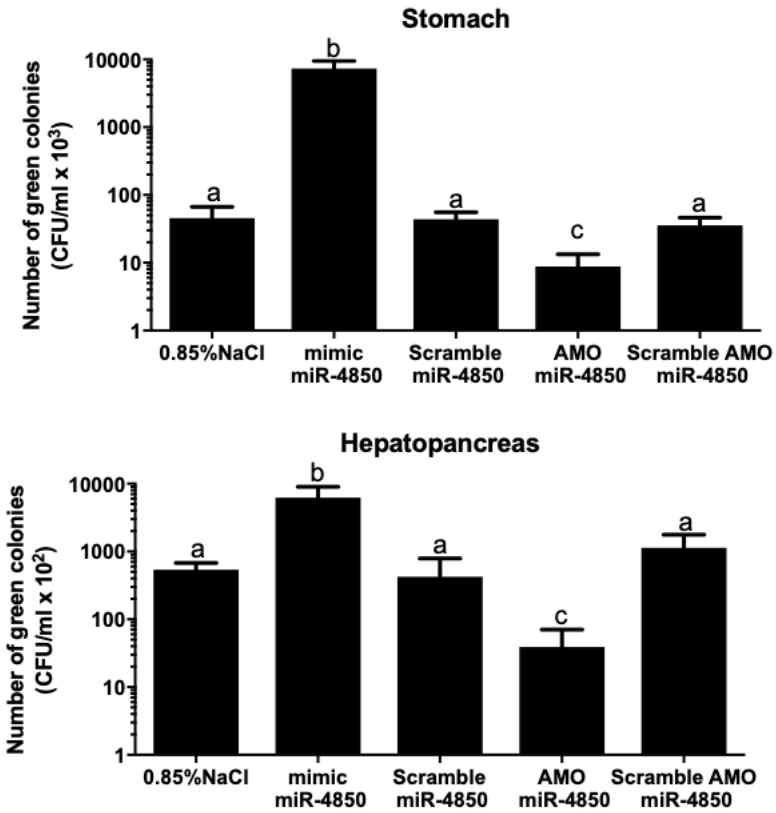

Figure 3.16 Effects of mimic and AMO lva-miR-4850 on the number of bacteria in stomach and hepatopancreas of VP_{AHPND} infected *P. vannamei*. Shrimp were injected with mimic-lva-miR-4850, scramble mimic-lva-miR-4850, AMO-lva-miR-4850, scramble AMO-lva-miR-4850, or 0.85% NaCl. After 24 h, shrimp were infected with 1×10^6 CFU/ml VP_{AHPND} by immersion. Stomach and hepatopancreas were individually collected to determine the amount of VP_{AHPND} by dotting on TCBS agar at 24 h post VP_{AHPND} challenge. Following overnight incubation, the total number of viable green colonies (CFUs) were evaluated. The experiment was performed in triplicate. Data are presented as means ± standard deviations. The small letters indicate significant differences at $P < 0.05$.

3.3. Functional characterization of a WSSV-responsive miRNA from *P. monodon*

3.3.1 Expression of pmo-miR-315 in tissues of WSSV-infected shrimp

Previously, the differentially expressed miRNAs in hemocytes of WSSV-infected shrimp were identified (Kaewkascholkul et al, 2016). Among them, the pmo-miR-315 was highly up-regulated at 48 h post WSSV infection. The pmo-miR-315 expression level in various tissues including hemocytes, gill, lymphoid organ, and stomach in WSSV-infected shrimp at 0, 6, 24, and

48 hhpi was further studied. Although, the pmo-miR-315 expression was observed in all tissues tested, the significant response to WSSV infection were found only in hemocytes, in which it was up-regulated at 24 and 48 hpi for about 5- and 30-fold compared with that at 0 hpi (Figure 3.17). Our results suggested that the pmo-miR-315 was the WSSV-responsive miRNA that might have a function in shrimp immune response.

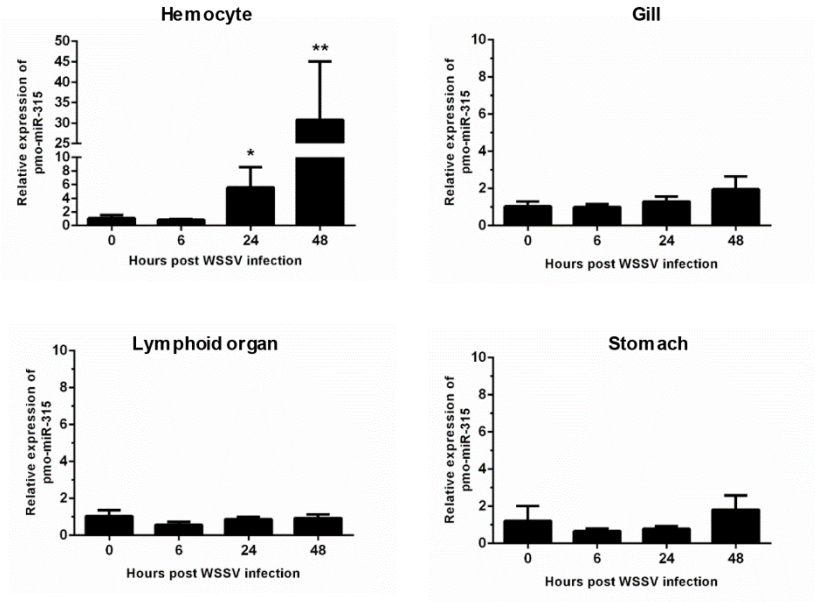

Figure 3.17 The expression of pmo-miR-315 in WSSV-infected *P. monodon* tissues. Quantitative stem-loop real-time RT-PCR was performed to determine the expression level of pmo-miR-315 in hemocytes, gill, lymphoid organ and stomach at 0, 6, 24 and 48 hpi. Using U6 as an internal control, the relative expression level of miR-315 was calculated. All experiments were performed in triplicate. The * and ** indicate the significant difference at $P < 0.05$ and $P < 0.01$, respectively.

3.3.2 Expression of pmo-miR-315 target gene in WSSV-infected shrimp hemocytes

As stated before, the target mRNA of pmo-miR-315 has been predicted as a putative prophenoloxidase-activating enzyme (*PmPPAE*) by bioinformatic approaches (Kaewkascholkul et al, 2016). The PPAE is known as an enzyme that converts the prophenoloxidase (proPO) to active phenoloxidase (PO) in cascades of the proPO system (Cerenius and Söderhäll 2004). Previously,

two isoforms of PPAEs including *Pm*PPAE1 and *Pm*PPAE2 were identified in *P. monodon* (Charoensapsri et al, 2009, 2011). Preliminary analysis showed that the sequence of target mRNA of pmo-miR-315 was a novel isoform of *PmPPAE*. Herein, therefore, it was named as *PmPPAE3*. The RNA hybrid software used to analyze the structure and stability of miRNA/mRNA duplex showed that the seed region of pmo-miR-315 was perfectly complementary to the target sequence located on the coding sequence of *PmPPAE3* mRNA (Figure 3.18A). The possibility of *PmPPAE3* transcript on being the pmo-miR-315 target was evaluated by the determination of the pattern of *PmPPAE3* gene expression in comparison to that of pmo-miR-315. The expression of *PmPPAE3* transcript was dramatically decreased by about 5-fold at 24 and 48 hpi compared with that at 0 hpi (Figure 3.18B). The negative correlation of expression pattern of pmo-miR-315 (Figure 3.17) and *Pm*PPAE3 (Figure 3.18B) during WSSV infection was noted, suggesting that the pmo-miR-315 was likely to inhibit the *PmPPAE3* expression.

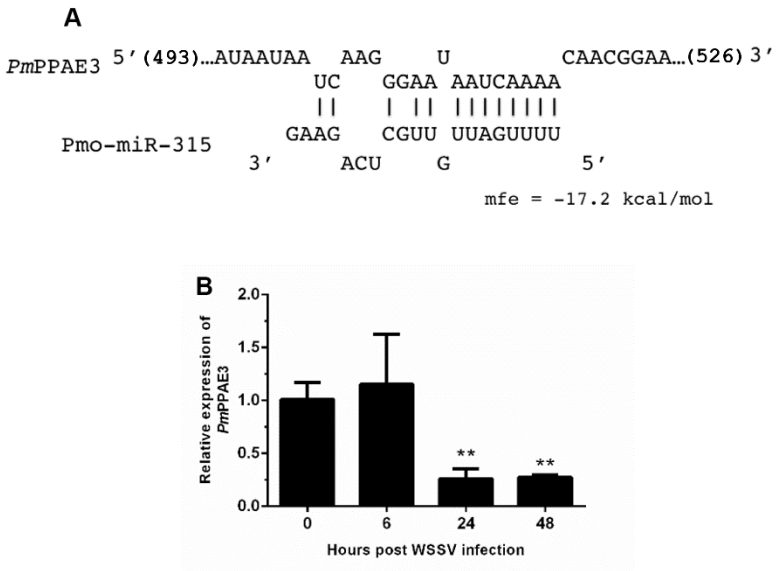

Figure 3.18 The pmo-miR-315 target mRNA, prophenoloxidase-activating enzyme 3 (*PmPPAE3*). **(A)** The pmo-miR-315/*PmPPAE3* base pairing and the binding energy was predicted using RNA hybrid software. **(B)** The relative expression level of *PmPPAE3* gene in *P. monodon* hemocyte at 0, 6, 24 and 48 h post-WSSV infection was investigated. The *EF-1α* gene was used as an internal control. All experiments were performed in triplicate. The ** indicates the significant difference at $P<0.05$.

3.3.3 Interaction between pmo-miR-315 and *PmPPAE3 in vitro*

The specific interaction of pmo-miR-315 with target mRNA binding site on *PmPPAE3* coding sequence was confirmed *in vitro* in HEK293T cell line. Either pmo-miR-315 mimic or its scramble miRNA and the luciferase reporter plasmid containing pmo-miR-315 binding site of *PmPPAE3* (pmir-T315) were co-transfected into HEK293T cells and then assayed for the luciferase activity. The results showed that in the presence of the mimic pmo-miR-315, the luciferase activity was reduced by about 36% compared with the reaction containing scramble miRNA (Figure 3.19). The reduction of luciferase activity suggested the specific binding of mimic pmo-miR-315 to miRNA-binding site of *PmPPAE3*.

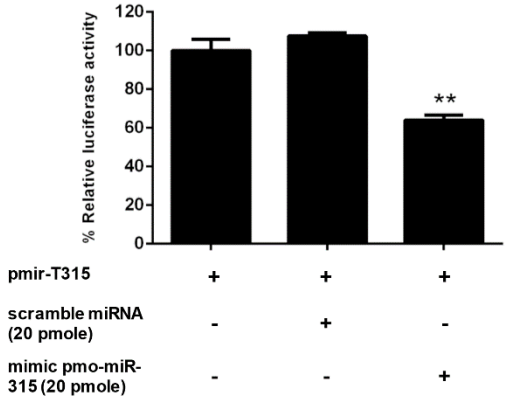

Figure 3.19 The pmo-miR-315/*PmPPAE3* interaction by luciferase reporter assay. The target sequence of pmo-miR-315 from *PmPPAE3* was amplified and cloned into the pmirGLO vector (pmir-T315). The pmo-miR-315 mimic or scramble pmo-miR-315 were co-transfected with pmir-T315 using Effectene transfection reagent (Qiagen) into HEK293T cells. At 48 h after transfection, the luciferase activity was measured using a Dual-luciferase® reporter assay system (Promega). The data shown is derived from triplicate experiments. The ** indicates significant difference ($P<0.01$).

3.3.4 Characterization of *PmPPAE3* gene

As mentioned above, the *Pm*PPAE3 entails the shrimp immunity against WSSV. The function of PPAE is generally involved in the proPO system as reported previously by Charoensapsri et al. (2009), and Charoensapsri et al. (2011). Therefore, the function of *Pm*PPAE3

in the proPO system was investigated. The full-length gene of *PmPPAE3* was identified. Using the 5′-RACE technique, the *PmPPAE3* full-length gene of 2,988 bp including 5′-UTR of 147 bp, 3′-UTR of 909 bp and the open reading frame (ORF) of 1,932 bp encoding for 643 amino acid residue protein was obtained.

The phylogenetic tree constructed based on the deduced amino acid sequences corresponding to the ORFs of PPAEs from crustaceans and insects showed that the PPAEs are clustered into the crustacean and insect lineages (Figure 3.20A). Amino acid sequence alignment of insect and crustacean PPAEs showed the conserved patterns of a clip domain, the serine proteinase domain, and the catalytic triad of histidine, aspartic acid, and serine residues (Figure 3.20B). Comparing with previously identified crustacean PPAEs, the *Pm*PPAE3 showed about 46.43%, 46.31% and 45.98% identity with *Fc*PPAE, *Lv*PPAE and *Pm*PPAE1, respectively. Like the *Pm*PPAE1 and *Pm*PPAE2, the *Pm*PPAE3 was specifically expressed in shrimp hemocytes (Figure 3.20C). Lastly, the function of *Pm*PPAE3 in the proPO system was further investigated by RNA interference (Figure 3.20D). The *PmPPAE3* gene knockdown dramatically reduced the PO activity in shrimp hemolymph (Figure 3.20E) suggesting its important role in the proPO system.

3.3.5 Role of pmo-miR-315 in WSSV-infected shrimp hemocytes

As stated in the previous experiment, suppression of *PmPPAE3* gene expression resulted in a decrease in PO activity in shrimp hemolymph and the pmo-miR-315 could bind to specific site in the open reading frame (ORF) of *PmPPAE3* gene. In order to reveal the role of pmo-miR-315 in WSSV-infected shrimp, overexpression of pmo-miR-315 by introducing the exogenous pmo-miR-315 mimic and the silencing of pmo-miR-315 by anti-pmo-miR-315 injection (AMO-miR-315) were performed in shrimp after WSSV infection. The expression of pmo-miR-315 and its target gene, *PmPPAE3*, was analyzed to confirm the regulatory role of pmo-miR-315 on *PmPPAE3* gene expression. As expected, the expression of *PmPPAE3* was decreased whereas that of pmo-miR-315 was highly increased (Figure 3.21A and B).

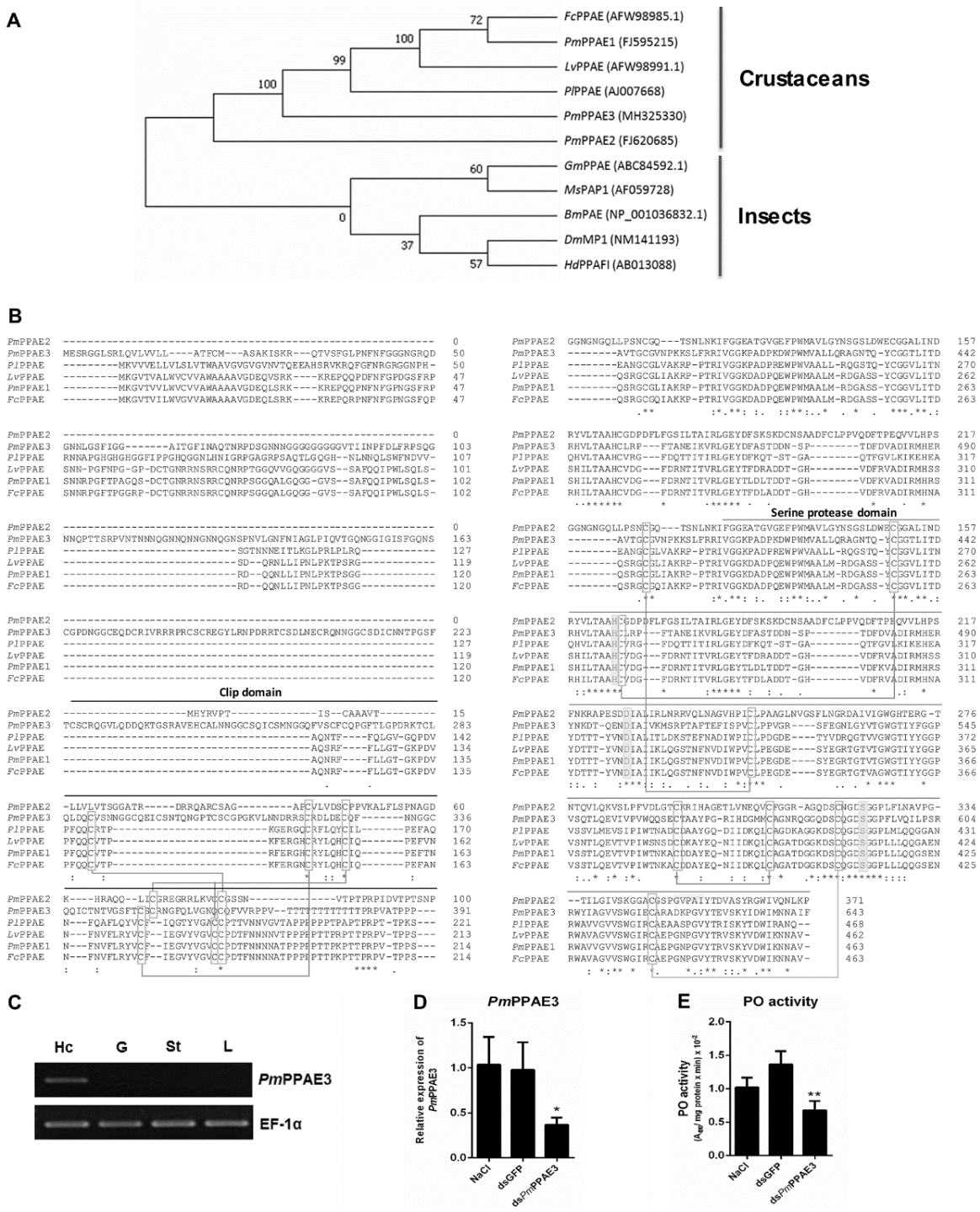

Figure 3.20 Characterization of *PmPPAE3* gene. (A) Phylogenetic analysis of PPAEs from various organisms including crustaceans and insects, e.g. *B. mori* PO-activating enzyme (*Bm*PAE); *M. sexta* proPO-activating proteinase 1 (*Ms*PAP1), *H. diomphalia* proPO-activating factor I (*Hd*PPAFI), *G. morsitans* (*Gm*PPAE) and *D. melanogaster* melanization protease1 (*Dm*MP1); shrimp *P. monodon* proPO-activating enzymes 1, 2 and 3 (*Pm*PPAE1, *Pm*PPAE2, *Pm*PPAE3), shrimp, *P. vannamei* proPO-activating enzyme (*Lv*PPAE), *F. chinensis* proPO-activating enzyme (*Fc*PPAE) and crayfish

P. leniusculus proPO-activating enzyme (*Pl*PPAE), was performed using ClustaX 2.1 and MEGA7 softwares. **(B)** Multiple alignment of the deduced amino acid sequences of *Pm*PPAE3 with other crustacean PPAEs was conducted using the Clustal Omega program. The conserved features of PPAEs such as the disulfide bond, the catalytic triad (histidine, aspartic acid, and serine residues), clip domain, and serine proteinase domain are shown. **(C)** The representative result of *PmPPAE3* gene tissue distribution analysis by semi-quantitative RT-PCR in the hemocytes (Hc), gill (G), stomach (St) and lymphoid organ (L), is shown. In this analysis, the *EF-1α* transcript was used as an internal control. All experiments were performed in triplicate. **(D)** The *PmPPAE3* gene knockdown using *PmPPAE3*-dsRNA was performed to reveal the functional role of *Pm*PPAE in proPO activating system. The effectiveness of the *PmPPAE3* gene knockdown is shown. Hemocytes collected from the control groups of 0.85% NaCl and dsGFP injected shrimp and from the experimental shrimp injected with *PmPPAE3*-dsRNA was analyzed for the expression of *PmPPAE3* gene by qRT-PCR using the *EF-1α* transcript as an internal control. **(E)** The PO activity was assayed in the *PmPPAE3* knockdown shrimp hemocytes. The data are derived from three independently replicated experiments. The * and ** indicate the significant difference at $P<0.05$ and $P<0.01$, respectively.

The PO activity was also determined in shrimp hemolymph to further elucidate the involvement of pmo-miR-315 in modulating the proPO system. The mimic pmo-miR-315 injected into the WSSV-infected shrimp resulted in a deduction of PO activity (Figure 3.21C), indicating that the pmo-miR-315 negatively regulated the shrimp proPO system. The WSSV copy number was also analyzed in hemocytes to determine the effect of introducing the pmo-miR-315 on WSSV replication in shrimp. Interestingly, as compared with those of control groups of saline and scramble miR-315 injection, the WSSV copy number was significantly increased in WSSV-challenged shrimp if the mimic pmo-miR-315 was introduced (Figure 3.21D). Conversely, silencing of pmo-miR-315 in WSSV-infected shrimp caused an increase in PO activity because of the up-regulation of *PmPPAE3* (Figure 3.21C). The inhibition of pmo-miR-315 activity by AMO-miR-315 slightly reduced the WSSV copy number when compared to that of pmo-miR-315 injection; however, it was still higher than the control groups (Figure 3.21D).

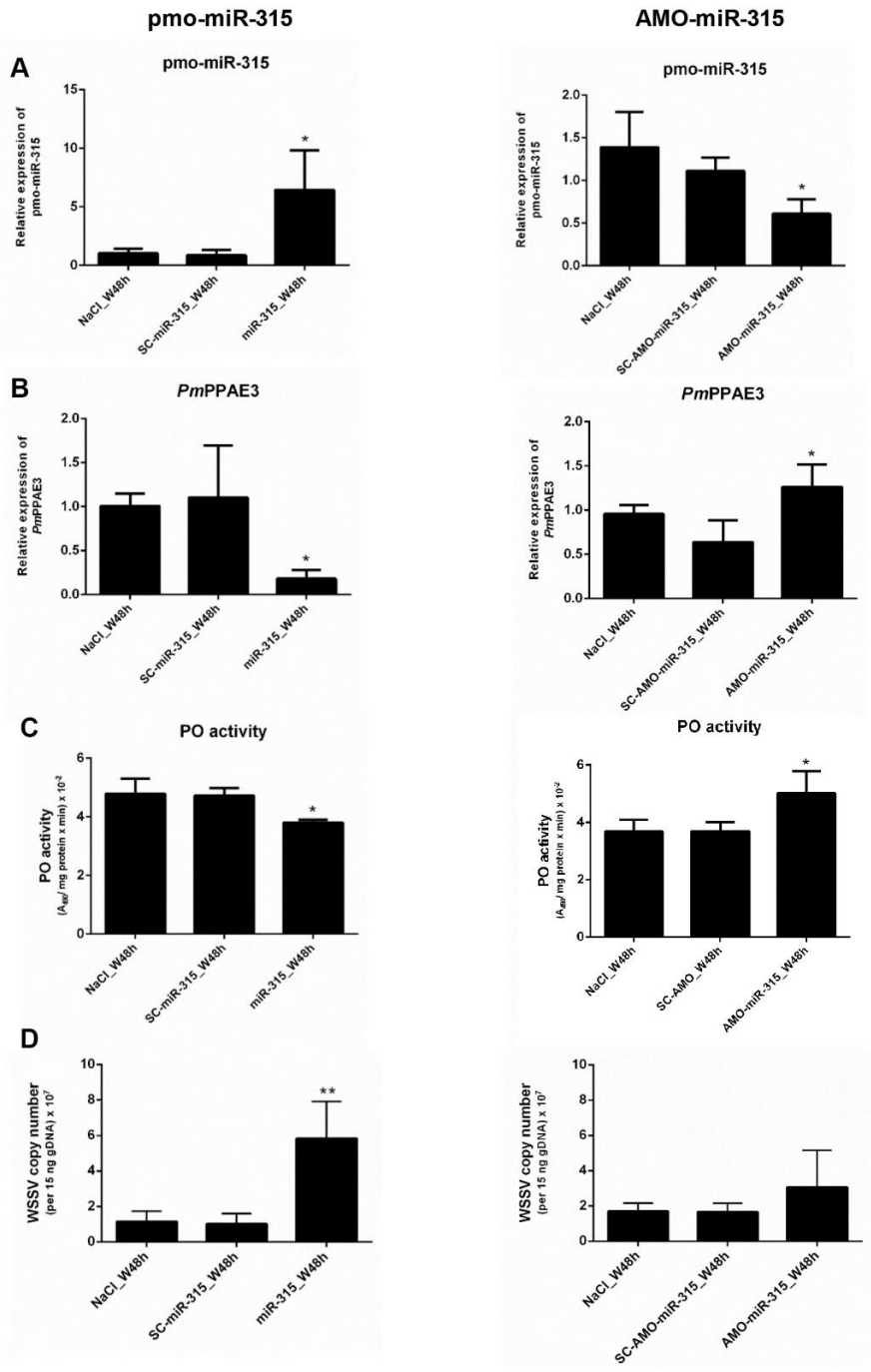

Figure 3.21 The role of pmo-miR-315 in WSSV-infected *P. monodon* hemocytes. In this experiment, either pmo-miR-315 mimic or AMO-miR-315 was injected into WSSV-infected shrimp. Then, several parameters were investigated including the expression level of **(A)** pmo-miR-315, **(B)** *PmPPAE3* gene, **(C)** PO activity and **(D)** WSSV copy number. The U6 and *EF-1α* was used as internal controls for pmo-miR-315 and *PmPPAE3* expression, respectively. All experiments were performed in triplicate. The * and ** indicate the significant difference at $P<0.05$ and $P<0.01$, respectively.

4. Discussion

4.1 Integrated analysis of microRNA and mRNA expression profiles in shrimp hemocyte challenge with VP_{AHPND} under heat and non-heat stress conditions

The previous observation that non-lethal heat shock may enhance production of heat shock proteins and then increase the expression of some immune-related genes resulting in enhanced immunity (Loc et al., 2013) has become a promising research interest because of its potential application in developing preventive strategies for diseases in shrimp. For instance, short-term hyperthermic treatment that was suggested to reduce gill-associated virus replication in *P. monodon* (de la Vega et al., 2006) may prove to be a simple and efficient prophylactic strategy. In this study, we have observed that chronic heat stress improves the survival of *P. vannamei*, which were challenged with AHPND-causing *V. parahaemolyticus* (VP_{AHPND}), revealing that non-lethal heat shock (NLHS) may indeed be an important immune-modulating factor to avoid mortalities caused by AHPND. However, *P. vannamei* tolerance to VP_{AHPND} infection was found to be influenced neither by Hsp70 accumulation nor the changes in tested immune-related proteins, such as proPO and hemocyanin (Loc et al., 2013). The mechanisms of tolerance to VP_{AHPND} infection under NLHS conditions, thus, still remain to be explored and explained by undescribed genes. To explore the microRNAs and gene networks that are involved in VP_{AHPND} infection and heat stress condition in *P. vannamei*, we performed smallRNA sequencing analysis and RNA-Seq (by Dr. Benedict A. Maralit) during VP_{AHPND} infection under NLHS and control conditions.

The small RNA libraries prepared from VP_{AHPND}-infected *P. vannamei* hemocyte under NLHS (NLHS-VP) generated 3 million reads across 3 individual libraries and identified 41 DEMs of 27 up-regulated and 14 down-regulated miRNA in NLHS-VP. Previously, 47 up-regulated and 36 down-regulated miRNA homologs were identified form VP_{AHPND} challenged *P. vannamei* hemocyte (Zheng et al., 2018). This evidence suggests that miRNAs might play an important role as regulators of shrimp immune system upon pathogen infection.

The qRT-PCR results were used to validate mRNA and miRNA expression level in NLHS-VP and NH-VP conditions. Eight genes selected from NGS data including *Relish*, *Lipoprotein receptor*, *Dynamin*, Importin7, *Juvenile hormone epoxide hydroxylase 1*; *JHEH-1*, *DNAJ5*, *Prophenoloxidase 1*; *PO1* and *Prophenoloxidase 2*; *PO2* were analyzed. It was found that NLHS-VP- and NH-VP responsive genes showed the expression profile similar to qRT-PCR. In the

meantime, 10 differentially expressed NLHS-VP-responsive miRNAs were selected to validate their expression. The results showed that lva-miR-7170-5p, lva-miR-2898, lva-miR-184, lva-miR-2169-3p, lva-miR-4901, lva-miR-92a-3p and lva-miR-61 were significantly differenced in NLHS-VP condition as the same to our smallRNA-Seq data.

The transcriptome reflects the mRNAs and miRNAs that are actively expressed under a particular condition. We attempted to acquire the miRNA-mRNA pairs through the use of DEMs and DEGs datasets and miRNA-targeting information. In most cases, the negative correlation between miRNAs and their target mRNAs is often considered proof of miRNA targeting (Alshalalfa et al., 2012). Previously, a total of 407 miRNA-mRNA interaction sites were predicted were identified involved in VP_{AHPND} infected *P. vannamei*. Among them, 11 DEMs might regulate 37 DE genes related to shrimp immune-responsive genes in response to VP_{AHPND} infection (Zheng et al., 2018). In the present study, a total of 779 pairs of NLHS-VP responsive miRNA-mRNA were identified with a negative correlation with the involvement of 19 DEMs and 707 DEGs. Among the interaction identified, only 11 heat-VP_{AHPND} responsive miRNAs might regulate shrimp immune-responsive genes/path ways such as homocyte homeostasis, AMP production and prophenoloxidase system.

Caspase and transglutaminase (TGase) are 2 proteins that play important role in hemocyte homeostasis in crustacean species (Apitanyasai et al., 2015; Lin et la., 2008). Caspase is a key player in apoptosis (Fiandalo et al., 2012). In *M. japonicus*, apoptosis pathway suppression using dsRNA could reduce the cumulative mortality of shrimp after challenge with *Vibrio alginolyticus* (Wang et al., 2018). TGase is known to be involved in blood coagulation, a conserved defense mechanism among invertebrates. In 2012, Fagutao et al. reported that suppression of TGase resulted in low haemocyte counts and high bacterial counts in *M. japonicas* (Fagutao et al., 2012). In our study, up-regulation of TGase and down-regulation of caspase identified from the NGS in shrimp hemocyte upon VP_{AHPND} infection under heat stress condition suggests that hemocyte homeostasis pathway might help shrimp tolerate to VP_{AHPND} infection after heat treatment.

Prophenoloxidase system is a major innate defense system in invertebrates that can kill pathogens and damaged shrimp tissues (Cerenius et al., 2004). Generally, phenoloxidase (PO), the key enzyme of the proPO-system, catalyzes the non-enzymatic conversion of phenolic substances to quinones, leading to the production of cytotoxic intermediates and melanin

(Christensen et al., 2005). Proteinases and their inhibitor such as specific serine proteinases, non-catalytic serine proteinase homologs (SPH) as protein cofactors, and proteinase inhibitors cascade are the important cascade that regulated proPO-system to prevent excessive production of these toxic substances (Cerenius et al., 2004). In shrimp, suppression of proPO-system by gene silencing could increase susceptibility to bacterial infection (Charoensapsri et al., 2009). In 2018, it was found that the up-regulation of the two *Lv*proPO transcripts in shrimp *P. vannamei* might increase disease resistance to VP_{AHPND} (Chomwong et al., 2018). In this study, genes related-proPO system were highly up-regulated after VP_{AHPND} infection under heat treatment condition. This suggests that proPO-system plays crucial role in bacterial defense leading to shrimp tolerance to VP_{AHPND} infection.

The Toll and IMD pathways are regarded as the main pathways regulating the immune response of invertebrates. They play a key role in the response to pathogen infection by regulating a large set of genes including antimicrobial peptide genes, many small peptides with unknown function as well as components of the melanization and clotting cascades to fight against pathogen infection (Li et al., 2013). Anti-lipopolysaccharide factor is a type of antimicrobial peptides (AMPs) with a vital role in antimicrobial defense (Gu et al., 2018). In shrimp, it was found that ALF and AMP are regulated by Toll and IMD pathways (Tassanakajon et al., 2018). Silencing of *Lv*ALF along with VP_{AHPND} and VP_{AHPND} toxin challenge resulted in increasing of cumulative mortality rate (Tinwongger et al., 2019; Maralit et al., 2018). Similar to this study, AMPs were up-regulated in NLHS-VP condition. To proof that AMP gene upregulation is modulated though signaling pathway, genes in each Toll and IMD pathway were analyzed their expression under NLHS-VP condition. We found that genes in IMD pathway including *IMD*, *IKK*ε and *Relish* were highly expressed in NLHS-VP condition. This suggests that NLHS treatment might modulate the up-regulation of IMD pathway resulting in overexpression of AMP production system that play important role in bacterial defense.

In conclusions, the integrated analysis of miRNA and mRNA transcriptome analysis suggested that NLHS-VP miRNAs and their predicted target may have strong influence on tolerance to VP_{AHPND} infection under NLHS treatment method. In total, 3 immune-related pathways were identified based on the miRNA targets function, including proPO-system, IMD pathway, and hemocyte homeostasis. These findings improve our current understanding of the effect of NLHS treatment that mediate the immunity of shrimp against VP_{AHPND} infection. Our

present study provides a new insight into the potential molecular mechanism of VP_{AHPND} infection under NLHS condition is a multiply miRNAs and mRNA caused biological change.

4.2 Function analysis of VP_{AHPND}-responsive miRNA in *P. vannamei* hemocyte

In this study, we used next-generation sequencing to survey the miRNA and miRNA expression profiles in VP_{AHPND} infection group and a control group of shrimp *P. vannamei*. This allowed us to determine the degree of changes in gene expression and miRNA expression. These results also revealed the distinct patterns of miRNA deregulation and predict the miRNA–mRNA regulatory network of *P. vannamei* upon VP_{AHPND} infection. Previously in *Scylla paramamosain*, 161 miRNAs were significantly differentially expressed during the VPAHPND challenge and the potential targets of these differentially expressed miRNAs were predicted as genes in innate immunity (Li et al., 2013). In shrimp *P. vannamei*, a total of 83 miRNAs were significantly differentially expressed in *P. vannamei* upon VP_{AHPND} infection (Zheng et al., 2018). In our study, 19 miRNAs were identified as a differentially expressed miRNA homologs in shrimp hemocyte upon VP_{AHPND} infection. Our study identified miRNA homologs against vertebrate and invertebrate species whereas the NGS from Zheng et al., 2018 identified miRNA homologs against only invertebrate species. Among both NGS data, only lva-miR-71 shared the same trend of the expression profiles. The qRT-PCR results were used to validate miRNA expression level in VP_{AHPND} challenge shrimp hemocyte. It was found that 4 from 10 miRNAs including lva-miR-9000, lva-miR-7170-5p, lva-miR-92a-3p and lva-miR-2169-3p were significantly differenced in shrimp hemocyte upon VP_{AHPND} infection at 6 hpi as same as our smallRNA-Seq data. Among the expression analysis, the 10 miRNAs were differentially expressed after VP_{AHPND} challenge.

According to Zheng et al., 2018, 12 miRNAs and their predicted target genes are possibly involved in modulating several immune-related processes in the pathogenesis of AHPND. In our study, the differentially expressed miRNAs were predicted against the transcriptomic data of VP_{AHPND} challenge *P. vannamei*. It was found that VP_{AHPND} responsive miRNAs might regulate several shrimp immune genes. Based on miRNA target function, the miR-4850 targeting *PO2* gene was characterized.

Upon bacterial infection, the shrimp proPO system takes part in shrimp antibacterial immunity by producing melanin and cytotoxic intermediate for bacterial sequestration (Li et al., 2008). The phenoloxidase (PO) is a key enzyme in the melanization cascade that also participates in cuticle sclerotization and wound healing. Sclerotized cuticle presents a barrier to infection,

and melanization around pathogens help to kill invading pathogens (Amparyup et al., 2013). In our study, *PO2* were predicted as a target gene of lva-miR-4850. It was significantly increased after 6 and 24 h post-VP_{AHPND} infection. As expected, the negative correlation of lva-miR-4850 expression and *PO2* gene expression was observed in hemocytes after VP_{AHPND} infection. In our study, an increase in the bacterial number in hepatopancreas and stomach of VP_{AHPND}-infected shrimp after lva-miR-4850 mimic injection indicated that the lva-miR-4850 functioned in enhancing VP_{AHPND}-infection by regulating the proPO system through the inhibition of PO2 gene expression. On the other hand, the amount of AMO-lva-miR-4850 challenged shrimp was lower than that of VP_{AHPND}-infected shrimp challenged with exogenous lva-miR-4850. In conclusions, the lva-miR-4850 was reduced in shrimp hemocyte after VP_{AHPND} infection resulted in increasing of PO2 gene in prophenoloxidase system.

4.3 Functional characterization of a WSSV-responsive miRNA form *P. monodon*

In 2007, the miR-315 from *Drosophila* was found to act as a potent activator of Wingless (Wg) signaling, a conserved pathway that regulates growth and tissue specification (Silver et al, 2007). Previously, the miR-315s from *M. japonicas, P. vannamei, P. monodon* and *F. chinensis* have been identified as a viral responsive miRNA in WSSV-infected shrimp hemocytes (Huang et al, 2012, Kaewkascholkul et al, 2016, Li et al, 2017, Zeng et al, 2015, Sun et al, 2016) suggesting that the shrimp miR-315 might be involved in antiviral immunity. Therefore, the pmo-miR-315 function was further characterized in this research.

The expression of pmo-miR-315 was detected in various shrimp tissues including hemocytes, gill, lymphoid organ and stomach. Interestingly, the expression level of pmo-miR-315 in hemocytes was significantly up-regulated, more than 30 times at 48 h post-WSSV infection, implying the specific role of pmo-miR-315 in shrimp antiviral response in hemocytes. Although the target gene of pmo-miR-315 was predicted as putative prophenoloxidase-activating enzyme *Pm*PPAE3 and serine/threonine protein kinase (Kaewkascholkul et al, 2016), in this research we focused on confirming the regulatory role of pmo-miR-315 on the expression of *PmPPAE3*.

Generally, the miRNA binds to the 3′-UTR of its target gene to regulate the translational repression and mRNA destabilization. Nevertheless, the binding site of miRNA can also be located at the 5′-UTR and coding sequence (CDS), albeit the regulatory activity may be different (Hausser et al. 2013; Brümmer and Hausser 2014). According to our prediction, the pmo-miR-315 can bind to CDS of *PmPPAE3* gene (Kaewkascholkul et al, 2016). The luciferase reporter assay revealed

that the pmo-miR-315 mimic could interact with the specific binding site on *PmPPAE3* CDS, which was indicated by almost 36% reduction in luciferase activity.

Melanization activated by the prophenoloxidase (proPO) system is a principal innate immune response in shrimp. Upon pathogen invasion, the binding of Pattern Recognition Proteins (PRPs) to the microbial cell wall components activates the serine proteinase cascade that finally activates the final proteinases, called proPO-activating enzymes (PPAEs). The PPAEs, then, cleave the inactive proPOs to active POs leading to the initiation of melanin formation (Tassanakajon et al, 2018). In *P. monodon*, the active *Pm*PPAE1 and *Pm*PPAE2 cleaves *Pm*proPO1 and *Pm*proPO2 generating the active PO1 and PO2, respectively (Amparyup et al, 2013). The *Pm*PPAE3 whose mRNA is the target of pmo-miR-315 is a novel isoform of *Pm*PPAE characterized herein. It was mainly expressed in shrimp hemocytes and significantly suppressed after 24 and 48 h post WSSV infection. As expected, the negative correlation of pmo-miR-315 expression and *PmPPAE3* gene expression was observed in hemocytes after WSSV infection.

The full-length gene of *PmPPAE3* was identified in this study and its deduced amino acid sequence was compared with other *Pm*PPAEs from various species as well as the *Pm*PPAE1 and *Pm*PPAE2 (Charoensapsri et al, 2009, 2011). The multiple alignment of different PPAE amino acid sequences revealed that the *Pm*PPAE3 was closely related to *Fc*PPAE, *Lv*PPAE and *Pm*PPAE1. The phylogenetic analysis showed that the shrimp PPAEs and a crayfish PPAE belonged to the crustaceans cluster. Besides, the *PmPPAE3* gene was hemocyte specific like *Pm*PPAE1 and *Pm*PPAE2. The function of *Pm*PPAE3 in proPO system was confirmed using the RNA interference technique. Therefore, the *Pm*PPAE3 was considered as a novel clips serine proteinase that function in the proPO system.

As mentioned above, the melanization reaction is activated through the proPO cascade after pathogen infection and unavoidably generates highly toxic molecules. These toxic intermediates are not only involved in pathogen killing but also cause the damage of the host cells (Amparyup et al. 2013; Charoensapsri et al. 2014). Therefore, the activation cascade is needed to be tightly regulated. To date, several proteinase inhibitors of melanization cascade have been reported in shrimp, including the melanization inhibition protein (MIP), serine proteinase inhibitors (serpins), alpha-2-macroglobulin (A2M) and pacifastin (Tassanakajon et al, 2018). Furthermore, the small RNAs can also regulate the proPO system. The shrimp miR-100, which was up-regulated after

WSSV or *V. alginolyticus* infection, can regulate several shrimp immune reactions including proPO activity, SOD activity and phagocytosis (Wang et al, 2017).

The involvement of proPO system upon WSSV infection has been reported. The PO activity is strongly decreased after WSSV-infection in shrimp (Sutthangkul et al, 2015). Later, it is found that the WSSV453 binds to and interferes with the pro*Pm*PPAE2 activation to active *Pm*PPAE2 resulting in the suppression of shrimp melanization (Sutthangkul et al. 2017; Sutthangkul et al. 2015)**.** In our research, the role of pmo-miR-315 and *Pm*PPAE3 in proPO system during WSSV infection in shrimp was explored. Injection of pmo-miR-315 mimic into the shrimp resulted in a reduction of *PmPPAE3* gene expression and the PO activity as expected. On the other hand, inhibition of pmo-miR-315 by AMO-miR-315 increased the *PmPPAE3* gene expression leading to the increase in PO activity in WSSV-infected shrimp hemocytes. Therefore, we can conclude that the pmo-miR-315 regulates the proPO system via *PmPPAE3* post-transcriptional repression.

Upon WSSV infection, the shrimp proPO system takes part in shrimp antiviral immunity by producing melanin and cytotoxic intermediate for viral sequestration. However, the WSSV can overcome shrimp antiviral immunity partly by proPO system suppression. Several crustacean miRNAs have been reported to promote WSSV propagation. In *M. rosenbergii,* the host miR-9041 and miR-9850 play positive roles in WSSV replication by targeting the *STAT* gene (Huang et al. 2016). In crabs, *E. sinensis,* the miR-217 leads to a decrease in the transcript level of *Tube* gene resulting in the enhancement of WSSV copies (Huang et al, 2017). Meanwhile, the survival rate of miR-100 silenced shrimp after WSSV infection is increased as the PO activity (Wang et al, 2017). According to our research, an increase in the viral copy number in WSSV-infected shrimp after pmo-miR-315 mimic injection indicated that the pmo-miR-315 functioned in enhancing viral replication by regulating the proPO system through the inhibition of *PmPPAE3* gene expression. On the other hand, the viral copy number of AMO-miR-315 challenged shrimp was lower than that of WSSV-infected shrimp challenged with exogenous pmo-miR-315 but was not lower than the control groups as expected (Figure 21D). This might be because the pmo-miR-315 was not totally silenced. Since the whole genome sequence of *P. monodon* has not been reported yet, it was possible that the AMO-miR-315 could also target other unknown genes that might affect the WSSV propagation.

Taken together, our research offer a new mechanism on how WSSV inhibits proPO system by triggering host miRNA. The WSSV infection causes the pmo-miR-315 over-expression and subsequently inhibits the *PmPPAE3* expression leading to a decrease in PO activity and increase in WSSV copy number in WSSV-infected shrimp hemocytes. Therefore, the pmo-miR-315 regulates the proPO system through the suppression of *PPAE3* gene expression which leads to the promotion of viral propagation in shrimp hemocytes during WSSV infection

References

Afgan E, Baker D, Van den Beek M, Blankenberg D, Bouvier D, Čech M, Chilton J, Clements D, Coraor N, Eberhard C, Grüning B. The Galaxy platform for accessible, reproducible and collaborative biomedical analyses: 2016 update. Nucleic acids research. 2016 May 2;44(W1):W3-10.

Alshalalfa M. MicroRNA response elements-mediated miRNA-miRNA interactions in prostate cancer. Advances in bioinformatics. 2012;2012.

Altschul SF, Gish W, Miller W, Myers EW, Lipman DJ. Basic local alignment search tool. Journal of molecular biology. 1990 Oct 5;215(3):403-10.

Amparyup P, Charoensapsri W, Tassanakajon A. Prophenoloxidase system and its role in shrimp immune responses against major pathogens. Fish & shellfish immunology. 2013 Apr 1;34(4):990-1001.

Apitanyasai K, Amparyup P, Charoensapsri W, Senapin S, Tassanakajon A. Role of *Penaeus monodon* hemocyte homeostasis associated protein (*Pm*HHAP) in regulation of caspase-mediated apoptosis. Developmental & Comparative Immunology. 2015 Nov 1;53(1):234-43.

Ashburner M, Ball CA, Blake JA, Botstein D, Butler H, Cherry JM, Davis AP, Dolinski K, Dwight SS, Eppig JT, Harris MA. Gene ontology: tool for the unification of biology. Nature genetics. 2000 May 1;25(1):25.

Azzam G, Smibert P, Lai EC, Liu JL. *Drosophila* Argonaute 1 and its miRNA biogenesis partners are required for oocyte formation and germline cell division. Developmental biology. 2012 May 15;365(2):384-94.

Bartel DP. MicroRNAs: genomics, biogenesis, mechanism, and function. cell. 2004 Jan 23;116(2):281-97.

Bradford MM. A rapid and sensitive method for the quantitation of microgram quantities of protein utilizing the principle of protein-dye binding. Anal Biochem (1976);72(1-2):248-54. doi: 10.1016/0003-2697(76)90527-3

Brümmer A, Hausser J. MicroRNA binding sites in the coding region of mRNAs: Extending the repertoire of post-transcriptional gene regulation. Bioessays. 2014 Jun;36(6):617-26.

Cerenius L, Söderhäll K. The prophenoloxidase-activating system in invertebrates. Immunological reviews. 2004 Apr;198(1):116-26.

Christensen BM, Li J, Chen CC, Nappi AJ. Melanization immune responses in mosquito vectors. Trends in parasitology. 2005 Apr 1;21(4):192-9.

Charoensapsri W, Amparyup P, Hirono I, Aoki T, Tassanakajon A. Gene silencing of a prophenoloxidase activating enzyme in the shrimp, *Penaeus monodon*, increases susceptibility to *Vibrio harveyi* infection. Developmental & Comparative Immunology. 2009 Jul 1;33(7):811-20.

Charoensapsri W, Amparyup P, Hirono I, Aoki T, Tassanakajon A. *Pm*PPAE2, a new class of crustacean prophenoloxidase (proPO)-activating enzyme and its role in PO activation. Developmental & Comparative Immunology. 2011 Jan 1;35(1):115-24.

Chomwong S, Charoensapsri W, Amparyup P, Tassanakajon A. Two host gut-derived lactic acid bacteria activate the proPO system and increase resistance to an AHPND-causing strain of *Vibrio parahaemolyticus* in the shrimp *Litopenaeus vannamei*. Developmental & Comparative Immunology. 2018 Dec 1;89:54-65.

Conesa A, Götz S, García-Gómez JM, Terol J, Talón M, Robles M. Blast2GO: a universal tool for annotation, visualization and analysis in functional genomics research. Bioinformatics. 2005 Aug 4;21(18):3674-6.

de la Vega E, Hall MR, Degnan BM, Wilson KJ. Short-term hyperthermic treatment of *Penaeus monodon* increases expression of heat shock protein 70 (HSP70) and reduces replication of gill associated virus (GAV). Aquaculture. 2006 Mar 31;253(1-4):82-90.

Eulalio A, Schulte L, Vogel J. The mammalian microRNA response to bacterial infections. RNA biology. 2012 Jun 1;9(6):742-50.

Fagutao FF, Maningas MB, Kondo H, Aoki T, Hirono I. Transglutaminase regulates immune-related genes in shrimp. Fish & shellfish immunology. 2012 May 1;32(5):711-5.

Fiandalo MV, Kyprianou N. Caspase control: protagonists of cancer cell apoptosis. Experimental oncology. 2012 Oct;34(3):165.

Finn RD, Clements J, Eddy SR. HMMER web server: interactive sequence similarity searching. Nucleic acids research. 2011 May 18;39(suppl_2):W29-37.

Grabherr MG, Haas BJ, Yassour M, Levin JZ, Thompson DA, Amit I, Adiconis X, Fan L, Raychowdhury R, Zeng Q, Chen Z. Full-length transcriptome assembly from RNA-Seq data without a reference genome. Nature biotechnology. 2011 Jul;29(7):644.

Gong Y, Ju C, Zhang X. The miR-1000-p53 pathway regulates apoptosis and virus infection in shrimp. Fish & shellfish immunology. 2015 Oct 1;46(2):516-22.

Gu HJ, Sun QL, Jiang S, Zhang J, Sun L. First characterization of an anti-lipopolysaccharide factor (ALF) from hydrothermal vent shrimp: Insights into the immune function of deep-sea crustacean ALF. Developmental & Comparative Immunology. 2018 Jul 1;84:382-95.

Hausser J, Syed AP, Bilen B, Zavolan M. Analysis of CDS-located miRNA target sites suggests that they can effectively inhibit translation. Genome research. 2013 Apr 1;23(4):604-15.

He Y, Yang K, Zhang X. Viral microRNAs targeting virus genes promote virus infection in shrimp in vivo. Journal of virology. 2014 Jan 15;88(2):1104-12.

Huang T, Cui Y, Zhang X. Involvement of viral microRNA in the regulation of antiviral apoptosis in shrimp. Journal of virology. 2014 Mar 1;88(5):2544-54.

Huang T, Xu D, Zhang X. Characterization of host microRNAs that respond to DNA virus infection in a crustacean. Bmc Genomics. 2012 Dec;13(1):159.

Huang Y, Wang W, Ren Q. Two host microRNAs influence WSSV replication via *STAT* gene regulation. Scientific reports. 2016 Mar 31;6:23643.

Huang Y, Han K, Wang W, Ren Q. Host microRNA-217 promotes white spot syndrome virus infection by targeting *tube* in the Chinese mitten crab (*Eriocheir sinensis*). Frontiers in cellular and infection microbiology. 2017 May 4;7:164.

Junprung W, Supungul P, Tassanakajon A. HSP70 and HSP90 are involved in shrimp *Penaeus vannamei* tolerance to AHPND-causing strain of *Vibrio parahaemolyticus* after non-lethal heat shock. Fish & shellfish immunology. 2017 Jan 1;60:237-46.

Kaewkascholkul N, Somboonviwat K, Asakawa S, Hirono I, Tassanakajon A, Somboonwiwat K. Shrimp miRNAs regulate innate immune response against white spot syndrome virus infection. Developmental & Comparative Immunology. 2016 Jul 1;60:191-201.

Kanehisa M, Goto S, Sato Y, Furumichi M, Tanabe M. KEGG for integration and interpretation of large-scale molecular data sets. Nucleic acids research. 2011 Nov 10;40(D1):D109-14.

Krogh A, Larsson B, Von Heijne G, Sonnhammer EL. Predicting transmembrane protein topology with a hidden Markov model: application to complete genomes. Journal of molecular biology. 2001 Jan 19;305(3):567-80.

Krüger J, Rehmsmeier M. RNAhybrid: microRNA target prediction easy, fast and flexible. Nucleic acids research. 2006 Jul 1;34(suppl_2):W451-4.

Kumar S, Stecher G, Tamura K. MEGA7: molecular evolutionary genetics analysis version 7.0 for bigger datasets. Molecular biology and evolution. 2016 Mar 22;33(7):1870-4.

Lagos-Quintana M, Rauhut R, Yalcin A, Meyer J, Lendeckel W, Tuschl T. (2002) Identification of tissue-specific microRNAs from mouse. Curr Biol. 30: 735-739.

Lin X, Söderhäll K, Söderhäll I. Transglutaminase activity in the hematopoietic tissue of a crustacean, Pacifastacus leniusculus, importance in hemocyte homeostasis. BMC immunology. 2008 Dec;9(1):58.

Li X, Meng X, Luo K, Luan S, Shi X, Cao B, Kong J. The identification of microRNAs involved in the response of Chinese shrimp *Fenneropenaeus chinensis* to white spot syndrome virus infection. Fish & shellfish immunology. 2017 Sep 1;68:220-31.

Li F, Xiang J. Signaling pathways regulating innate immune responses in shrimp. Fish & shellfish immunology. 2013 Apr 1;34(4):973-80.

Li S, Zhu S, Li C, Zhang Z, Zhou L, Wang S, Wang S, Zhang Y, Wen X. Characterization of microRNAs in mud crab *Scylla paramamosain* under *Vibrio parahaemolyticus* infection. PLoS One. 2013 30:e73392.

Loc NH, MacRae TH, Musa N, Abdullah MD, Wahid ME, Sung YY. Non-lethal heat shock increased Hsp70 and immune protein transcripts but not *Vibrio* tolerance in the white-leg shrimp. PloS one. 2013 Sep 9;8(9):e73199.

Lu LF, Liston A. MicroRNA in the immune system, microRNA as an immune system. Immunology. 2009 127: 291-298.

Maralit BA, Jaree P, Boonchuen P, Tassanakajon A, Somboonwiwat K. Differentially expressed genes in hemocytes of *Litopenaeus vannamei* challenged with *Vibrio parahaemolyticus* AHPND (VPAHPND) and VP_{AHPND} toxin. Fish & shellfish immunology. 2018 Oct 1;81:284-96.

Mendoza-Cano F, Sánchez-Paz A. Development and validation of a quantitative real-time polymerase chain assay for universal detection of the White Spot Syndrome Virus in marine crustaceans. Virology journal. 2013 Dec;10(1):186

Petersen TN, Brunak S, Von Heijne G, Nielsen H. SignalP 4.0: discriminating signal peptides from transmembrane regions. Nature methods. 2011 Oct;8(10):785.

Pfaffl MW. A new mathematical model for relative quantification in real-time RT–PCR. Nucleic acids research. 2001 May 1;29(9):e45-.

Powell S, Szklarczyk D, Trachana K, Roth A, Kuhn M, Muller J, Arnold R, Rattei T, Letunic I, Doerks T, Jensen LJ. eggNOG v3. 0: orthologous groups covering 1133 organisms at 41 different taxonomic ranges. Nucleic acids research. 2011 Nov 16;40(D1):D284-9.

Punta M, Coggill PC, Eberhardt RY, Mistry J, Tate J, Boursnell C, Pang N, Forslund K, Ceric G, Clements J, Heger A. The Pfam protein families database. Nucleic acids research. 2011 Nov 29;40(D1):D290-301.

Robinson MD, McCarthy DJ, Smyth GK. edgeR: a Bioconductor package for differential expression analysis of digital gene expression data. Bioinformatics. 2010 Jan 1;26(1):139-40.

Rungrassamee W, Leelatanawit R, Jiravanichpaisal P, Klinbunga S, Karoonuthaisiri N. Expression and distribution of three heat shock protein genes under heat shock stress and under exposure to *Vibrio harveyi* in *Penaeus monodon*. Developmental & Comparative Immunology. 2010 Oct 1;34(10):1082-9.

Shu L, Li C, Zhang X. The role of shrimp miR-965 in virus infection. Fish & shellfish immunology. 2016 Jul 1;54:427-34.

Siddle KJ, Tailleux L, Deschamps M, Loh YH, Deluen C, Gicquel B, Antoniewski C, Barreiro LB, Farinelli L, Quintana-Murci L. Bacterial infection drives the expression dynamics of microRNAs and their isomiRs. PLoS genetics. 2015 Mar 20;11(3):e1005064.

Silver SJ, Hagen JW, Okamura K, Perrimon N, Lai EC. Functional screening identifies miR-315 as a potent activator of Wingless signaling. Proceedings of the National Academy of Sciences. 2007 Nov 13;104(46):18151-6.

Somboonwiwat K, Chaikeeratisak V, Wang HC, Lo CF, Tassanakajon A. Proteomic analysis of differentially expressed proteins in *Penaeus monodon* hemocytes *after Vibrio harveyi* infection. Proteome science. 2010 Dec;8(1):39.

Sun X, Liu QH, Yang B, Huang J. Differential expression of microRNAs of *Litopenaeus vannamei* in response to different virulence WSSV infection. Fish & shellfish immunology. 2016 Nov 1;58:18-23.

Sung YY, Van Damme EJ, Sorgeloos P, Bossier P. Non-lethal heat shock protects gnotobiotic Artemia franciscana larvae against virulent *Vibrios*. Fish & shellfish immunology. 2007 Apr 1;22(4):318-26.

Sun Y, Zhang X. Role of DCP1-DCP2 complex regulated by viral and host microRNAs in DNA virus infection. Fish & shellfish immunology. 2019 Sep 92, 21-30.

Sutthangkul J, Amparyup P, Eum JH, Strand MR, Tassanakajon A. Anti-melanization mechanism of the white spot syndrome viral protein, WSSV453, via interaction with shrimp proPO-activating enzyme, *Pm*proPPAE2. Journal of General Virology. 2017 Apr 28;98(4):769-78.

Sutthangkul J, Amparyup P, Charoensapsri W, Senapin S, Phiwsaiya K, Tassanakajon A. Suppression of shrimp melanization during white spot syndrome virus infection. Journal of Biological Chemistry. 2015 Mar 6;290(10):6470-81.

Taganov, K. D., et al. NF-kappaB-dependent induction of microRNA miR-146, an inhibitor targeted to signaling proteins of innate immune responses, Proc Natl Acad Sci U S A, 2006 103(33), 12481-12486.

Tassanakajon A, Rimphanitchayakit V, Visetnan S, Amparyup P, Somboonwiwat K, Charoensapsri W, Tang S. Shrimp humoral responses against pathogens: antimicrobial peptides and melanization. Developmental & Comparative Immunology. 2018 Mar 1;80:81-93.

Tran L, Nunan L, Redman RM, Mohney LL, Pantoja CR, Fitzsimmons K, Lightner DV. Determination of the infectious nature of the agent of acute hepatopancreatic necrosis syndrome affecting penaeid shrimp. Diseases of aquatic organisms. 2013 Jul 9;105(1):45-55.

Triboulet R, Mari B, Lin YL, Chable-Bessia C, Bennasser Y, Lebrigand K, Cardinaud B, Maurin T, Barbry P, Baillat V, Reynes J. Suppression of microRNA-silencing pathway by HIV-1 during virus replication. Science. 2007 Mar 16;315(5818):1579-82.

Tinwongger S, Thawonsuwan J, Kondo H, Hirono I. Identification of an anti-lipopolysaccharide factor AV-R isoform (LvALF AV-R) related to Vp_PirAB-like toxin resistance in Litopenaeus vannamei. Fish & shellfish immunology. 2019 Jan 1;84:178-88.

Umbach JL, Cullen BR. The role of RNAi and microRNAs in animal virus replication and antiviral immunity. Genes & development. 2009 May 15;23(10):1151-64.

Untergasser A, Cutcutache I, Koressaar T, Ye J, Faircloth BC, Remm M, Rozen SG. Primer3—new capabilities and interfaces. Nucleic acids research. 2012 Jun 21;40(15):e115-.

Wang B, Li F, Dong B, Zhang X, Zhang C, Xiang J. Discovery of the genes in response to white spot syndrome virus (WSSV) infection in *Fenneropenaeus chinensis* through cDNA microarray. Marine Biotechnology. 2006 Oct 1;8(5):491-500.

Wang Z, Sun B, Zhu F. The shrimp hormone receptor acts as an anti-apoptosis and anti-inflammatory factor in innate immunity. Fish & shellfish immunology. 2018 Jan 1;72:581-92.

Wang Z, Zhu F. MicroRNA-100 is involved in shrimp immune response to white spot syndrome virus (WSSV) and *Vibrio alginolyticus* infection. Scientific reports. 2017 Feb 9;7:42334.

Wu TH, Pan CY, Lin MC, Hsieh JC, Hui CF, Chen JY. In vivo screening of zebrafish microRNA responses to bacterial infection and their possible roles in regulating immune response genes after lipopolysaccharide stimulation. Fish Physiol Biochem. 2012 38:1299-1310.

Xu X, Yuan J, Yang L, Weng S, He J, Zuo H. The Dorsal/miR-1959/Cactus feedback loop facilitates the infection of WSSV in *Litopenaeus vannamei.* Fish & shellfish immunology. 2016 Sep 1;56:397-401.

Yang YT, Chen IT, Lee CT, Chen CY, Lin SS, Hor LI, Tseng TC, Huang YT, Sritunyalucksana K, Thitamadee S, Wang HC. Draft genome sequences of four strains of *Vibrio parahaemolyticus*, three of which cause early mortality syndrome/acute hepatopancreatic necrosis disease in shrimp in China and Thailand. Genome Announc. 2014 Oct 30;2(5):e00816-14.

Yang L, Yang G, Zhang X. The miR-100-mediated pathway regulates apoptosis against virus infection in shrimp. Fish & shellfish immunology. 2014 Sep 1;40(1):146-53.

Zeng D, Chen X, Xie D, Zhao Y, Yang Q, Wang H, Li Y, Chen X. Identification of highly expressed host microRNAs that respond to white spot syndrome virus infection in the Pacific white shrimp *Litopenaeus vannamei* (Penaeidae). Genet Mol Res. 2015 Oct;14(2):4818-28.

Zhou J, Wang WN, He WY, Zheng Y, Wang L, Xin Y, Liu Y, Wang AL. Expression of HSP60 and HSP70 in white shrimp, *Litopenaeus vannamei* in response to bacterial challenge. Journal of invertebrate pathology. 2010 Mar 1;103(3):170-8.

Zheng Z, Aweya JJ, Wang F, Yao D, Lun J, Li S, Ma H, Zhang Y. Acute Hepatopancreatic Necrosis Disease (AHPND) related microRNAs in *Litopenaeus vannamei* infected with AHPND-causing strain of *Vibrio parahemolyticus*. BMC genomics. 2018 Dec;19(1):335.

ผลงานจากงานวิจัย (output)

1. ผลงานตีพิมพ์ในวารสารวิชาการนานาชาติ

มีการตีพิมพ์เผยแพร่ผลงานวิจัยในวารสารระดับนานาชาติ 1 เรื่อง มีผลงานวิจัยที่ส่งเพื่อตีพิมพ์ (submitted) 1 เรื่อง และอยู่ระหว่างจัดเตรียมบทความอีก 1 เรื่อง

1.1 Jaree P, Wongdontri C, Somboonwiwat K. White spot syndrome virus-induced shrimp miR-315 attenuates prophenoloxidase activation via PPAE3 gene suppression. Frontiers in Immunology. Front Immunol. 2018, 25;9:2184

1.2 Boonchuen P, Maralit BA, Jaree P, Tassanakajon A, Somboonwiwat K. MicroRNA and mRNA interactions contribute to coordinating the immune response in chronic non-lethal heat stressed *Litopenaeus vannamei* against acute hepatopancreatic necrosis disease-causing strain of *Vibrio parahaemolyticus*. PLOS Pathogens. (submitted)

1.3 Boonchuen P, Somboonviwat K, Tassanakajon A, Somboonwiwat K. Identification of miRNA from *Penaeus vannamei* in response to *Vibrio parahaemolyticus* AHPND infection (manuscript in preparation)

2. การได้รับเชิญไปเป็นวิทยากร

2.1 รศ.ดร. กุลยา สมบูรณ์วิวัฒน์ ได้รับเชิญให้ไปบรรยายในงานประชุมวิชาการต่างๆ ดังนี้

2.1.1 ได้รับเชิญให้เป็น Invited Spearker ในงานประชุมวิชาการ International Mini-symposium on Frontier Aquaculture Science ซึ่งจัดขึ้นในวันที่ 9 ธันวาคม 2560 ที่ National Cheng Kung University ประเทศไต้หวัน บรรยายในหัวข้อ “The shrimp antimicrobial peptide antilipopolysaccharide factor (ALF): Basic and protential applications”

2.1.2 ได้รับเชิญให้เป็น Invited Spearker ในงานประชุมวิชาการวิทยาศาสตร์และเทคโนโลยีแห่งประเทศไทย ครั้งที่ 43 (วทท.43) ซึ่งจัดขึ้นระหว่างวันที่ 17-19 ธันวาคม 2560 ที่ จุฬาลงกรณ์มหาวิทยาลัย กรุงเทพมหานคร บรรยายในหัวข้อ “The shrimp antimicrobial peptide antilipopolysaccharide factor (ALF): Basic and potential applications”

3. การเสนอผลงานในที่ประชุมวิชาการ

มีผลงานนำเสนอในที่ประชุมวิชาการรวมทั้งสิ้น ? เรื่อง โดยแบ่งเป็นผลงานที่นำเสนอในที่ประชุมวิชาการระดับนานาชาติ ? เรื่อง และผลงานที่นำเสนอในที่ประชุมวิชาการระดับชาติ ? เรื่อง

3.1 การเสนอผลงานในที่ประชุมระดับนานาชาติ

มีผลงานนำเสนอในที่ประชุมวิชาการระดับนานาชาติรวม 7 เรื่อง โดยแบ่งเป็นประเภทบรรยาย 4 เรื่อง และโปสเตอร์ 3 เรื่อง ดังนี้

3.1.1 ประเภทบรรยาย

3.1.1.1 Boonchuen P, Jaree P, Somboonwiwat K. (2016). Differential expression of mRNAs from *Penaeus vannamei* upon *Vibrio parahaemolyticus* AHPND infection. 21st Biological Sciences Graduate Congress (BSGC). 15–16 December 2016. University Of Malaya, Malaysia.

3.1.1.2 Somboonwiwat K, Maralit BA, Jaree P, Boonchuen P, Luangtrakul W, Tassanakajon T. (2017). Efffect of chronic heat stress response on hemocyte transcriptome of *Penaeus vannamei* challenged with *Vibrio parahaemolyticus* AHPND. The 10th Symposium on Diseases in Asian Aquaculture (DAA10). 28 August–1 September 2017. The Anvaya Beach Resort, Kuta, Bali, Indonesia.

3.1.1.3 Boonchuen P. (2017). Identification of miRNAs from *Penaeus vannamei* in response to *Vibrio parahaemolyticus* AHPND infection and heat stress. The 22nd Biological Sciences Graduate Congress (BSGC2017). 19–21 December 2017. University Town, NUS, Singapore.

3.1.1.4 Somboonwiwat K, Boonchuen P, Maralit BA, Tassanakajon A. Integrated miRNA AND mRNA transcriptome analyses of *Penaeus vannamei* hemocyte reveals the effect of non-lethal heat stress on shrimp antibacterial immunity. Aquaculture 2019. 7-11 March 2019. New Orleans, Louisiana, USA

3.1.2 ประเภทโปสเตอร์

3.1.2.1 Boonchuen P, Methatham T, Jaree P, Tassanakajon A, Somboonwiwat K. (2017). Hemocyanin of *Litopenaeus vannamei* agglutinates *Vibrio parahaemolyticus* AHPND (VP_{AHPND}) and neutralizes VP_{AHPND} toxin. The 10th Symposium on Diseases in Asian Aquaculture (DAA10). 28 August–1 September 2017. The Anvaya Beach Resort, Kuta, Bali, Indonesia.

3.1.2.2 Boonchuen P, Somboonwiwat K. (2018). Identification of miRNAs from *Penaeus vannamei* in response to *Vibrio parahaemolyticus* AHPND infection. The 6th International Conference on Biochemistry and Molecular Biology (BMB). 20–22 June 2018. Rayong, Thailand.

3.1.2.3 Wongdontri C, Somboonwiwat K. (2018). Characterization of shrimp miRNAs involved in pathogen–challenged responses. The 6th International Conference on Biochemistry and Molecular Biology (BMB). 20–22 June 2018. Rayong, Thailand.

3.2 การเสนอผลงานในที่ประชุมระดับชาติ

มีผลงานนำเสนอในที่ประชุมวิชาการระดับชาติ 2 เรื่อง โดยแบ่งเป็นประเภทบรรยาย 1 เรื่อง และ โปสเตอร์ 1 เรื่อง ดังนี้

3.2.1 ประเภทบรรยาย

3.2.1.1 Jaree P, Tassanakajon A, Somboonwiwat K. (2015). Characterization of mir–315 function in shrimp, *Penaeus monodon*, antiviral immunity. The 41st Congress on Science and Technology of Thailand (STT41). 6–8 November 2015. Nakhonratchasima, Thailand.

3.2.2 ประเภทโปสเตอร์

3.2.2.1 Kanoksinwuttipong N, Wongdontri C, Somboonwiwat K. (2017). Expression analysis of miRNAs involved in pathogen challenge in shrimp. The 43rd Congress on Science and Technology of Thailand (STT43). 17–19 December 2017. Chulalongkorn University, Bangkok, Thailand.

4. รางวัล

4.1 รางวัลจากหน่วยงานต่างๆ

อาจารย์และนักวิจัยได้รับรางวัลจากหน่วยงานต่างๆ ดังนี้

4.1.1 รศ.ดร. กุลยา สมบูรณ์วิวัฒน์ ได้รับรางวัล Young Protein Scientist of Thailand Award ปี 2561 จากผลงานทางด้าน “Molecular Mechanism of Immune-Related Proteins in Shrimp Immunity” จากสมาคมโปรตีนแห่งประเทศไทย รับรางวัลวันที่ 9 สิงหาคม 2561

4.1.2 ดร. ภัทรันดา จารีย์ ได้รับรางวัล ผลงานวิจัยดีเด่นสำหรับนิสิตระดับปริญญาเอก จากผลงานวิทยานิพนธ์เรื่อง “ลักษณะสมบัติเชิงหน้าที่ของโปรตีนในระบบภูมิคุ้มกันจากกุ้งกุลาดำ *Penaeus monodon* ในการตอบสนองต่อการติดเชื้อโรค” จาก กองทุนรัชดาภิเษกสมโภช ประจำปี 2559

4.2 รางวัลจากการเสนอผลงานในที่ประชุมวิชาการต่างๆ

นิสิต และนักวิจัย ได้รับรางวัลจากการเสนอผลงานในที่ประชุมวิชาการต่างๆ ดังนี้

4.2.1 ประเภทบรรยาย

4.2.1.1 นาย ภาคภูมิ บุญชื่น ได้รับรางวัล Third Place Award for Oral Presentation ในงานประชุม 21st Biological Sciences Graduate Congress (BSGC) จากผลงานวิจัยเรื่อง "Differential expression of mRNAs from *Penaeus vannamei* upon *Vibrio parahaemolyticus* AHPND infection” รับรางวัลวันที่ 17 ธันวาคม 2559

4.2.2 ประเภทโปสเตอร์

4.2.2.1 นาย ภาคภูมิ บุญชื่น ได้รับรางวัล 2nd Winner Poster Presentation ในงานประชุม The 10th Symposium on Diseases in Asian Aquaculture (DAA10) จากผลงานวิจัยเรื่อง “Hemocyanin of *Litopenaeus vannamei* agglutinates *Vibrio parahaemolyticus* AHPND (VP_{AHPND}) and neutralizes VP_{AHPND} toxin” รับรางวัลวันที่ 1 กันยายน 2560

4.2.2.2 นายภาคภูมิ บุญชื่น ได้รับรางวัล Outstanding poster presentation ในงานประชุม The 6th International Conference on Biochemistry and Molecular Biology (BMB) จากผลงานวิจัยเรื่อง "Identification of miRNAs from *Penaeus vannamei* in response to *Vibrio parahaemolyticus* AHPND infection" รับรางวัลวันที่ 22 มิถุนายน 2561

4.2.2.3 นางสาว ฉันทกา วงษ์ดนตรี ได้รับรางวัล Outstanding poster presentation ในงานประชุม The 6th International Conference on Biochemistry and Molecular Biology (BMB) จากผลงานวิจัยเรื่อง “Characterization of shrimp miRNAs involved in pathogen-challenged responses” รับรางวัลวันที่ 22 มิถุนายน 2561

5. ความก้าวหน้าในการสร้างทีมวิจัย

ได้รับนักวิจัยหลังปริญญาเอกเพื่อทำงานวิจัยภายในโครงการ 2 คน คือ ดร. ภัทรันดา จารีย์ และ Dr. Benedict Maralit ซึ่งปัจจุบันทั้งสองคนได้เป็นอาจารย์และนักวิจัยในมหาวิทยาลัย และ นอกจากนี้ได้มีนิสิตปริญญาเอกและปริญญาโทที่ช่วยในงานวิจัยดังนี้

นิสิตระดับปริญญาเอก สาขาวิชา ชีวเคมีและชีววิทยาโมเลกุล ภาควิชาชีวเคมี คณะวิทยาศาสตร์ จุฬาลงกรณ์มหาวิทยาลัย

1. นาย ภาคภูมิ บุญชื่น
2. นางสาว ฉันทกา วงษ์ดนตรี
3. นางสาววรันธร เหลืองตระกูล

นิสิตระดับปริญญาโท สาขาวิชา ชีวเคมีและชีววิทยาโมเลกุล ภาควิชาชีวเคมี คณะวิทยาศาสตร์ จุฬาลงกรณ์มหาวิทยาลัย

1. นางสาว ณิชาพัฒน์ กนกสินวุฒิพงศ์

ผลงานจากงานวิจัย (output)

1. ผลงานตีพิมพ์ในวารสารวิชาการนานาชาติ

มีการตีพิมพ์เผยแพร่ผลงานวิจัยในวารสารระดับนานาชาติ 1 เรื่อง มีผลงานวิจัยที่ส่งเพื่อตีพิมพ์ (submitted) 1 เรื่อง และอยู่ระหว่างจัดเตรียมบทความอีก 1 เรื่อง

1.1 Jaree P, Wongdontri C, Somboonwiwat K. White spot syndrome virus-induced shrimp miR-315 attenuates prophenoloxidase activation via PPAE3 gene suppression. Frontiers in Immunology. Front Immunol. 2018, 25;9:2184

1.2 Boonchuen P, Maralit BA, Jaree P, Tassanakajon A, Somboonwiwat K. MicroRNA and mRNA interactions contribute to coordinating the immune response in chronic non-lethal heat stressed *Litopenaeus vannamei* against acute hepatopancreatic necrosis disease-causing strain of *Vibrio parahaemolyticus*. PLOS Pathogens. (submitted)

1.3 Boonchuen P, Somboonviwat K, Tassanakajon A, Somboonwiwat K. Identification of miRNA from *Penaeus vannamei* in response to *Vibrio parahaemolyticus* AHPND infection (manuscript in preparation)

2. การได้รับเชิญไปเป็นวิทยากร

2.1 รศ.ดร. กุลยา สมบูรณ์วิวัฒน์ ได้รับเชิญให้ไปบรรยายในงานประชุมวิชาการต่างๆ ดังนี้

2.1.1 ได้รับเชิญให้เป็น Invited Spearker ในงานประชุมวิชาการ International Mini-symposium on Frontier Aquaculture Science ซึ่งจัดขึ้นในวันที่ 9 ธันวาคม 2560 ที่ National Cheng Kung University ประเทศไต้หวัน บรรยายในหัวข้อ “The shrimp antimicrobial peptide antilipopolysaccharide factor (ALF): Basic and protential applications”

2.1.2 ได้รับเชิญให้เป็น Invited Spearker ในงานประชุมวิชาการวิทยาศาสตร์และเทคโนโลยีแห่งประเทศไทย ครั้งที่ 43 (วทท.43) ซึ่งจัดขึ้นระหว่างวันที่ 17-19 ธันวาคม 2560 ที่ จุฬาลงกรณ์มหาวิทยาลัย กรุงเทพมหานคร บรรยายในหัวข้อ “The shrimp antimicrobial peptide antilipopolysaccharide factor (ALF): Basic and potential applications”

3. การเสนอผลงานในที่ประชุมวิชาการ

มีผลงานนำเสนอในที่ประชุมวิชาการรวมทั้งสิ้น 9 เรื่อง โดยแบ่งเป็นผลงานที่นำเสนอในที่ประชุมวิชาการระดับนานาชาติ 7 เรื่อง และผลงานที่นำเสนอในที่ประชุมวิชาการระดับชาติ 2 เรื่อง

3.1 การเสนอผลงานในที่ประชุมระดับนานาชาติ

มีผลงานนำเสนอในที่ประชุมวิชาการระดับนานาชาติรวม 7 เรื่อง โดยแบ่งเป็นประเภทบรรยาย 4 เรื่อง และโปสเตอร์ 3 เรื่อง ดังนี้

3.1.1 ประเภทบรรยาย

3.1.1.1 Boonchuen P, Jaree P, Somboonwiwat K. (2016). Differential expression of mRNAs from *Penaeus vannamei* upon *Vibrio parahaemolyticus* AHPND infection. 21st Biological Sciences Graduate Congress (BSGC). 15–16 December 2016. University Of Malaya, Malaysia.

3.1.1.2 Somboonwiwat K, Maralit BA, Jaree P, Boonchuen P, Luangtrakul W, Tassanakajon T. (2017). Efffect of chronic heat stress response on hemocyte transcriptome of *Penaeus vannamei* challenged with *Vibrio parahaemolyticus* AHPND. The 10th Symposium on Diseases in Asian Aquaculture (DAA10). 28 August–1 September 2017. The Anvaya Beach Resort, Kuta, Bali, Indonesia.

3.1.1.3 Boonchuen P. (2017). Identification of miRNAs from *Penaeus vannamei* in response to *Vibrio parahaemolyticus* AHPND infection and heat stress. The 22nd Biological Sciences Graduate Congress (BSGC2017). 19–21 December 2017. University Town, NUS, Singapore.

3.1.1.4 Somboonwiwat K, Boonchuen P, Maralit BA, Tassanakajon A. Integrated miRNA AND mRNA transcriptome analyses of *Penaeus vannamei* hemocyte reveals the effect of non-lethal heat stress on shrimp antibacterial immunity. Aquaculture 2019. 7-11 March 2019. New Orleans, Louisiana, USA

3.1.2 ประเภทโปสเตอร์

3.1.2.1 Boonchuen P, Methatham T, Jaree P, Tassanakajon A, Somboonwiwat K. (2017). Hemocyanin of *Litopenaeus vannamei* agglutinates *Vibrio parahaemolyticus* AHPND (VP_{AHPND}) and neutralizes VP_{AHPND} toxin. The 10th Symposium on Diseases in Asian Aquaculture (DAA10). 28 August–1 September 2017. The Anvaya Beach Resort, Kuta, Bali, Indonesia.

3.1.2.2 Boonchuen P, Somboonwiwat K. (2018). Identification of miRNAs from *Penaeus vannamei* in response to *Vibrio parahaemolyticus* AHPND infection. The 6th International Conference on Biochemistry and Molecular Biology (BMB). 20–22 June 2018. Rayong, Thailand.

3.1.2.3 Wongdontri C, Somboonwiwat K. (2018). Characterization of shrimp miRNAs involved in pathogen–challenged responses. The 6th International Conference on Biochemistry and Molecular Biology (BMB). 20–22 June 2018. Rayong, Thailand.

3.2 การเสนอผลงานในที่ประชุมระดับชาติ

มีผลงานนำเสนอในที่ประชุมวิชาการระดับชาติ 2 เรื่อง โดยแบ่งเป็นประเภทบรรยาย 1 เรื่อง และ โปสเตอร์ 1 เรื่อง ดังนี้

3.2.3 ประเภทบรรยาย

3.2.3.1 Jaree P, Tassanakajon A, Somboonwiwat K. (2015). Characterization of mir–315 function in shrimp, *Penaeus monodon*, antiviral immunity. The 41st Congress on Science and Technology of Thailand (STT41). 6–8 November 2015. Nakhonratchasima, Thailand.

3.2.4 ประเภทโปสเตอร์

3.2.4.1 Kanoksinwuttipong N, Wongdontri C, Somboonwiwat K. (2017). Expression analysis of miRNAs involved in pathogen challenge in shrimp. The 43rd Congress on Science and Technology of Thailand (STT43). 17–19 December 2017. Chulalongkorn University, Bangkok, Thailand.

4. รางวัล

4.1 รางวัลจากหน่วยงานต่างๆ

อาจารย์และนักวิจัยได้รับรางวัลจากหน่วยงานต่างๆ ดังนี้

4.1.1 รศ.ดร. กุลยา สมบูรณ์วิวัฒน์ ได้รับรางวัล Young Protein Scientist of Thailand Award ปี 2561 จากผลงานทางด้าน “Molecular Mechanism of Immune-Related Proteins in Shrimp Immunity” จากสมาคมโปรตีนแห่งประเทศไทย รับรางวัลวันที่ 9 สิงหาคม 2561

4.1.2 ดร. ภัทรันดา จารีย์ ได้รับรางวัล ผลงานวิจัยดีเด่นสำหรับนิสิตระดับปริญญาเอก จากผลงานวิทยานิพนธ์เรื่อง “ลักษณะสมบัติเชิงหน้าที่ของโปรตีนในระบบภูมิคุ้มกันจากกุ้งกุลาดำ *Penaeus monodon* ในการตอบสนองต่อการติดเชื้อโรค” จาก กองทุนรัชดาภิเษกสมโภช ประจำปี 2559

4.2 รางวัลจากการเสนอผลงานในที่ประชุมวิชาการต่างๆ

นิสิต และนักวิจัย ได้รับรางวัลจากการเสนอผลงานในที่ประชุมวิชาการต่างๆ ดังนี้

4.2.1 ประเภทบรรยาย

4.2.1.1 นาย ภาคภูมิ บุญชื่น ได้รับรางวัล Third Place Award for Oral Presentation ในงานประชุม 21st Biological Sciences Graduate Congress (BSGC) จากผลงานวิจัยเรื่อง "Differential expression of mRNAs from *Penaeus vannamei* upon *Vibrio parahaemolyticus* AHPND infection” รับรางวัลวันที่ 17 ธันวาคม 2559

4.2.2 ประเภทโปสเตอร์

4.2.2.1 นาย ภาคภูมิ บุญชื่น ได้รับรางวัล 2nd Winner Poster Presentation ในงานประชุม The 10th Symposium on Diseases in Asian Aquaculture (DAA10) จากผลงานวิจัยเรื่อง “Hemocyanin of *Litopenaeus vannamei* agglutinates *Vibrio parahaemolyticus* AHPND (VP_{AHPND}) and neutralizes VP_{AHPND} toxin” รับรางวัลวันที่ 1 กันยายน 2560

4.2.2.2 นายภาคภูมิ บุญชื่น ได้รับรางวัล Outstanding poster presentation ในงานประชุม The 6th International Conference on Biochemistry and Molecular Biology (BMB) จากผลงานวิจัยเรื่อง "Identification of miRNAs from *Penaeus vannamei* in response to *Vibrio parahaemolyticus* AHPND infection" รับรางวัลวันที่ 22 มิถุนายน 2561

4.2.2.3 นางสาว ฉันทกา วงษ์ดนตรี ได้รับรางวัล Outstanding poster presentation ในงานประชุม The 6th International Conference on Biochemistry and Molecular Biology (BMB) จากผลงานวิจัยเรื่อง “Characterization of shrimp miRNAs involved in pathogen-challenged responses” รับรางวัลวันที่ 22 มิถุนายน 2561

5. ความก้าวหน้าในการสร้างทีมวิจัย

ได้รับนักวิจัยหลังปริญญาเอกเพื่อทำงานวิจัยภายในโครงการ 2 คน คือ ดร. ภัทรันดา จารีย์ และ Dr. Benedict Maralit ซึ่งปัจจุบันทั้งสองคนได้เป็นอาจารย์และนักวิจัยในมหาวิทยาลัย และ นอกจากนี้ได้มีนิสิตปริญญาเอกและปริญญาโทที่ช่วยในงานวิจัยดังนี้

นิสิตระดับปริญญาเอก สาขาวิชาชีวเคมีและชีววิทยาโมเลกุล ภาควิชาชีวเคมี คณะวิทยาศาสตร์ จุฬาลงกรณ์มหาวิทยาลัย

1. นาย ภาคภูมิ บุญชื่น (คาดว่าจะจบการศึกษา ภาคต้น ปีการศึกษา 2562)
2. นางสาววรันธร เหลืองตระกูล (คาดว่าจะจบการศึกษา ภาคต้น ปีการศึกษา 2563)
3. นางสาว ฉันทกา วงษ์ดนตรี (คาดว่าจะจบการศึกษา ภาคปลาย ปีการศึกษา 2563)

นิสิตระดับปริญญาโท สาขาวิชา ชีวเคมีและชีววิทยาโมเลกุล ภาควิชาชีวเคมี คณะวิทยาศาสตร์ จุฬาลงกรณ์มหาวิทยาลัย

1. นางสาว ณิชาพัฒน์ กนกสินวุฒิพงศ์ (จบการศึกษา ภาคปลาย ปีการศึกษา 2561)

frontiers in Immunology

ORIGINAL RESEARCH
published: 25 September 2018
doi: 10.3389/fimmu.2018.02184

White Spot Syndrome Virus-Induced Shrimp miR-315 Attenuates Prophenoloxidase Activation via *PPAE3* Gene Suppression

Phattarunda Jaree[1†], *Chantaka Wongdontri*[1] *and Kunlaya Somboonwiwat*[1,2*]

[1] Center of Excellence for Molecular Biology and Genomics of Shrimp, Department of Biochemistry, Faculty of Science, Chulalongkorn University, Bangkok, Thailand, [2] Omics Sciences and Bioinformatics Center, Faculty of Science, Chulalongkorn University, Bangkok, Thailand

OPEN ACCESS

Edited by:
Chu-Fang Lo,
National Cheng Kung University, Taiwan

Reviewed by:
Arun K. Dhar,
University of Arizona, United States
Chia-Ying Chu,
National Taiwan University, Taiwan

***Correspondence:**
Kunlaya Somboonwiwat
kunlaya.s@chula.ac.th

†Present Address:
Phattarunda Jaree,
Institue of Molecular Biosciences, Mahidol University, Salaya, Thailand

Specialty section:
This article was submitted to Comparative Immunology, a section of the journal Frontiers in Immunology

Received: 07 June 2018
Accepted: 04 September 2018
Published: 25 September 2018

Citation:
Jaree P, Wongdontri C and Somboonwiwat K (2018) White Spot Syndrome Virus-Induced Shrimp miR-315 Attenuates Prophenoloxidase Activation via PPAE3 Gene Suppression. Front. Immunol. 9:2184. doi: 10.3389/fimmu.2018.02184

MicroRNAs (miRNAs), the small non-coding RNAs, play a pivotal role in post-transcriptional gene regulation in various cellular processes. However, the miRNA function in shrimp antiviral response is not clearly understood. This research aims to uncover the function of pmo-miR-315, a white spot syndrome virus (WSSV)-responsive miRNAs identified from *Penaeus monodon* hemocytes during WSSV infection. The expression of the predicted pmo-miR-315 target mRNA, a novel *PmPPAE* gene called *PmPPAE3*, was negatively correlated with that of the pmo-miR-315. Furthermore, the luciferase assay indicated that the pmo-miR-315 directly interacted with the target site in *PmPPAE3* suggesting the regulatory role of pmo-miR-315 on *PmPPAE3* gene expression. Introducing the pmo-miR-315 into the WSSV-infected shrimp caused the reduction of the *PmPPAE3* transcript level and, hence, the PO activity activated by the *Pm*PPAE3 whereas the WSSV copy number in the shrimp hemocytes was increased. Taken together, our findings state a crucial role of pmo-miR-315 in attenuating proPO activation via *PPAE3* gene suppression and facilitating the WSSV propagation in shrimp WSSV infection.

Keywords: microRNA, viral infection, invertebrates, *Penaeus monodon*, prophenoloxidase

INTRODUCTION

MicroRNAs (miRNAs) are small non-coding RNA molecules transcribed from the genome and subsequently processed by Drosha and Dicer nucleases (1). Generally, when miRNA complementary binds to the 3′-untranslated regions (3′-UTRs) of mRNAs, it can cleave the target mRNAs or inhibits the mRNA translation, thus, down-regulating the corresponding gene expression. In addition, it has been reported that the miRNAs can also bind to the 5′-untranslated regions (5′-UTR) (2) or even within the coding sequence of mRNAs (3). Accordingly, miRNA's function involves the regulation of various biological processes including the host-virus interaction upon viral infection. During virus infection, viral miRNAs downregulate specific viral and cellular mRNAs to establish a host environment conducive to the completion of viral life cycle. At the same time, the host miRNAs modulate both cellular and viral transcripts exerting influence over immune responses (4).

In crustaceans, there are many reports showing that the host miRNAs can regulate the expression of the host and viral genes and vice versa. In 2012, the first large-scale miRNA characterization in white spot syndrome virus (WSSV)-infected *Marsupenaeus japonicas* lymphoid organ has been reported (5). Several cellular WSSV-responsive miRNAs play important roles in shrimp immunity including apoptosis pathway (6, 7), phagocytosis (8), NF-kB pathway (9), and JAK/STAT pathway (10). Furthermore, the WSSV miRNAs were also identified and probably could target either the host or viral genes. In the WSSV-infected *M. japonicas,* the viral miRNAs could target virus transcripts and further promote virus infection (11). In the meantime, a viral miRNA, WSSV-miR-N24, could target the shrimp apoptotic gene, caspase 8, and further represses the apoptosis of shrimp hemocytes (12). Despite this, the study on the host miRNAs-virus relationship in shrimp is still very limited.

In *Penaeus monodon*, the 60 known miRNA homologs that are expressed in the hemocytes of WSSV-challenged shrimp at the early and late phases of infection have been identified (13). Their immune-related gene targets in apoptosis pathway, antimicrobial peptide, prophenoloxidase system, signal transduction, proteinase and proteinase inhibitor, blood clotting system, and heat shock protein have also been predicted. Among them, the pmo-miR-315 was found to be a highly up-regulated miRNA in response to WSSV challenge and its target gene was predicted to be a novel prophenoloxidase-activating enzyme, called *PmPPAE3* (13). According to the previous reports, the miR-315 was also up-regulated after WSSV infection in lymphoid organ of *M. japonicas* (5) and hepatopancreas of *F. chinensis* (14). However, the function of miR-315 in shrimp immunity against WSSV infection is still unknown. In this research, the cellular mRNA target of pmo-miR-315 was confirmed. Moreover, the role of pmo-miR-315 in WSSV-infected shrimp was investigated.

MATERIALS AND METHODS

Shrimp and WSSV

Healthy black tiger shrimp, *P. monodon*, of about 3–5 and 15–20 g in size were purchased from a farm in Surat Thani Province, Thailand. Due to the Ethical Principles and Guidelines for the use of animals for scientific purposes by the National Research Council of Thailand, this project was conducted according to the animal use protocol number 1823006 approved by the Chulalongkorn University Animal Care And Use Committee (CU-ACUC). The animals were reared in laboratory tanks at ambient temperature, and maintained in aerated water with a salinity of 15 ppt for at least 7 days before use.

The WSSV stock used for the experimental infection was prepared according to the method described by Xie et al. (15) and stored at −80°C until used. One microliter of WSSV stock was 10-fold serially diluted with 0.85% NaCl to 10^{-7} dilution. The diluted WSSV of 50 μL was injected into the second abdominal segment of the shrimp. The mortality was recorded daily. This dosage caused 100% mortality within 3–4 days after injection and was used for all subsequent viral infection experiment.

This project has been reviewed and approved by the CU-IBC (Approval number: SCI-01-001) to be in accordance with the levels of risk in pathogens and animal toxins listed in the Risk Group of Pathogen and Animal Toxin (2017) published by the Department of Medical Sciences, Ministry of Public Health, the Pathogen and Animal Toxin Act (2015) and Biosafety Guidelines for Modern Biotechnology, BIOTEC (2016).

Pmo-miR-315 Mimic and Its Scramble miRNA

The mimic microRNAs used in this research were synthesized by a commercial service GenePharma (Shanghai). The sequences of mimic pmo-miR-315 and pmo-miR-315 scramble were 5′-UUU UGAUUGUUGCUCAGAAG-3′ and 5′-GUGGUUAGCGUUA AUUCUAU-3′, respectively. The sequences of miR-315 inhibitor (AMO-miR-315) and miR-315 inhibitor scramble were 5′-CUU CUGAGCAACAAUCAAAA-3′ and 5′-ACGAACCUACGAUA AUAAUC-3′.

Pmo-miR-315 Expression in WSSV-Infected Shrimp Tissues

The expression of pmo-miR-315 in various shrimp tissues including hemocytes, gill, lymphoid organ and stomach of WSSV-infected *P. monodon* was determined by stem-loop quantitative real time RT-PCR (qRT-PCR). The pooled total RNA of each tissue from 3 WSSV-infected individuals at 0, 6, 24, and 48 hpi was prepared using mirVana miRNA Isolation Kit (Life Technologies) and 1 μg was used as templates for the first strand stem-loop cDNA synthesis using Superscript III Reverse Transcriptase (Invitrogen). The qPCR was performed using SsoFast^{TM} EvaGreen® Supermix (Bio-Rad) on CFX96 touch real-time PCR detection system (Bio-Rad), where each sample was analyzed in triplicate. The amplification condition was 98°C for 2 min, followed by 40 cycles of 95°C for 5 s and 60°C for 30 s. A non-coding small nuclear RNA, U6, was used as a reference. The primer sequences for stem-loop cDNA synthesis, pmo-miR-315: RT-pmo-miR315_F and RT-pmo-miR315_R, and for U6: RT-U6-F and RT-U6-R, are shown in **Table 1**. The miRNA relative expression level was calculated using the equation by Pfaffl (16).

In addition, the expression of the target mRNA of pmo-miR-315, a putative prophenoloxidase-activating enzyme (*Pm*PPAE3), was determined in hemocytes of shrimp infected with WSSV at 0, 6, 24, and 48 hpi. The total RNA from hemocytes of 3 individuals was reverse-transcribed into the first strand cDNA using oligo (dT) as a primer following the manufacturer's instruction for RevertAid First Strand cDNA Synthesis Kit (Thermo scientific). Quantitative real-time PCR was performed as described previously using *EF-1α* gene as an internal control.

Specificity and Inhibitory Activity of Pmo-miR-315 on Target *PmPPAE3* mRNA

First, the pmirGLO vector (Promega) harboring the 200 bp *Pm*PPAE3 gene fragment that contained the pmo-miR-315 binding region (**Figure 2A**) was constructed. The *PmPPAE3* gene fragment was PCR amplified from *P. monodon* hemocyte cDNAs using the gene specific primers, pmirG_*Pm*PPAE_F and pmirG_*Pm*PPAE_R (**Table 1**), digested with *Sac*I and *Xba*I

TABLE 1 | List of primers used in this study.

Primer name	Sequence (5′-3′)
Stem-loop pmo-miR-315	GTCGTATCCAGTGCAGGGTCCGAGGTATTCGCAC TGGATACGACCTTCTG
RT-pmo-miR315_F	CGGGCGTTTTGATTGTTGCTCAG
RT-pmo-miR315_R	CCAGTGCAGGGTCCGAGGTA
RT-U6-F	CTCGCTTCGGCAGCACA
RT-U6-R	AACGCTTCACGAATTTGCGT
RT-*Pm*PPAE3-F	GGACGAGTGCCAGTTCAACA
RT-*Pm*PPAE3-R	GGTCGTTGTGGTGGTGGTCACT
RT-EF1α-F	GGTGCTGGACAAGCTGAAGGC
RT-EF1α-R	CGTTCCGGTGATCATGTTCTTGATG
knPPAE3-F	CAACATTGCCGGACTGCCTA
knPPAE3-R	GGCAGAAGCACGACACGAAC
knPPAE3-T7-F	TAATACGACTCACTATAGGCAACATTGCCGGACTG CCTA
knPPAE3-T7-R	TAATACGACTCACTATAGGGGCAGAAGCACGACA CGAAC
knGFP-F	ATGGTGAGCAAGGGGGAGGA
knGFP-R	TTACTTGTACAGCTCGTCCA
knGFP-T7-F	GGATCCTAATACGACTCACTATAGGATGGTGAGCA AGGGGGAGGA
knGFP-T7-R	GGATCCTAATACGACTCACTATAGGTTACTTGTACA GCTCGTCCA
pmirG_*Pm*PPAE3_F	CTAGCGAGCTCCCAACGACCAGTAGGCCTGTGA
pmirG_*Pm*PPAE3_R	CTAGCTCTAGAGGCAGAAGCACGACACGAA
VP28-140Fw	AGGTGTGGAACAACACATCAAG
VP28-140Rv	TGCCAACTTCATCCTCATCA
pri-*Pm*PPAE3	GGTCGTTGTGGTGGTGGTCACT
nested *Pm*PPAE3	TCCTGACATCCTCCGTTGTTGCTCAC

(New England Biolabs), cloned into the likewise double digested pmirGLO, and transformed into an *Escherichia coli* stain XL1-blue. The recombinant plasmid, pmir-T315, was extracted and sequenced to confirm the correctness of the sequences (Macrogen, Korea).

To investigate the inhibitory activity of pmo-miR-315 on the *PmPPAE3* gene target sequence, dual-luciferase activity assay was performed. The HEK293T cell culture of 8×10^4 cells/well was seeded into a 24-well plate. At 24 h after seeding, 200 ng of pmir-T315 and 20 pmole of mimic miRNA (pmo-miR-315 or scramble) were co-transfected into the HEK293T cells using the Effectene® transfection reagent (Qiagen). The luciferase activity was measured using Dual-luciferase® Reporter Assay System (Promega) at 48 h post-transfection. The control cells were transfected with pmir-T315 alone and co-transfected pmir-T315 with mimic miRNA scramble.

Introducing and Silencing of Pmo-miR-315 in WSSV-Infected Shrimp

To confirm the inhibitory effect of pmo-miR-315 on the *PmPPAE3* target gene expression in shrimp after WSSV infection, the exogenous pmo-miR-315 mimic and anti-pmo-miR-315 (AMO-miR-315) were introduced into the WSSV-infected shrimp and the expression levels of pmo-miR-315 and target gene were quantified.

To study the effect of pmo-miR-315 *in vivo*, the exogenous pmo-miR-315 was introduced into the shrimp by injection. For pmo-miR-315 silencing, the AMO-miR-315 was injected into the shrimp. In these experiments, shrimp were divided into five groups of three individuals each. The first group was injected with 0.85% NaCl used as an injection control. The miRNA and AMO control groups were shrimp injected with scramble miRNA or scramble AMO-miR-315, respectively. The two test groups were shrimp injected with pmo-miR-315 mimic or AMO-miR-315. At 2 h after the first injection, all groups were muscularly injected with WSSV. After 48 h post-WSSV infection, shrimp hemolymph was collected. The total RNA was extracted and used for the first-strand cDNA production. The expression level of pmo-miR-315 and putative *PmPPAE3* was determined by qRT-PCR.

Analysis of WSSV Copy Number Using qRT-PCR

To study the effect of pmo-miR-315 on WSSV replication, the WSSV copy number was also investigated according to a method described by Mendoza-Cano and Sánchez-Paz (17). The genomic DNA of WSSV-infected shrimp hemocytes was extracted using a FavorPrep™ Tissue Genomic DNA Extraction Mini Kit (Favorgen). The quantity and quality of genomic DNA was determined by NanoDrop 2000c spectrophotometer (Thermo Sciencetific) and 1.2% agarose gel electrophoresis.

The qRT-PCR was performed in triplicates of 10 μL reaction containing 5 μL Luna® Universal qPCR Master mix (New England Biolabs) and 1.5 μL genomic DNA template (10 ng/μL) and 250 nM VP28-140Fw and VP28-140Rv (**Table 1**). The amplification condition was 98°C for 2 min, followed by 40 cycles of 95°C for 5 s and 61°C for 30 s. The plasmid containing a highly conserved region of the WSSV *VP28* gene, was used to generate a standard curve for the determination of WSSV copy number.

Phenoloxidase Activity Assay

The phenoloxidase (PO) activity was determined in the hemolymph of WSSV- infected shrimp. The shrimp hemolymph was collected at 48 h post-WSSV infection and the PO activity was measured using a method modified from Sutthangkul et al. (18). Briefly, 50 μL of hemolymph was mixed with 25 μL of 3 mg/mL freshly prepared L-3, 4-dihydroxyphenylalanine (L-DOPA; Fluka) and 25 μL of 20 mM Tris-HCl pH 8.0. The absorbance at 490 nm was monitored. The amount of hemolymph proteins was measured by the Bradford method (19). The PO activity was recorded as A_{490}/mg total protein/min.

Identification of Full-Length cDNA of Putative *PmPPAE3*

According to our previous report on pmo-miR-315 target prediction (13), the partial nucleotide sequence of *PmPPAE3* was obtained from *P. monodon* EST database. To identify the full-length cDNA, the 5′-RACE was performed using a SMARTer™ RACE cDNA Amplification Kit (Clontech, USA) according to the manufacturer's instructions. The specific primers of partial putative *PmPPAE3* gene were designed, which are pri-*Pm*PPAE3

and nested *Pm*PPAE3 (**Table 1**). The primary and nested-PCR were used to amplify the 5′-RACE cDNA library using Advantage® 2 polymerase mix (Clontech). The PCR product was analyzed by 1.2% agarose gel electrophoresis. The nested PCR product was purified and cloned into the pGEM-T easy vector (Promega) and transformed into *E. coli* XL1-blue. The positive clone was selected and sequenced by a commercial service (Macrogen, Korea). The 5′-RACE *PmPPAE3* nucleotide sequence was analyzed and combined with the starting *PmPPAE3* sequence from the EST library.

The full-length cDNA of putative *PmPPAE3* was analyzed using a Blast program (http://www.ncbi.nlm.nih.gov/BLAST/). The open reading frame (ORF) and the encoded amino acid sequence were predicted using ExPASy software (http://web.expasy.org/translate/). The putative signal peptide cleavage site was predicted by SignalP 4.1 server (http://www.cbs.dtu.dk/services/SignalP/). Moreover, the structural protein domains were analyzed by a simple modular architecture research tool program (SMART) (http://smart.embl-heidelberg.de/).

Multiple amino acid sequence alignment was performed using the Clustal Omega program (http://www.ebi.ac.uk//Tools/msa/clustalo/). The deduced amino acid sequence of *Pm*PPAE3 was aligned with other insect and crustacean PPAEs including *Bombyx mori* PO-activating enzyme (*Bm*PAE: NP_001036832.1); *Manduca sexta* proPO-activating proteinase 1 (*Ms*PAP1: AF059728), *Holotrichia diomphalia* proPO-activating factor I (*Hd*PPAFI: AB013088), *Glossina morsitans* (*Gm*PPAE: ABC84592) and *Drosophila melanogaster* melanization protease1 (*Dm*MP1: NM141193); *P. monodon* proPO-activating enzyme 1, 2, and 3 (*Pm*PPAE1: FJ595215, *Pm*PPAE2: FJ620685, *Pm*PPAE3: MH325330), *Litopenaeus vannamei* proPO-activating enzyme (*Lv*PPAE: AFW98991.1), *Fenneropenaeus chinensis* proPO-activating enzyme (*Fc*PPAE: AFW98985.1) and *Pacifastacus leniusculus* proPO-activating enzyme (*Pl*PPAE: AJ007668). An unrooted phylogenetic tree was constructed by the neighbor-joining method based on the amino acid sequences using MEGA 7 software (20). The bootstrap sampling was reiterated 1000 times.

Tissue Distribution Analysis of *PmPPAE3* Gene

The *PmPPAE3* gene expression in various tissues including hemocytes, gill, lymphoid organ, and stomach of healthy unchallenged *P. monodon* was analyzed by semi-quantitative RT-PCR. The total RNA of each tissue was extracted by Tri reagent (Geneaid) and used for the first-strand cDNA synthesis using RevertAid First Strand cDNA Synthesis Kit (Thermo Scientific). The PCR reaction was performed using the *PmPPAE3* specific primer pair (**Table 1**) and the *EF-1α* was used as an internal control. The expression profile was analyzed by 1.5% agarose gel electrophoresis.

Effect of *PmPPAE3* Gene Silencing on PO Activity in Shrimp

The function of *Pm*PPAE3 in shrimp was characterized using a RNA interference technique. The *PmPPAE3* DNA template was amplified from normal shrimp cDNA with gene specific primers (knPPAE3-F, knPPAE3-R, knPPAE3-T7-F, and knPPAE3-T7-R) as shown in **Table 1**. In addition, the dsRNA of the green fluorescent protein (*GFP*) as the negative control, was prepared from the pEGFP-1 vector (Clontech) using the knGFP-F, knGFP-R, knGFP-T7-F, and knGFP-T7-R (**Table 1**). The *PmPPAE3*-dsRNA and GFP-dsRNA were prepared using T7 RiboMAX™ Express Large Scale RNA Production System (Promega) according to the manufacturer's instruction.

The *P. monodon* of approximately 3 g body weight were divided into two groups of three individuals each. The first (control) group was injected with 5 μg/g shrimp of *GFP*-dsRNA, whilst the second group, the *PmPPAE3* knockdown, was injected with 5 μg/g shrimp *PmPPAE3*-dsRNA. The hemolymph of individual shrimp was collected at 48 h post-injection. Then, the expression level of *PmPPAE3* gene and also the PO activity were measured as described above.

Statistical Analysis

All experiments were performed in triplicate. One-way ANOVA with Duncan's multiple range test was used to identify statistically significant differences with SPSS software (version 17.0). Data are presented as means ± 1 standard deviations of three biological replications. The statistical significance of differences among means was calculated by the paired-samples *t*-test where the significance was accepted at the P-value < 0.05.

RESULTS

Expression of Pmo-miR-315 in Tissues of WSSV-Infected Shrimp

Previously, the differentially expressed miRNAs in hemocytes of WSSV-infected shrimp were identified (13). Among them, the pmo-miR-315 was highly up-regulated at 48 h post-WSSV infection. The pmo-miR-315 expression level in various tissues including hemocytes, gill, lymphoid organ, and stomach in WSSV-infected shrimp at 0, 6, 24, and 48 hpi was further studied. Although, the pmo-miR-315 expression was observed in all tissues tested, the significant response to WSSV infection were found only in hemocytes, in which it was up-regulated at 24 and 48 hpi for about 5- and 30-fold compared with that at 0 hpi (**Figure 1**). Our results suggested that the pmo-miR-315 was the WSSV-responsive miRNA that might have a function in shrimp immune response.

Expression of Pmo-miR-315 Target Gene in WSSV-Infected Shrimp Hemocytes

As stated before, the target mRNA of pmo-miR-315 has been predicted as a putative prophenoloxidase-activating enzyme (*PmPPAE*) by bioinformatic approaches (13). The PPAE is known as an enzyme that converts the prophenoloxidase (proPO) to active phenoloxidase (PO) in cascades of the proPO system (21). Previously, two isoforms of PPAEs including *Pm*PPAE1 and *Pm*PPAE2 were identified in *P. monodon* (22, 23). Preliminary analysis showed that the sequence of target mRNA of pmo-miR-315 was a novel isoform of *PmPPAE*. Herein, therefore, it was named as *PmPPAE3*. The RNA hybrid software used to analyze the structure and stability of miRNA/mRNA duplex showed that the seed region of pmo-miR-315 was perfectly complementary to

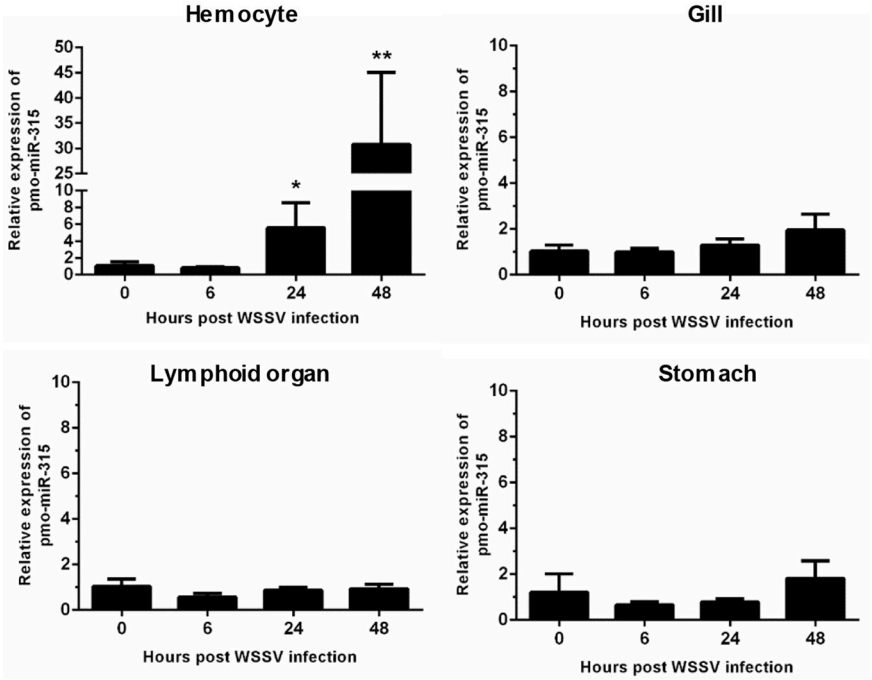

FIGURE 1 | The expression of pmo-miR-315 in WSSV-infected shrimp tissues. Quantitative stem-loop real-time RT-PCR was performed to determine the expression level of pmo-miR-315 in hemocytes, gill, lymphoid organ and stomach at 0, 6, 24, and 48 hpi. Using U6 as an internal control, the relative expression level of miR-315 was calculated. All experiments were performed in triplicate. The * and ** indicate the significant difference at $P < 0.05$ and $P < 0.01$, respectively.

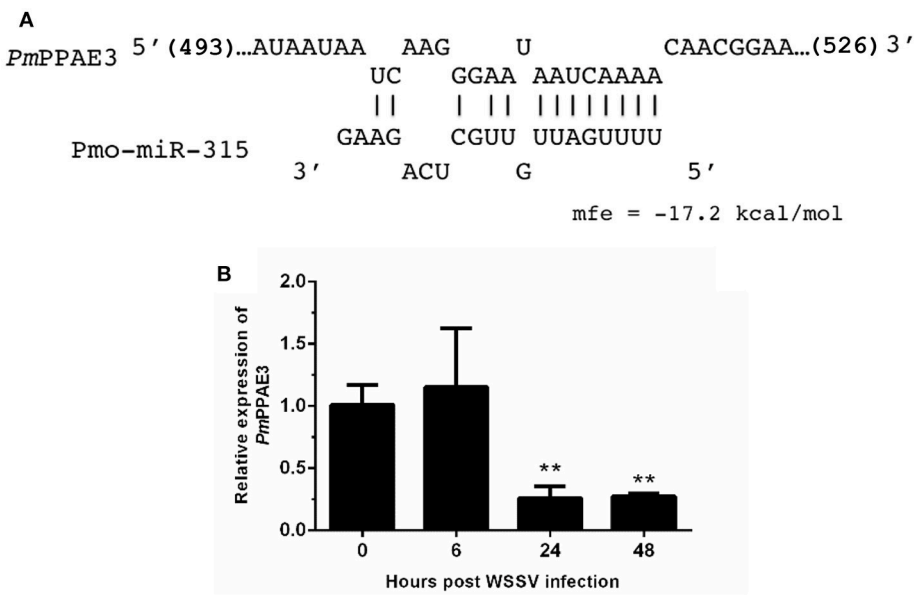

FIGURE 2 | The pmo-miR-315 target mRNA, prophenoloxidase-activating enzyme 3 (*PmPPAE3*). **(A)** The pmo-miR-315/*PmPPAE3* base pairing and the binding energy was predicted using RNA hybrid software. The number in bracket indicates the position of nucleotide of pmo-miR-315 target site on the *PmPPAE3* CDS. **(B)** The relative expression level of *PmPPAE3* gene at 0, 6, 24, and 48 h post-WSSV infection was investigated. The *EF-1α* gene was used as an internal control. All experiments were performed in triplicate. The ** indicates the significant difference at $P < 0.05$.

the target sequence located on the coding sequence of *PmPPAE3* mRNA (**Figure 2A**).

The possibility of *PmPPAE3* transcript on being the pmo-miR-315 target was evaluated by the determination of the pattern of *PmPPAE3* gene expression in comparison to that of pmo-miR-315. The expression of *PmPPAE3* transcript was dramatically decreased by about 5-fold at 24 and 48 hpi compared with that at 0 hpi (**Figure 2B**). The negative correlation of expression pattern of pmo-miR-315 (**Figure 1A**) and *Pm*PPAE3 (**Figure 2B**) during WSSV infection was noted, suggesting that the pmo-miR-315 was likely to inhibit the *PmPPAE3* expression.

Interaction Between Pmo-miR-315 and *PmPPAE3 in vitro*

The specific interaction of pmo-miR-315 with target mRNA binding site on *PmPPAE3* coding sequence was confirmed *in vitro* in HEK293T cell line. Either pmo-miR-315 mimic or its scramble miRNA and the luciferase reporter plasmid containing pmo-miR-315 binding site of *PmPPAE3* (pmir-T315) were co-transfected into HEK293T cells and then assayed for the luciferase activity. The results showed that in the presence of the mimic pmo-miR-315, the luciferase activity was reduced by about 36% compared with the reaction containing scramble miRNA (**Figure 3**). The reduction of luciferase activity suggested the specific binding of mimic pmo-miR-315 to miRNA-binding site of *PmPPAE3*.

Characterization of *PmPPAE3* Gene

As mentioned above, the *Pm*PPAE3 entails the shrimp immunity against WSSV. The function of PPAE is generally involved in the proPO system as reported previously by Charoensapsri et al. (22), and Charoensapsri et al. (23). Therefore, the function of *Pm*PPAE3 in the proPO system was investigated. The full-length gene of *PmPPAE3* was identified (**Supplementary Figure 1**). Using the 5′-RACE technique, the *PmPPAE3* full-length gene of 2,988 bp including 5′-UTR of 147 bp, 3′-UTR of 909 bp and the ORF of 1,932 bp encoding for 643 amino acid residue protein was obtained.

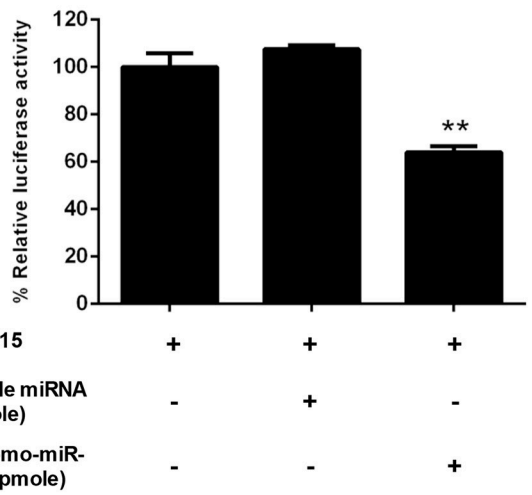

FIGURE 3 | The pmo-miR-315/*PmPPAE3* interaction by luciferase reporter assay. The target sequence of pmo-miR-315 from *PmPPAE3* was amplified and cloned into the pmirGLO vector (pmir-T315). The pmo-miR-315 mimic or scramble pmo-miR-315 were co-transfected with pmir-T315 using Effectene transfection reagent (Qiagen) into HEK293T cells. At 48 h after transfection, the luciferase activity was measured using a Dual-luciferase® reporter assay system (Promega). The data shown is derived from triplicate experiments. The ** indicates significant difference ($P < 0.01$).

The phylogenetic tree constructed based on the deduced amino acid sequences corresponding to the ORFs of PPAEs from crustaceans and insects showed that the PPAEs are clustered into the crustacean and insect lineages. (**Figure 4A**). Amino acid sequence alignment of insect and crustacean PPAEs showed the conserved patterns of a clip domain, the serine proteinase domain, and the catalytic triad of histidine, aspartic acid, and serine residues (**Figure 4B**). Comparing with previously identified crustacean PPAEs, the *Pm*PPAE3 showed about 46.43, 46.31, and 45.98% identity with *Fc*PPAE, *Lv*PPAE and *Pm*PPAE1, respectively. Like the *Pm*PPAE1 and *Pm*PPAE2, the *Pm*PPAE3 was specifically expressed in shrimp hemocytes (**Figure 4C**). Lastly, the function of *Pm*PPAE3 in the proPO system was further investigated by RNA interference (**Figure 4D**). The *PmPPAE3* gene knockdown dramatically reduced the PO activity in shrimp hemolymph (**Figure 4E**) suggesting its important role in the proPO system.

Role of Pmo-miR-315 in WSSV-Infected Shrimp Hemocytes

As stated in the previous experiment, suppression of *PmPPAE3* gene expression resulted in a decrease in PO activity in shrimp hemolymph and the pmo-miR-315 could bind to specific site in the ORF of *PmPPAE3* gene. In order to reveal the role of pmo-miR-315 in WSSV-infected shrimp, overexpression of pmo-miR-315 by introducing the exogenous pmo-miR-315 mimic and the silencing of pmo-miR-315 by anti-pmo-miR-315 injection (AMO-miR-315) were performed in shrimp after WSSV infection. The expression of pmo-miR-315 and its target gene, *PmPPAE3*, was analyzed to confirm the regulatory role of pmo-miR-315 on *PmPPAE3* gene expression. As expected, the expression of *PmPPAE3* was decreased whereas that of pmo-miR-315 was highly increased (**Figures 5A,B**).

The PO activity was also determined in shrimp hemolymph to further elucidate the involvement of pmo-miR-315 in modulating the proPO system. The mimic pmo-miR-315 injected into the WSSV-infected shrimp resulted in a deduction of PO activity (**Figure 5C**, **Supplementary Table S1**), indicating that the pmo-miR-315 negatively regulated the shrimp proPO system. The WSSV copy number was also analyzed in hemocytes to determine the effect of introducing the pmo-miR-315 on WSSV replication in shrimp. Interestingly, as compared with those of control groups of saline and scramble miR-315 injection, the WSSV copy number was significantly increased in WSSV-challenged shrimp if the mimic pmo-miR-315 was introduced (**Figure 5D**). Conversely, silencing of pmo-miR-315 in WSSV-infected shrimp caused an increase in PO activity because of the up-regulation of *PmPPAE3* (**Figure 5C**, **Supplementary Table S2**). The inhibition

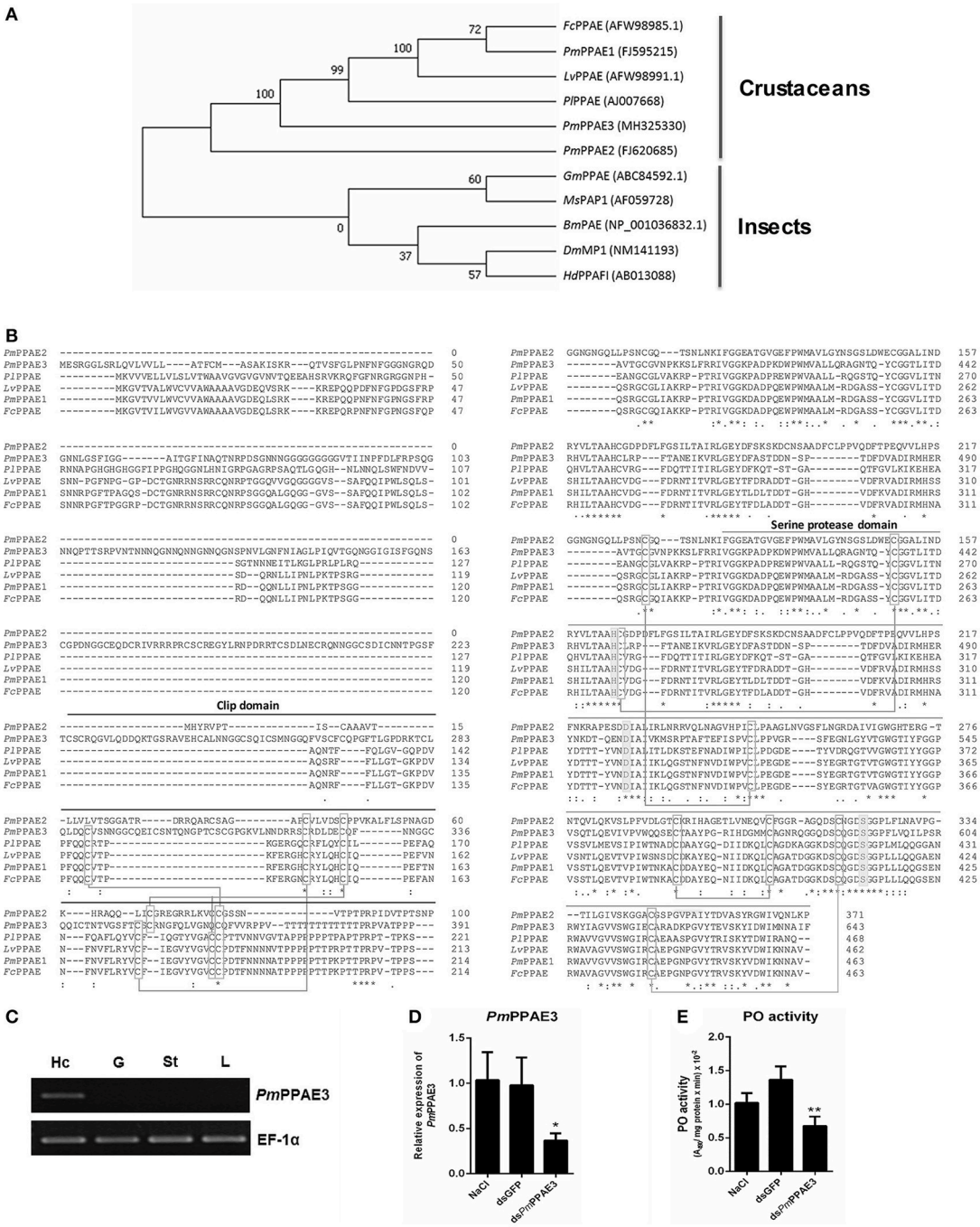

FIGURE 4 | Characterization of *PmPPAE3* gene. **(A)** Phylogenetic analysis of PPAEs from various organisms including crustaceans and insects, e.g., *B. mori* PO-activating enzyme (*Bm*PAE); *M. sexta* proPO-activating proteinase 1 (*Ms*PAP1), *H. diomphalia* proPO-activating factor I (*Hd*PPAFI), *G. morsitans* (*Gm*PPAE) and *D. melanogaster* melanization protease1 (*Dm*MP1); shrimp *P. monodon* proPO-activating enzymes 1, 2 and 3 (*Pm*PPAE1, *Pm*PPAE2, *Pm*PPAE3), shrimp, *L. vannamei* proPO-activating enzyme (*Lv*PPAE), *F. chinensis* proPO-activating enzyme (*Fc*PPAE), and crayfish *P. leniusculus* proPO-activating enzyme (*Pl*PPAE), was performed using ClustaX 2.1 and MEGA7 softwares. **(B)** Multiple alignment of the deduced amino acid sequences of *Pm*PPAE3 with other crustacean PPAEs was conducted using the Clustal Omega program. The conserved features of PPAEs such as the disulfide bond, the catalytic triad (histidine, aspartic acid, and serine residues), the clip domain, and the serine proteinase domain are shown. **(C)** The representative result of *PmPPAE3* gene tissue distribution analysis by semi-quantitative RT-PCR in the hemocytes (Hc), gill (G), stomach (St), and lymphoid organ (L), is shown. In this analysis, the *EF-1α* transcript was used as an internal control. All experiments were performed in triplicate. **(D)** The *PmPPAE3* gene knockdown using *PmPPAE3*-dsRNA was performed to reveal the functional role of *Pm*PPAE in proPO activating system. The effectiveness of the *PmPPAE3* gene knockdown is shown. Hemocytes collected from the control groups of 0.85% NaCl and dsGFP injected shrimp and from the experimental shrimp injected with *PmPPAE3*-dsRNA was analyzed for the expression of *PmPPAE3* gene by qRT-PCR using the *EF-1α* transcript as an internal control. **(E)** The PO activity was assayed in the *PmPPAE3* knockdown shrimp hemocytes. The data are derived from three independently replicated experiments. The * and ** indicate the significant difference at $P < 0.05$ and $P < 0.01$, respectively.

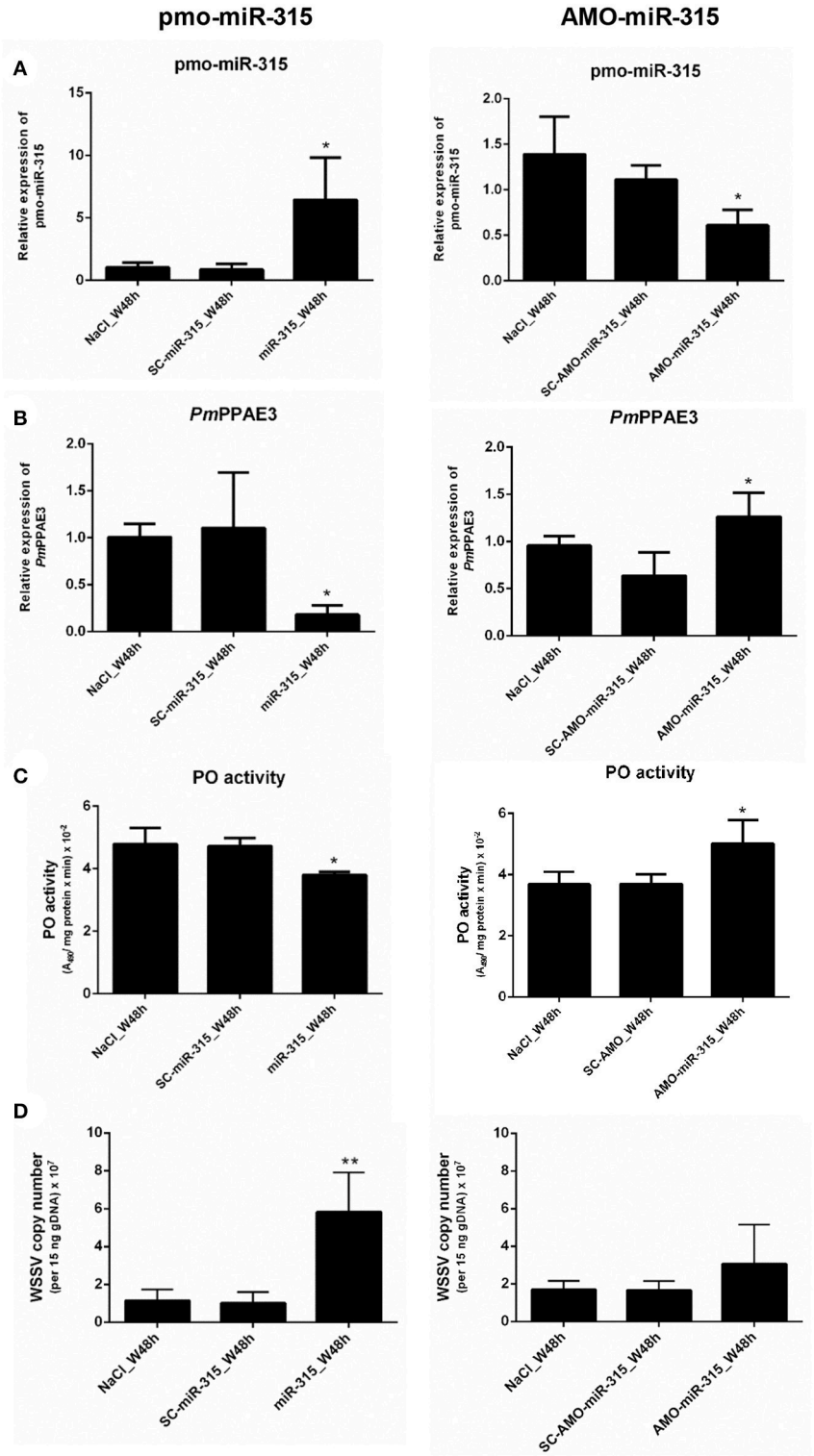

FIGURE 5 | The role of pmo-miR-315 in WSSV-infected shrimp hemocytes. In this experiment, either pmo-miR-315 mimic or AMO-miR-315 was injected into WSSV-infected shrimp. Then, several parameters were investigated including **(A)** pmo-miR-315 and **(B)** *PmPPAE3* gene expression level, **(C)** PO activity and **(D)** WSSV copy number. The U6 and *EF-1α* were used as internal controls for pmo-miR-315 and *PmPPAE3* expression, respectively. All experiments were performed in triplicate. The * and ** indicate the significant difference at $P < 0.05$ and $P < 0.01$, respectively.

of pmo-miR-315 activity by AMO-miR-315 slightly reduced the WSSV copy number when compared to that of pmo-miR-315 injection; however, it was still higher than the control groups (**Figure 5D**).

DISCUSSION

In 2007, the miR-315 from *Drosophila* was found to act as a potent activator of Wingless (Wg) signaling, a conserved pathway that regulates growth and tissue specification (24). Previously, the miR-315s from *M. japonicas, L. vannamei, P. monodon,* and *F. chinensis* have been identified as a viral responsive miRNA in WSSV-infected shrimp hemocytes(5, 13, 14, 25, 26) suggesting that the shrimp miR-315 might be involved in antiviral immunity. Therefore, the pmo-miR-315 function was further characterized in this research.

The expression of pmo-miR-315 was detected in various shrimp tissues including hemocytes, gill, lymphoid organ, and stomach. Interestingly, the expression level of pmo-miR-315 in hemocytes was significantly up-regulated, more than 30 times at 48 h post-WSSV infection, implying the specific role of pmo-miR-315 in shrimp antiviral response in hemocytes. Although the target gene of pmo-miR-315 was predicted as putative prophenoloxidase-activating enzyme *Pm*PPAE3 and serine/threonine protein kinase (13), in this research we focused on confirming the regulatory role of pmo-miR-315 on the expression of *PmPPAE3*.

Generally, the miRNA binds to the 3′-UTR of its target gene to regulate the translational repression and mRNA destabilization. Nevertheless, the binding site of miRNA can also be located at the 5′-UTR and coding sequence (CDS), albeit the regulatory activity may be different (27, 28). According to our prediction, the pmo-miR-315 can bind to CDS of *PmPPAE3* gene (13). The luciferase reporter assay revealed that the pmo-miR-315 mimic could interact with the specific binding site on *PmPPAE3* CDS, which was indicated by almost 36% reduction in luciferase activity.

Melanization activated by the prophenoloxidase (proPO) system is a principal innate immune response in shrimp. Upon pathogen invasion, the binding of Pattern Recognition Proteins (PRPs) to the microbial cell wall components activates the serine proteinase cascade that finally activates the final proteinases, called proPO-activating enzymes (PPAEs). The PPAEs, then, cleave the inactive proPOs to active POs leading to the initiation of melanin formation (29). In *P. monodon*, the active *Pm*PPAE1 and *Pm*PPAE2 cleaves *Pm*proPO1 and *Pm*proPO2 generating the active PO1 and PO2, respectively (30). The *Pm*PPAE3 whose mRNA is the target of pmo-miR-315 is a novel isoform of *Pm*PPAE characterized herein. It was mainly expressed in shrimp hemocytes and significantly suppressed after 24 and 48 h post-WSSV infection. As expected, the negative correlation of pmo-miR-315 expression and *PmPPAE3* gene expression was observed in hemocytes after WSSV infection.

The full-length gene of *PmPPAE3* was identified in this study and its deduced amino acid sequence was compared with other *Pm*PPAEs from various species as well as the *Pm*PPAE1 and *Pm*PPAE2 (22, 23). The multiple alignment of different PPAE amino acid sequences revealed that the *Pm*PPAE3 was closely related to *Fc*PPAE, *Lv*PPAE, and *Pm*PPAE1. The phylogenetic analysis showed that the shrimp PPAEs and a crayfish PPAE belonged to the crustaceans cluster. Besides, the *PmPPAE3* gene was hemocyte specific like *Pm*PPAE1 and *Pm*PPAE2. The function of *Pm*PPAE3 in proPO system was confirmed using the RNA interference technique. Therefore, the *Pm*PPAE3 was considered as a novel clips serine proteinase that function in the proPO system.

As mentioned above, the melanization reaction is activated through the proPO cascade after pathogen infection and unavoidably generates highly toxic molecules. These toxic intermediates are not only involved in pathogen killing but also cause the damage of the host cells (30, 31). Therefore, the activation cascade is needed to be tightly regulated. To date, several proteinase inhibitors of melanization cascade have been reported in shrimp, including the melanization inhibition protein (MIP), serine proteinase inhibitors (serpins), alpha-2-macroglobulin (A2M) and pacifastin (29). Furthermore, the small RNAs can also regulate the proPO system. The shrimp miR-100, which was up-regulated after WSSV or *V. alginolyticus* infection, can regulate several shrimp immune reactions including proPO activity, SOD activity and phagocytosis (32).

The involvement of proPO system upon WSSV infection has been reported. The PO activity is strongly decreased after WSSV-infection in shrimp (33). Later, it is found that the WSSV453 binds to and interferes with the pro*Pm*PPAE2 activation to active *Pm*PPAE2 resulting in the suppression of shrimp melanization (18, 33). In our research, the role of pmo-miR-315 and *Pm*PPAE3 in proPO system during WSSV infection in shrimp was explored. Injection of pmo-miR-315 mimic into the shrimp resulted in a reduction of *PmPPAE3* gene expression and the PO activity as expected. On the other hand, inhibition of pmo-miR-315 by AMO-miR-315 increased the *PmPPAE3* gene expression leading to the increase in PO activity in WSSV-infected shrimp hemocytes. Therefore, we can conclude that the pmo-miR-315 regulates the proPO system via *PmPPAE3* post-transcriptional repression.

Upon WSSV infection, the shrimp proPO system takes part in shrimp antiviral immunity by producing melanin and cytotoxic intermediate for viral sequestration. However, the WSSV can overcome shrimp antiviral immunity partly by proPO system suppression. Several crustacean miRNAs have been reported to promote WSSV propagation. In *M. rosenbergii,* the host miR-s9041 and miR-9850 play positive roles in WSSV replication by targeting the *STAT* gene (10). In crabs, *E. sinensis,* the miR-217 leads to a decrease in the transcript level of *Tube* gene resulting in the enhancement of WSSV copies (34). Meanwhile, the survival rate of miR-100 silenced shrimp after WSSV infection is increased as the PO activity (32). According to our research, an increase in the viral copy number in WSSV-infected shrimp after pmo-miR-315 mimic injection indicated that the pmo-miR-315 functioned in enhancing viral replication by regulating the proPO system through the inhibition of *PmPPAE3* gene expression. On the other hand, the viral copy number of AMO-miR-315 challenged shrimp was lower than that of WSSV-infected shrimp challenged with exogenous pmo-miR-315 but

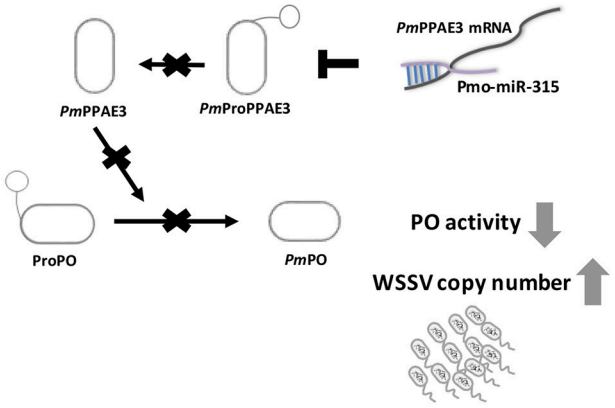

FIGURE 6 | A schematic representation of the pmo-miR-315 role in modulating proPO activity by *PmPPE3* suppression during WSSV infection.

was not lower than the control groups as expected (**Figure 5D**). This might be because the pmo-miR-315 was not totally silenced. Since the whole genome sequence of *P. monodon* has not been reported yet, it was possible that the AMO-miR-315 could also target other unknown genes that might affect the WSSV propagation.

Taken together, our research offer a new mechanism on how WSSV inhibits proPO system by triggering host miRNA, as illustrated in **Figure 6**. The WSSV infection causes the pmo-miR-315 over-expression and subsequently inhibits the *PmPPAE3* expression leading to a decrease in PO activity and increase in WSSV copy number in WSSV-infected shrimp hemocytes. Therefore, the pmo-miR-315 regulates the proPO system through the suppression of *PPAE3* gene expression which leads to the promotion of viral propagation in shrimp hemocytes during WSSV infection.

AUTHOR CONTRIBUTIONS

KS participated in funding acquisition and supervision of this works. KS and PJ designed and provided the resources for the study. PJ performed *in vivo* experiments. PJ and CW performed *in vitro* experiments. All the authors analyzed, investigated the data and also wrote, reviewed, and edited the manuscript.

FUNDING

This research is supported by the Ratchadaphiseksomphot Endowment Fund of Chulalongkorn University (CU-56-462-FW). Additional support from the Thailand Research Fund to KS (Grant No. RSA5980055) is acknowledged. Also, the scholarship to develop research potential for the Department of Biochemistry, Faculty of Science, Chulalongkorn University to CW and Postdoctoral Fellowship to PJ from Ratchadaphiseksomphot Endowment Fund of Chulalongkorn University are greatly appreciated. We would like to thank the support to Omics Sciences and Bioinformatics Center under the Outstanding Research Performance Program: Chulalongkorn Academic Advancement into Its 2nd Century Project (CUAASC).

ACKNOWLEDGMENTS

We thank Prof. Dr. Vichien Rimphanitchayakit (from Chulalongkorn University) for commenting on the manuscript.

SUPPLEMENTARY MATERIAL

The Supplementary Material for this article can be found online at: https://www.frontiersin.org/articles/10.3389/fimmu.2018.02184/full#supplementary-material

REFERENCES

1. Bartel DP. MicroRNAs: genomics, biogenesis, mechanism, and function. *Cell* (2004) 116:281–97. doi: 10.1016/S0092-8674(04)00045-5
2. Jopling CL, Yi M, Lancaster AM, Lemon SM, Sarnow P. Modulation of hepatitis C virus RNA abundance by a liver-specific microRNA. *Science* (2005) 309:1577–81. doi: 10.1126/science.1113329
3. Forman JJ, Coller HA. The code within the code: microRNAs target coding regions. *Cell Cycle* (2010) 9:1533–41. doi: 10.4161/cc.9.8.11202
4. Skalsky RL, Cullen BR. Viruses, microRNAs, and host interactions. *Annu Rev Microbiol.* (2010) 64:123–41. doi: 10.1146/annurev.micro.112408.134243
5. Huang T, Xu D, Zhang X. Characterization of host microRNAs that respond to DNA virus infection in a crustacean. *BMC Genomics* (2012) 13:159. doi: 10.1186/1471-2164-13-159
6. Yang L, Yang G, Zhang X. The miR-100-mediated pathway regulates apoptosis against virus infection in shrimp. *Fish Shellfish Immunol.* (2014) 40:146–53. doi: 10.1016/j.fsi.2014.06.019
7. Gong Y, Ju C, Zhang X. The miR-1000-p53 pathway regulates apoptosis and virus infection in shrimp. *Fish Shellfish Immunol.* (2015) 46:516–22. doi: 10.1016/j.fsi.2015.07.022
8. Shu L, Li C, Zhang X. The role of shrimp miR-965 in virus infection. *Fish Shellfish Immunol.* (2016) 54:427–34. doi: 10.1016/j.fsi.2016.04.129
9. Xu X, Yuan J, Yang L, Weng S, He J, Zuo H. The dorsal/miR-1959/cactus feedback loop facilitates the infection of WSSV in *Litopenaeus vannamei*. *Fish Shellfish Immunol.* (2016) 56:397–401. doi: 10.1016/j.fsi.2016.07.039
10. Huang Y, Wang W, Ren Q. Two host microRNAs influence WSSV replication via *STAT* gene regulation. *Sci Rep.* (2016) 6:23643. doi: 10.1038/srep23643
11. He Y, Yang K, Zhang X. Viral microRNAs targeting virus genes promote virus infection in shrimp *in vivo*. *J Virol.* (2014) 88:1104–12. doi: 10.1128/JVI.02455-13
12. Huang T, Cui Y, Zhang X. Involvement of viral microRNA in the regulation of antiviral apoptosis in shrimp. *J Virol.* (2014) 88:2544–54. doi: 10.1128/JVI.03575-13
13. Kaewkascholkul N, Somboonviwat K, Asakawa S, Hirono I, Tassanakajon A, Somboonwiwat K. Shrimp miRNAs regulate innate immune response against white spot syndrome virus infection. *Dev Comp Immunol.* (2016) 60:191–201. doi: 10.1016/j.dci.2016.03.002
14. Li X, Meng X, Luo K, Luan S, Shi X, Cao B, et al. The identification of microRNAs involved in the response of Chinese shrimp *Fenneropenaeus chinensis* to white spot syndrome virus infection. *Fish Shellfish Immunol.* (2017) 68:220–31. doi: 10.1016/j.fsi.2017.05.060
15. Xie X, Li H, Xu L, Yang F. A simple and efficient method for purification of intact white spot syndrome virus (WSSV) viral particles. *Virus Res.* (2005) 108:63–7. doi: 10.1016/j.virusres.2004.08.002

16. Pfaffl MW. A new mathematical model for relative quantification in real-time RT–PCR. *Nucleic Acids Res.* (2001) 29:e45. doi: 10.1093/nar/29.9.e45
17. Mendoza-Cano F, Sánchez-Paz A. Development and validation of a quantitative real-time polymerase chain assay for universal detection of the white spot syndrome virus in marine crustaceans. *Virol J.* (2013) 10:186. doi: 10.1186/1743-422X-10-186.
18. Sutthangkul J, Amparyup P, Eum J-H, Strand MR, Tassanakajon A. Anti-melanization mechanism of the white spot syndrome viral protein, WSSV453, via interaction with shrimp proPO-activating enzyme, *Pm*proPPAE2. *J Gen Virol.* (2017) 98:769–78. doi: 10.1099/jgv.0.000729
19. Bradford MM. A rapid and sensitive method for the quantitation of microgram quantities of protein utilizing the principle of protein-dye binding. *Anal Biochem.* (1976) 72:248–54. doi: 10.1016/0003-2697(76)90527-3
20. Kumar S, Stecher G, Tamura K. MEGA7: molecular evolutionary genetics analysis version 7.0 for bigger datasets. *Mol Biol Evol.* (2016) 33:1870–4. doi: 10.1093/molbev/msw054
21. Cerenius L, Söderhäll K. The prophenoloxidase-activating system in invertebrates. *Immunol Rev.* (2004) 198:116–26. doi: 10.1111/j.0105-2896.2004.00116.x
22. Charoensapsri W, Amparyup P, Hirono I, Aoki T, Tassanakajon A. Gene silencing of a prophenoloxidase activating enzyme in the shrimp, *Penaeus monodon*, increases susceptibility to *Vibrio harveyi* infection. *Dev Comp Immunol.* (2009) 33:811–20. doi: 10.1016/j.dci.2009.01.006
23. Charoensapsri W, Amparyup P, Hirono I, Aoki T, Tassanakajon A. *Pm*PPAE2, a new class of crustacean prophenoloxidase (proPO)-activating enzyme and its role in PO activation. *Dev Comp Immunol.* (2011) 35:115–24. doi: 10.1016/j.dci.2010.09.002
24. Silver SJ, Hagen JW, Okamura K, Perrimon N, Lai EC. Functional screening identifies miR-315 as a potent activator of Wingless signaling. *Proc Natl Acad Sci USA.* (2007) 104:18151–6. doi: 10.1073/pnas.0706673104
25. Zeng D, Chen X, Xie D, Zhao Y, Yang Q, Wang H, et al. Identification of highly expressed host microRNAs that respond to white spot syndrome virus infection in the Pacific white shrimp *Litopenaeus vannamei* (Penaeidae). *Genet Mol Res.* (2015) 14:4818–28. doi: 10.4238/2015
26. Sun X, Liu Q-h, Yang B, Huang J. Differential expression of microRNAs of *Litopenaeus vannamei* in response to different virulence WSSV infection. *Fish Shellfish Immunol.* (2016) 58:18–23. doi: 10.1016/j.fsi.2016.08.062
27. Hausser J, Syed AP, Bilen B, Zavolan M. Analysis of CDS-located miRNA target sites suggests that they can effectively inhibit translation. *Genome Res.* (2013) 23:604–15. doi: 10.1101/gr.139758.112
28. Brümmer A, Hausser J. MicroRNA binding sites in the coding region of mRNAs: extending the repertoire of post-transcriptional gene regulation. *Bioessays* (2014) 36:617–26. doi: 10.1002/bies.201300104
29. Tassanakajon A, Rimphanitchayakit V, Visetnan S, Amparyup P, Somboonwiwat K, Charoensapsri W, et al. Shrimp humoral responses against pathogens: antimicrobial peptides and melanization. *Dev Comp Immunol.* (2018) 80:81–93. doi: 10.1016/j.dci.2017.05.009
30. Amparyup P, Charoensapsri W, Tassanakajon A. Prophenoloxidase system and its role in shrimp immune responses against major pathogens. *Fish Shellfish Immunol.* (2013) 34:990–1001. doi: 10.1016/j.fsi.2012.08.019
31. Charoensapsri W, Amparyup P, Suriyachan C, Tassanakajon A. Melanization reaction products of shrimp display antimicrobial properties against their major bacterial and fungal pathogens. *Dev Comp Immunol.* (2014) 47:150–9. doi: 10.1016/j.dci.2014.07.010.
32. Wang Z, Zhu F. MicroRNA-100 is involved in shrimp immune response to white spot syndrome virus (WSSV) and *Vibrio alginolyticus* infection. *Sci Rep.* (2017) 7:42334. doi: 10.1038/srep42334
33. Sutthangkul J, Amparyup P, Charoensapsri W, Senapin S, Phiwsaiya K, Tassanakajon A. Suppression of shrimp melanization during white spot syndrome virus infection. *J Biol Chem.* (2015) 290:6470–81. doi: 10.1074/jbc.M114.605568
34. Huang Y, Han K, Wang W, Ren Q. Host microRNA-217 promotes white spot syndrome virus infection by targeting *Tube* in the Chinese mitten crab (*Eriocheir sinensis*). *Front Cell Infect Microbiol.* (2017) 7:164. doi: 10.3389/fcimb.2017.00164

Conflict of Interest Statement: The authors declare that the research was conducted in the absence of any commercial or financial relationships that could be construed as a potential conflict of interest.


CERTIFICATE OF AWARD
This is to Certify that
Kunlaya Somboonwiwat
Has received
2018 Professor M.R. Jisnuson Svasti
Young Protein Scientist of Thailand
The 13th International Symposium of The Protein Society of Thailand
Bangkok, Thailand, Held on August 7-9, 2018
Emeritus Prof. M.R. Jisnuson Svasti
Chair of the Organizing Committee
The Protein Society of Thailand
2018 Professor M.R. Jisnuson Svasti
Young Protein Scientist of Thailand Award
Presented to
Asst. Prof. Dr. Kunlaya Somboonwiwat
For her contribution on
"Molecular Mechanism of
Immune-Related Proteins
in Shrimp Immunity"
9 August 2018

ประกาศ จุฬาลงกรณ์มหาวิทยาลัย

เรื่อง รางวัลผลงานวิจัย กองทุนรัชดาภิเษกสมโภช ประจำปี 2559

ตามที่มหาวิทยาลัยได้มีประกาศ จุฬาลงกรณ์มหาวิทยาลัย เรื่องหลักเกณฑ์และการให้รางวัลการวิจัย กองทุนรัชดาภิเษกสมโภช พ.ศ. 2559 และได้เชิญชวนให้ผู้สนใจส่งผลงานวิจัย/วิทยานิพนธ์ เพื่อสมัครขอรับรางวัลผลงานวิจัย กองทุนรัชดาภิเษกสมโภช ประจำปี 2559 นั้น

บัดนี้คณะกรรมการพิจารณารางวัลการวิจัย กองทุนรัชดาภิเษกสมโภช ประจำปี 2559 ในการประชุม ครั้งที่ 2/2560 (วันที่ 21 กุมภาพันธ์ 2560) พิจารณาและมีมติอนุมัติรางวัลผลงานวิจัย กองทุนรัชดาภิเษกสมโภช ประจำปี 2559 จำนวนทั้งสิ้น 16 รางวัล ดังนี้

1. **รางวัลผลงานวิจัยสำหรับบุคลากรประจำของจุฬาลงกรณ์มหาวิทยาลัย**

1.1 <u>รางวัลผลงานวิจัยดีเด่น</u>

มี 4 รางวัล ผู้ได้รับรางวัล จะได้รับเงินรางวัล 60,000 บาท พร้อมกิตติบัตร จำนวน 1 เรื่อง

1.1.1 ผลงานวิจัยเรื่อง "การขนส่งนอกระบบในกรุงเทพมหานคร"
Embracing Informal Mobility in Bangkok
โดย ผู้ช่วยศาสตราจารย์ ดร.อภิวัฒน์ รัตนวราหะ และคณะ
ภาควิชาการวางแผนภาคและเมือง คณะสถาปัตยกรรมศาสตร์

1.2 <u>รางวัลผลงานวิจัยดีมาก</u>

มี 4 รางวัล ผู้ได้รับรางวัล จะได้รับเงินรางวัล 30,000 บาท พร้อมกิตติบัตร จำนวน 4 เรื่อง

1.2.1 ผลงานวิจัยเรื่อง "การคัดกรองภาวะออทิซึมสองขั้นตอนในเด็กที่มีพัฒนาการทางภาษาล่าช้าและเด็กปกติด้วยแบบสอบถาม M-CHAT"
Two-Step Screening of the Modified Checklist for Autism in Toddlers in Thai Children with Language Delay and Typically Developing Children
โดย ผู้ช่วยศาสตราจารย์ นายแพทย์วีระศักดิ์ ชลไชยะ และคณะ
ภาควิชากุมารเวชศาสตร์ คณะแพทยศาสตร์

1.2.2 ผลงานวิจัยเรื่อง "ข้อได้เปรียบของ Neutrophil Gelatinase Associated Lipocalin ในภาวะการติดเชื้อในกระแสเลือด โดยศึกษาจากโมเดลของหนูทดลองที่ถูกตัดไตออกทั้งสองข้างและการผูกท่อไตทั้งสองข้าง"
Advantage of Serum Neutrophil Gelatinase Associated Lipocalin in Sepsis, Impact of Bilateral Nephrectomy and Bilateral Ureter Obstruction Mouse Models
โดย อาจารย์ นายแพทย์ ดร.อัษฎาศ์ ลีฬหวนิชกุล และคณะ
ภาควิชาจุลชีววิทยา คณะแพทยศาสตร์

1.2.1 ผลงานวิจัยเรื่อง "การพัฒนาฟังก์ชันนัลพอลิเมอร์สำหรับการประยุกต์ทางด้านการตรวจวัดทางชีวภาพและชีวการแพทย์"
Development of Functional Polymers for Biosensing and Biomedical Applications
โดย รองศาสตราจารย์ ดร.วรวีร์ โฮเว่น
ภาควิชาเคมี คณะวิทยาศาสตร์

1.2.2 ผลงานวิจัยเรื่อง "การผลิตไบโอดีเซลและกลีเซอรอลความบริสุทธิ์สูงอย่างต่อเนื่องโดยใช้เทคโนโลยีการเร่งปฏิกิริยาวิวิธพันธุ์"
Continuous Production for Biodiesel and High-Purity Glycerol Using Heterogeneous Catalysis Technology
โดย รองศาสตราจารย์ ดร.ชวลิต งามจรัสศรีวิชัย และคณะ
ภาควิชาเคมีเทคนิค คณะวิทยาศาสตร์

2. รางวัลผลงานวิจัยดีเด่นสำหรับนิสิตระดับปริญญาเอก

มี 4 รางวัล ผู้ได้รับรางวัล จะได้รับเงินรางวัล 20,000 บาท พร้อมกิตติบัตร แต่เนื่องจากปีนี้มีผู้ได้คะแนนเท่ากัน ดังนั้นจึงมีผู้ได้รับรางวัลทั้งหมดเป็นจำนวน 5 รางวัลได้แก่

2.1 ผลงานวิทยานิพนธ์เรื่อง "การพัฒนาระบบการทดสอบแบบปรับเหมาะหลายขั้นตอนด้วยวิธีออนเดอะฟลายที่มีการสะท้อนข้อมูลย้อนกลับในการทดสอบมาตรฐานวิชาชีพของบุคลากรสาขาไอที"
System Development for On-The-Fly Assembled Multistage Adaptive Testing With Reflective Feedback in Information Technology Professional Examination
โดย ดร.ณภัทร ชัยมงคล
อาจารย์ที่ปรึกษาหลัก : รองศาสตราจารย์ ดร.โชติกา ภาษีผล
ภาควิชาวิจัยและจิตวิทยาการศึกษา คณะครุศาสตร์

2.2 ผลงานวิทยานิพนธ์เรื่อง "การพัฒนาอุปกรณ์วิเคราะห์ของไหลจุลภาคสำหรับการตรวจวัดโลหะหนัก"
Development of Microfluidic Analytical Device for Determination of Heavy Metals
โดย ดร.สุดเขต ไชโย
อาจารย์ที่ปรึกษาหลัก : ศาสตราจารย์ ดร.อรวรรณ ชัยลภากุล
ภาควิชาเคมี คณะวิทยาศาสตร์

2.3 ผลงานวิทยานิพนธ์เรื่อง "ลักษณะสมบัติเชิงหน้าที่ของโปรตีนในระบบภูมิคุ้มกันจากกุ้งกุลาดำ *Penaeus monodon* ในการตอบสนองต่อการติดเชื้อก่อโรค"
Functional Characterization of Immune-Related Proteins from Black Tiger Shrimp *Penaeus monodon* in Response to Pathogen Infection
โดย ดร.ภัทรันดา จารีย์
อาจารย์ที่ปรึกษาหลัก : ศาสตราจารย์ ดร.อัญชลี ทัศนาขจร
ภาควิชาชีวเคมี คณะวิทยาศาสตร์

2.4 ผลงานวิทยานิพนธ์เรื่อง "ลักษณะสมบัติเชิงหน้าที่ของโปรตีนรีลิชจากกุ้งกุลาดำ *Penaeus monodon*"
Functional Characterization of Relish Protein from Balck Tiger Shrimp *Penaeus monodon*"

โดย ดร.สุวัฒนา วิเศษนันท์

อาจารย์ที่ปรึกษาหลัก : ศาสตราจารย์ ดร.วิเชียร ริมพณิชยกิจ
ภาควิชาชีวเคมี คณะวิทยาศาสตร์

2.5 ผลงานวิทยานิพนธ์เรื่อง "ผลของกวาวเครือขาว *Pueraria mirifica* ต่อการออกฤทธิ์ป้องกันและรักษาภาวะเสื่อมของเซลล์ประสาทในสมองส่วนฮิปโปแคมปัสของหนูแรทที่ตัดรังไข่"
Effects of White Kwao Krua *Pueraria mirifica* on Neuroprotective and Neurotherapeutic Actions in Hippocampus of Ovariectomized Rats

โดย ผู้ช่วยศาสตราจารย์ ดร.กันยา อนุกูลธนากร

อาจารย์ที่ปรึกษาหลัก : ศาสตราจารย์ ดร.สุจินดา มาลัยวิจิตรนนท์
ภาควิชาชีววิทยา คณะวิทยาศาสตร์

หมายเหตุ ทั้งนี้ มีผลงานวิทยานิพนธ์ที่ดีเด่นเพิ่มขึ้นอีก 1 ราย จึงได้ขออนุมัติจากอธิการบดีเป็นกรณีพิเศษ

3. รางวัลผลงานวิจัยดีเด่นสำหรับนิสิตระดับปริญญาโท

มี 4 รางวัล ผู้ได้รับรางวัล จะได้รับเงินรางวัล 10,000 บาท พร้อมกิตติบัตร แต่เนื่องจากปีนี้มีผู้ได้คะแนนเท่ากัน ดังนั้นจึงมีผู้ได้รับรางวัลทั้งหมดเป็นจำนวน 5 รางวัลได้แก่

3.1 ผลงานวิทยานิพนธ์เรื่อง "ผลของการสอบระดับชาติที่ต่อครูและนักเรียน : การวิเคราะห์ปรากฏการณ์วอชแบค"
Effects of National Testing on Teachers and Students: a Washback Effect Analysis

โดย นางสาวปาริฉัตร ปิติสุทธิ

อาจารย์ที่ปรึกษาหลัก : ศาสตราจารย์ ดร.สุวิมล ว่องวาณิช
ภาควิชาวิจัยและจิตวิทยาการศึกษา คณะครุศาสตร์

3.2 ผลงานวิทยานิพนธ์เรื่อง "การพัฒนาตัวรับรู้ทางเคมีไฟฟ้าสำหรับการตรวจวัดกลูโคซามีนโดยใช้ระบบดรอปเล็ตไมโครฟลูอิดิก"
Development of Electrochemical Sensor for Determination of Glucosamine Using Droplet Microfluidic System

โดย นายอัคพล เสืองาม

อาจารย์ที่ปรึกษาหลัก : อาจารย์ ดร.มนพิชา ศรีสะอาด
ภาควิชาเคมี คณะวิทยาศาสตร์

3.3 ผลงานวิทยานิพนธ์เรื่อง "การเปลี่ยนแปลงสมบัติทางเคมีกายภาพของข้าวระหว่างการเก็บภายใต้ภาวะเร่ง"
Changes in Physicochemical Properties of Rice During Storage Under Accelerated Condition

โดย นายนนทชา ธนธรวรากุล

อาจารย์ที่ปรึกษาหลัก : รองศาสตราจารย์ ดร.ขนิษฐา ธนานุวงศ์
ภาควิชาเทคโนโลยีทางอาหาร คณะวิทยาศาสตร์

Winners of 21st BSGC 2016

THEME 1: BIODIVERSITY, ECOLOGY & SYSTEMATICS

ORAL

1. F. Gozde Cilingir (NUS)
2. Ian Z.W Chan (NUS) &
   Tan Ming Kai (NUS)
3. Ng Chin Soon Lionel (NUS)

POSTER

1. Lim Voon Ching (UM)
2. Delicia Ann Yong Cheen May (UM)
3. Low Liang Boon (UM)

THEME 2: APPLIED SCIENCES & BIOTECHNOLOGY

ORAL

1. Ourlad Alzeus G.Tantengco
   (University of the Phillipines)
2. Markyn Jared N.Kho
   (University of the Phillipines)

POSTER

1. Pinnapat Pinsorn (CU)
2. Mazni Omar (UM)
3. Jasdeep Kaur A/P Darsan Singh (UM)

THEME 3: BIOCHEMISTRY & PHYSIOLOGY

ORAL

1. Loh Su Yi (UM)
2. Ng Chuck Chuan (UM)
3. Nasiru Abdullahi (UM)

POSTER

1. Sunil Singh (NUS)
2. Anjali Gupta (NUS)
3. Angeline Oh Mei Feng (UM)

THEME 4: CELL & MOLECULAR BIOLOGY

ORAL

1. Nopphawitchayaphong Khrueasan (CU)
2. Yang Qiqi (NUS)
3. Pakpoom Boonchuen (CU)

POSTER

1. Xiaoyu Ma (NUS)
2. Xian Hongxu (NUS) &
   Zhang Rui (NUS)
3. Nurgul Imangali (NUS)

CU : Chulalongkorn University
UM : University of Malaya
NUS : National University of Singapore

UNIVERSITY OF MALAYA

NUS National University of Singapore

Chulalongkorn University
จุฬาลงกรณ์มหาวิทยาลัย

Biological Sciences Graduate Congress 21st BSGC 2016

Certificate of Participation

Third Place Award

presented to

PAKPOOM BOONCHUEN

for Oral Presentation at

21st Biological Sciences Graduate Congress 2016

That was held on
15th-16th of December 2016
At University of Malaya

.....

Professor Dr. Zanariah Abdullah
Dean
Faculty of Science
University of Malaya

.....

Associate Professor Dr. Subha Bhassu
Chairperson
21st BSGC 2016
University of Malaya

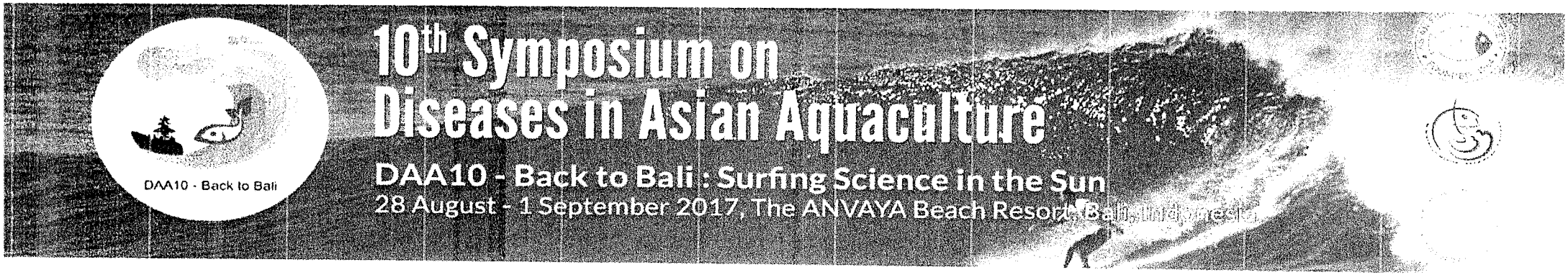

STUDENT POSTER AWARD

this Certificate goes to:

Pakpoom Boonchuen

Faculty of Science Chulalongkorn University- Thailand

as

2nd Winner Poster Presentation

TITLE: HEMOCYANIN OF *Litopenaeus vannamei* AGGLUTINATES *Vibrio parahaemolyticus* AHPND(VPAHPND) AND NEUTRALIZES VP_{AHPND} TOXIN (ID. 145F)

in

The 10th Symposium on Diseases in Asian Aquaculture (DAA10)

28 August to 1 September 2017, Bali - Indonesia

Dr. Phan Thi Van
Chairwoman
Fish Health Section - Asian Fisheries Society

Dr. Agus Sunarto
Vice Chairperson
Fish Health Section - Asian Fisheries Society

Biochemistry and Molecular Biology Section of the Science Society of Thailand Under the Patronage of His Majesty the King
and
Department of Biochemistry, Faculty of Science
Chulalongkorn University

Confer this

CERTIFICATE OF OUTSTANDING POSTER PRESENTATION

upon

Pakpoom Boonchuen

who presented during the 6th International Conference on Biochemistry and Molecular Biology (BMB 2018)
"Networking in Molecular Biosciences towards Creativity and Innovation"

June 20-22, 2018 at Rayong Resort, Rayong, Thailand

Associate Professor Dr. Tuangporn Suthiphongchai
Chair of the Biochemistry and Molecular Biology Section

Assistant Professor Dr. Kanoktip Packdibamrung
Chairperson of BMB 2018

Biochemistry and Molecular Biology Section of the Science Society of Thailand Under the Patronage of His Majesty the King
and
Department of Biochemistry, Faculty of Science
Chulalongkorn University

Confer this

CERTIFICATE OF OUTSTANDING POSTER PRESENTATION

upon

Chantaka Wongdontri

who presented during the 6th International Conference on Biochemistry and Molecular Biology (BMB 2018)
"Networking in Molecular Biosciences towards Creativity and Innovation"

June 20-22, 2018 at Rayong Resort, Rayong, Thailand

Associate Professor Dr. Tuangporn Suthiphongchai
Chair of the Biochemistry and Molecular Biology Section

Assistant Professor Dr. Kanoktip Packdibamrung
Chairperson of BMB 2018